Design, Implementation and Testing of an Underwater Global Positioning System

by

Emmett Donald Herbert Gamroth
B.Eng., University of Victoria, 2003

A Dissertation Submitted in Partial Fulfillment of the
Requirements for the Degree of

MASTER OF APPLIED SCIENCE

in the Department of Mechanical Engineering

Design, Implementation and Testing of an Underwater Global Positioning System

by

Emmett Donald Herbert Gamroth
B.Eng., University of Victoria, 2003

Supervisory Committee

Dr. C. Bradley, Supervisor
(Mechanical Engineering)

Dr. B. Buckham, Departmental Member
(Mechanical Engineering)

Dr. P. Kraeutner, Outside Member
(Electrical and Computer Engineering)

Supervisory Committee

Dr. C. Bradley, Supervisor
(Mechanical Engineering)

Dr. B. Buckham, Departmental Member
(Mechanical Engineering)

Dr. P. Kraeutner, Outside Member
(Electrical and Computer Engineering)

ABSTRACT

The purpose of this research project was to design, implement, and evaluate a prototype underwater positioning system which extends the reach of the terrestrial Global Positioning System (GPS) underwater. The GPS does not function underwater because the high-frequency low-power signals used by the GPS are not able to penetrate more than several meters in water. The Underwater Global Positioning System (UGPS), presented in this work, provides underwater position data to an unlimited number of underwater assets, such as autonomous vehicles. The user requirements are discussed and a design is presented that incorporates a topside surface buoy (satellite) and a subsurface receiver. The satellite is responsible for receiving GPS data and relaying the data, via acoustic signals, to the subsurface receiver. The receiver calculates its position using the coded acoustic signals. The implementation of the prototype UGPS satellite and subsurface receiver are discussed in detail; the custom electronics, software, data acquisition systems and mechanical housings are described. The key operating characteristics of the UGPS are investigated both experimentally and through the analysis of a model describing the entire UGPS. Employing the prototype UGPS, a series of sea-trials were performed that provides essential design data for developing the next version of the system. The main characteristics that were experimentally investigated were: the long and short-range accuracy; the repeatability; and the resolution. The experimental data was also employed to confirm the UGPS model performance. The prototype system demonstrated the feasibility of the UGPS concept and showed that a position accuracy of 6.5m should be attainable for an unlimited number of underwater receivers operating within a one square kilometer

workspace. The accuracy can be enhanced to sub-meter by employing more accurate GPS receivers in the satellites and using a sound velocity meter to measure the sound velocity profile of the acoustic workspace.

Contents

List of Tables

List of Figures

Nomenclature

Roman letters

$TDOA_{12}$	Time Difference of Arrival between signals from S1 and S2
$TDOA_{13}$	Time Difference of Arrival between signals from S1 and S3
f_0	Frequency of transmission
$f_{Doppler}$	Doppler Shift
V_{in}	Input Voltage
$v_{s,r}$	Velocity of source relative to the receiver
x_{r-t}	Horizontal distance between transmitter and receiver
z_b	Bottom depth
z_r	Receiver depth
z_t	Transmitter depth
A/D	Analog to Digital
APL	Applied Physics Laboratory
AUV	Autonomous Underwater Vehicle
BPSK	Binary Phase Shift Key
c	Speed of sound in water
CTD	Conductivity Temperature Depth
CW	Continuous Wave
D	Depth in km
D/A	Digital to Analog
DAQ	Data Acquisition
dB	Decibels
DOP	Dilution of Precision
DP	Dynamic Positioning
DVL	Doppler Velocity Logger
f	Frequency at which absorption coefficient is calculated
FSK	Frequency Shift Key
GPS	Global Positioning System
GUI	Graphical User Interface
HDOP	Horizontal Dilution of Precision
INS	Inertial Navigation System
ITC	International Transducer Corporation
LBL	Long Baseline
LUSBL	Long-Ultra-Short Baseline
NiMH	Nickel Metal Hydride
OCV	Open Circuit Voltage
OTL	Ocean Technology Laboratory
PC	Personal Computer
pH	Acidity
PPM	Parts Per Million
PVC	Polyvinyl Chloride
R	Distance from receiver
RF	Radio Frequency
RMS	Continuous Wave
ROV	Remotely Operated Vehicle

S	Salinity in parts per thousand
S1	Satellite 1
S2	Satellite 2
S3	Satellite 3
SBL	Short Baseline
SLAM	Simultaneous Localization and Mapping
SPL	Sound Pressure Level
SSBL	Super-Short Baseline
T	Temperature in degrees Celsius
TDOA	Time Difference of Arrival
TDOP	Time Dilution of Precision
TL	Transmission Loss
TOA	Time of Arrival
TVR	Transmit Voltage Response
UGPS	Underwater Global Positioning System
USBL	Ultra-Short Baseline
UTC	Coordinated Universal Time
UVic	University of Victoria
VDOP	Vertical Dilution of Precision
VENUS	Victoria Experimental Network Under the Sea
VRU	Vertical Reference Unit
WAAS	Wide Area Augmentation System

Greek letters

β	Bandwidth
ρ_{RES}	Distance measurement resolution
σ	Standard deviation
τ	Length of transmitted signal in meters

ACKNOWLEDGEMENTS

Many people contributed to the success of this effort and I would like to express my appreciation to them here. First of all, I would like to thank my supervisor Dr. Colin Bradley for his commitment to the work and guidance throughout this process. I could not have asked for a better supervisor. I would also like to thank Dr. Brad Buckham and Dr. Paul Kraeutner for being part of my supervisory committee and Dr. Ross Chapman for acting as my external examiner. I am indebted to Jeff Kennedy for his technical support and for the many hours spent cold and wet during field testing; most of all, for his friendship over the past 6 years. Rodney Katz for his knowledge and advice during the design of the test system. Kevin Jones for designing the initial prototype of the projector electronics. My brother, Darryl Gamroth, who was a constant source of knowledge and expertise during the entire design process. My parents, Don and Collette Gamroth who provided encouragement and motivation to complete this thesis. Finally, my wife Catherine. This thesis is a result of the contribution of many, but no one provided more technical, professional, and personal support than my wife. Thank you for your love and support.

DEDICATION

To Catherine.

Chapter 1

Introduction

The Ocean Technology Laboratory (OTL) at the University of Victoria is an engineering research laboratory that develops technologies such as underwater vehicles and high definition imaging systems. A key requirement of these projects is an underwater positioning system that would allow underwater objects such as vehicles to determine their positions, thereby allowing the vehicles to perform autonomous tasks. Although some positioning systems are commercially available, none of them meet the specific needs of these projects. The goal of this thesis is the preliminary design and implementation of an innovative underwater acoustic positioning system that will meet these requirements.

A scientific research project affiliated with the OTL is the Victoria Experimental Network Under the Sea (VENUS). In 2006, this cabled underwater ocean observatory was installed in the in-shore waters around Vancouver Island. VENUS, shown in Figure 1.1(a), has a total of three sites in Saanich Inlet and the Straight of Georgia. The Saanich Inlet site, for example, has a subsea node located in 100 m of water and situated approximately 3 km from shore. The Saanich Inlet node is shown in Figure 1.1(b). The underwater node, placed at a scientifically interesting location within the inlet, acts as a hub for scientific research and accommodates up to eight independent instrument packages.

(a) Node Locations

(b) Rendering of the Saanich Inlet Node

Figure 1.1: Victoria Experimental Network Under the Sea (VENUS) [1].

Underwater cabled observatories are promising venues for ocean science research, but have limitations because the instruments connected to each node are localized and the data are only collected in the immediate vicinity of the node. Therefore, there is a need for mobile underwater vehicles that can collect data at greater distances from the node [2].

Vehicles operating in the vicinity of an underwater node would be required to perform tasks such as repeatedly collecting data at pre-defined locations, responding to interesting events observed around the node, and performing maintenance on the node itself. All of these tasks require the vehicle to make critical control decisions based on an accurate knowledge of its location.

The need to determine the precise location of an object (such as a vehicle, diver or scientific instrument) is not limited to this particular project; it is crucially important in a diverse range of industries; for example, oil, gas and environmental monitoring [3], scientific research [4], and subsea construction [5]. The myriad of applications requiring underwater positioning strengthens the case to develop a new class of underwater

positioning system.

1.1 Project Motivation

There are two main categories of positioning systems in use today. They can be described in terms of where the majority of the tracking system is mounted: vessel or seafloor.

Vessel: Many commercially available underwater positioning systems are support vessel centric, i.e. they are designed to track an underwater asset from a vessel. Unfortunately with this class of system the underwater vehicle knows nothing of its own position. A vessel centric tracking system is not useful for underwater objects, such as autonomous underwater vehicles (AUVs), that require information from the positioning system to aid their own navigation.

Seafloor: Positioning systems that provide spatial information to the underwater target tend to be very complicated and require extensive initial surveying when the positioning system is installed. These systems utilize a network of underwater transponders that are located on the sea floor. Since the transponders are fixed to the seafloor they must be precisely surveyed when they are installed. This costly and difficult procedure makes these positioning system unusable for missions at arbitrary locations.

Underwater acoustic positioning systems use active tracking which relies on each target emitting an acoustic signal. The addition of each tracked target, therefore, adds acoustic noise to the working area. Hence, a relatively small number of targets can be tracked within an area before the targets (noise sources) start to interfere with one another.

The underwater positioning system proposed in this thesis is a rapidly deployable system allowing an unlimited number of receivers mounted on vehicles, divers, or any other underwater object, to determine their positions within the acoustic arena. A useful analogy is the terrestrial Global Positioning System (GPS) that enables vehicle drivers to know their precise location and relate it to a street map. This work presents the preliminary design of a subsea positioning system that functions in a similar manner to GPS.

1.2 Thesis Outline

The structure of this thesis is as follows:

Chapter 2 Underwater Positioning Methodologies

- Review of current underwater positioning systems; how they work; and their relative merits and weaknesses.
- Description of a proposed design for an underwater positioning system, called UGPS (Underwater Global Positioning System).

Chapter 3 Theory of Operation of the Proposed UGPS

- Explanation of the theory underlying trilateration, multilateration and recognition of received signals, as it applies to the UGPS.
- Identification of the contributing factors affecting the accuracy of the system.

Chapter 4 Description of the UGPS Model and Experimental Apparatus

- Presentation of the design of a test system used to verify time-of-flight accuracy, coding techniques, and multi-path rejection.
- Description of a model designed to be used as a preliminary means of analyzing the test system under a variety of operational scenarios.

Chapter 5 Evaluation of the UGPS Model and Experimental Apparatus

- Results of experiments performed in an underwater environment with the test system to verify the model and explore different acoustic signal modulation schemes.
- Verification of the model by comparing experimental and modeled results.
- Discussion of the results obtained with the test system.

Chapter 6 Future Work and Conclusions

- Summary of the overall UGPS, UGPS model, and evaluation of the performance of the system.
- Recommendations for future research and development.

Chapter 2

Underwater Positioning Methodologies

Underwater positioning systems are subject to constraints imposed by the unique underwater environment. As a result, many of the common techniques used in land and space based positioning systems cannot be directly applied, including optical, radio frequency (RF) and inertial systems. However, acoustic techniques are well-suited to the underwater environment, and can be used in combination with many standard positioning methodologies and algorithms such as those used in the Global Positioning System (GPS).

Optical positioning requires a line-of-sight path between the tracker and tracked object. This method is unreliable in murky water (due to path reflection) and impractical over large distances (due to absorption). These problems also affect camera-based navigation schemes such as Simultaneous Localization and Mapping (SLAM). Positioning using RF signals is impractical under water for ranges in excess of 10 m due to high attenuation of RF in water [6]. Inertial systems are widely used for underwater navigation, but have the inherent problem of spatial error accumulation over time. This problem can be mitigated using highly precise sensors such as laser ring gyros and Doppler velocity loggers but these sensors are prohibitively expensive ($> \$10000$/unit), particularly when multiple units are required.

In the ocean, the most appropriate form of radiation for long range propagation is sound [7]. Therefore, positioning using acoustic signals is the preferred underwater technology. Employing acoustic receivers and transmitters as the base technology, many of the terrestrial and space-based methodologies and algorithms are employed in underwater applications.

This chapter describes and motivates the proposed Underwater Global Positioning

System (UGPS) as follows:

1. Introduction to the aspects of GPS technologies that influence the proposed UGPS.

2. Review of current underwater positioning systems and their advantages and disadvantages.

3. Description of the proposed UGPS design.

2.1 Global Positioning System (GPS)

Since the launch of Sputnik 1 in 1957, satellites have been used for a variety of applications such as: optical monitoring of the Earths surface, telephony, cartography, and satellite based navigation. The observed Doppler shift on the radio waves emanating from Sputnik 1 lead the researchers at the Applied Physics Laboratory (APL) to propose an innovative satellite-based Doppler navigation system [8] called Transit. Transit was the precursor of the modern day GPS.

The GPS was developed in the early 1970's by the United States Department of Defense as a next generation tracking system for the military. In 1978 the first GPS satellite was launched and by 1993 a total of 24 satellites were in orbit. The following year the Federal Aviation Agency declared the GPS ready for aviation use [9].

The Global Positioning System, depicted in Figure 2.1 has three segments: space, control, and user. The space segment consists of 24 functional satellites that transmit positioning signals which cover the entire planet. The GPS was designed so that at least 4 satellites will be in view of a GPS receiver anywhere on the planet [8]. Each satellite transmits signals, which include information about the position and orbit of the satellite, so each GPS receiver can calculate its position. The control segment is a worldwide series of ground-based stations that track the position and health of the GPS satellites and relay this information to a master control station in Colorado Springs, Colorado. This information is used to provide corrections to the satellites so that precision positioning can be attained. The user segment includes military and consumer receivers, such as the GPS receivers now integrated into vehicles. The receivers are able to monitor the GPS signals transmitted from the visible satellites to calculate the position of the receiver.

A receiver uses a technique called trilateration to calculate its position. The distance between each satellite and the receiver is measured using the time-of-flight of

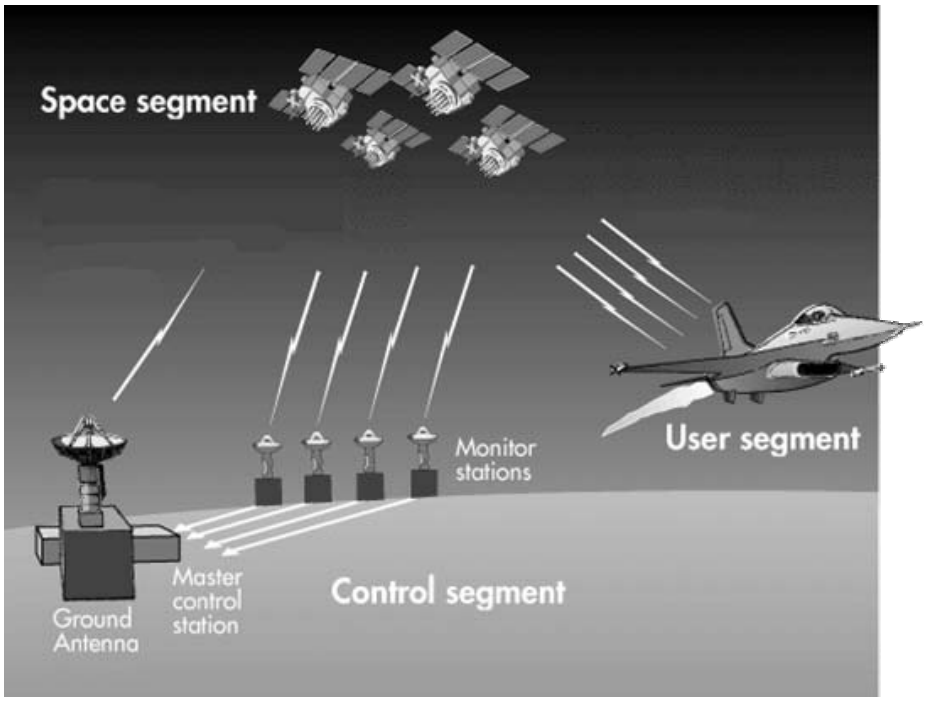

Figure 2.1: The three segments of the Global Positioning System (reproduced from [10]).

the radio signals traveling between the satellites and the receiver. Because the position of each satellite is precisely known, the position of the receiver can be calculated. Integral to the GPS, and position calculation, is a knowledge of a precise timing signal obtained from the satellites. This benefit allows receivers around the world to be time synchronized with the GPS's network time.

2.2 Underwater Positioning Systems Employing Acoustic Techniques

Currently available underwater acoustic positioning systems can be divided into four classes: Long Baseline (LBL), Short Baseline (SBL), Ultra-Short Baseline (USBL) (also called Super-Short Baseline (SSBL)), and Combined Systems. The classes are distinguished by the baseline, or distance between their fixed acoustic elements. Each of these systems is based on the technique of using one or more fixed acoustic devices to track a mobile target. In this section, the pros and cons of each class will be discussed, along with examples of each.

2.2.1 Long Baseline

The long baseline (LBL) positioning system provides accurate acoustic positioning over a large area. LBL systems are used to track multiple targets relative to a fixed set of underwater transponders moored to the seafloor. Typical applications for LBL systems include: dynamic positioning (DP) systems for positioning multiple offshore targets, such as oil rigs and large ships, in water depths up to 7000m; offshore construction, survey and metrology work [11]; and tracking autonomous underwater vehicles (AUVs) and remotely operated vehicles (ROVs) [12].

LBL systems are comprised of two types of components: mobile transceivers and fixed transponders. A transceiver is a device mounted on each tracked target and can both transmit and receive acoustic signals. A transponder is a self-contained device moored at an underwater location and responds to an acoustic interrogation with an acoustic reply. Figure 2.2 depicts a LBL system used to track the relative position of the oil rig above the ocean floor. The transceiver is mounted on the oil rig, while the transponders, labelled T1 through T4, are moored below. For LBL positioning, a minimum of three transponders are moored at underwater locations separated by a distance of up to several kilometers.

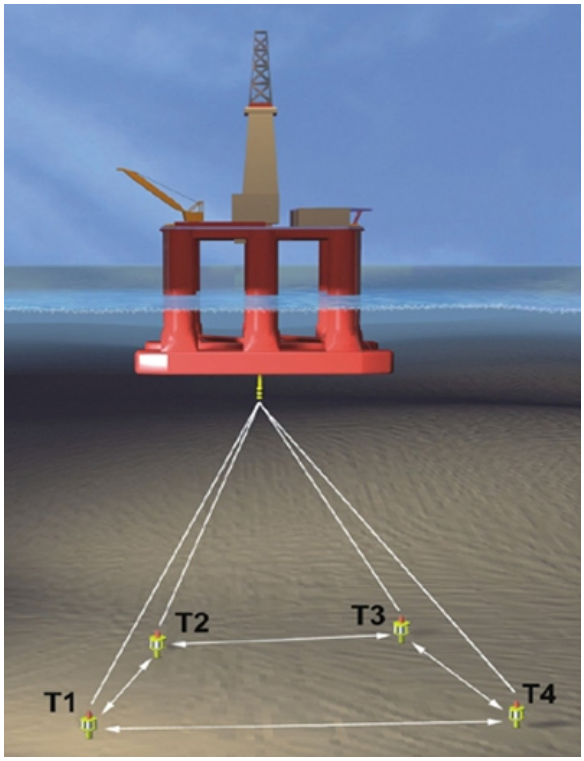

Figure 2.2: Computer generated rendering of a long baseline underwater acoustic positioning system used for monitoring the location of an oil platform (reproduced from [13]).

Long baseline systems use the trilateration technique (Section 3.1.1) to calculate the position of the target using the distances calculated between the target and each of the moored transponders. The target transceiver starts the tracking process by emitting an acoustic signal. Each underwater transponder receives this signal and sends back an acoustic reply. The transceiver receives the acoustic replies from the transponders and measures the time between transmitting the starting acoustic signal and receiving the replies from each of the transponders. The advantages and disadvantages of LBL systems are summarized in Table 2.1.

Table 2.1: Advantages and disadvantages of a LBL positioning system.

Advantages	**Disadvantages**
• very good position accuracy independent of depth • operates over large areas and great depth • only a single small transducer is required on the tracked object	• complex system requiring skilled operators • large array of expensive equipment • time consuming to setup the array of moored transponders

Most manufacturers of LBL systems (e.g. Sonardyne, Kongsberg, Linkquest and Nautronix) have developed their own proprietary spread spectrum technique to increase the accuracy of LBL systems and provide a better signal-to-noise ratio for the acoustic signals without increasing the amplitude of the acoustic waves [14]. Spread spectrum signals also have the advantage of allowing simultaneous tracking of multiple receivers operating in the same area.

Hypothesis grids have been proposed as a means of quantifying the quality of an acoustic range measurement using prior association probability. Each range observation is quantified as direct path, multi-path, or outlier [15]. This technique uses subsequent measurements to produce a better overall solution to range measurements, instead of taking each measurement as an independent event.

Another improvement to LBL systems is to incorporate inertial navigation to increase the accuracy for long range (>6000m) LBL systems [16]. A subset of adding inertial navigation to LBL systems is Synthetic Long Baseline [17], also known as Virtual Long Baseline [18]. This method uses inertial navigation systems to simplify the LBL system so that only a single transponder is required. Synthetic LBL uses the inertial navigation system of an underwater vehicle to supplement the acoustic positioning system. The single transponder is used to measure the distance between the transponder and the vehicle as the vehicle moves around, providing an absolute reference to the inertial navigation solution.

2.2.2 Short Baseline

Short baseline (SBL) acoustic positioning systems are used to track multiple targets relative to a fixed set of transceivers mounted on a vessel. SBL systems are used for Dynamic Positioning (DP) of vessels relative to a fixed reference on the seafloor and also for tracking ROVs and AUVs [19].

SBL systems, depicted in Figure 2.3, use similar equipment as LBL systems, i.e. transponders and transceivers. A minimum of three transceivers are mounted to the hull of a ship and are connected to a main control station. A single transponder, labelled T1 in Figure 2.3, is mounted to the tracked object. SBL systems can operate in several different modes (pinger, responder and transponder), with the transponder mode most common.

In transponder mode, one of the vessels transceivers emits an acoustic signal. Upon reception of this signal, by the transponder, an acoustic reply is emitted. SBL systems use triangulation to determine the position of the underwater transponder by measuring the range and bearing of the target relative to the surface vessel. The SBL system determines the bearing of the underwater transponder by measuring the relative times of arrival of the acoustic reply at each transceiver. The range to the tracked object is calculated using the travel-time of the acoustic signal transmitted from the transceiver to the reception of the acoustic reply. The defining feature of a SBL system is the distance between the transceivers, also called the baseline. For SBL systems the baseline is typically 20-50m [20].

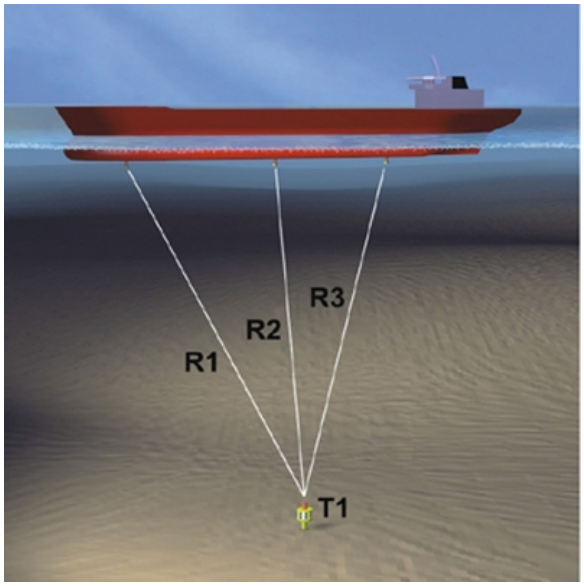

Figure 2.3: Computer generated rendering of a short baseline underwater acoustic positioning system (reproduced from [13]).

This vessel-centric system provides the position of the tracked underwater asset relative to the position and orientation of the vessel. Relating the relative position of the receiver to the absolute position of the sea floor is a challenging task that requires the addition of several sensors. A vertical reference unit (VRU), surface navigation unit and a gyro are required to report the position of the underwater target relative to the sea floor.

SBL systems have lost market share, in recent years, to the lighter, smaller USBL systems. Since a SBL system does not provide the excellent position accuracy of the LBL system, nor the ease of deployment of the USBL system, it is rarely chosen for use in new applications. In fact, manufacturers of SBL systems (e.g. Sonardyne) have discontinued their production of SBL systems altogether.

The advantages and disadvantages of SBL systems are summarized in Table 2.2.

Table 2.2: Advantages and disadvantages of a SBL positioning system.

Advantages	Disadvantages
• low system complexity makes SBL an easy tool to use • good range accuracy • quick to deploy since no transponders are deployed on the seafloor • small transducers on the ship	• large baselines are required for accuracy • transceiver positions must be accurately surveyed on vessel, generally requires dry dock • absolute position accuracy depends on additional sensors (gyro, VRU) • $\geq$3 transducers must be rigidly mounted on the ship

2.2.3 Ultra Short Baseline

Ultrashort baseline (USBL) positioning systems, also called super-short baseline (SSBL), have become the standard acoustic positioning system used for AUV and ROV tracking and homing. The ease of deployment and portability of the system makes the USBL system a good choice for AUV and ROV missions. USBL systems are used to track multiple targets that are generally in close proximity to the tracking vessel (<4km) because the accuracy of a USBL system is inversely proportional to the slant range (the distance between the ship and the target).

USBL systems, depicted in Figure 2.4, use a single transceiver mounted to a vessel to track an underwater transponder (T1). Unlike the SBL transceiver, the USBL transceiver is composed of several acoustic elements separated by a baseline of approximately 10cm. Since all of the acoustic elements are housed in a single enclosure, their position relative to one another is accurately measured during manufacturing, thereby eliminating in the field calibration of the transceiver.

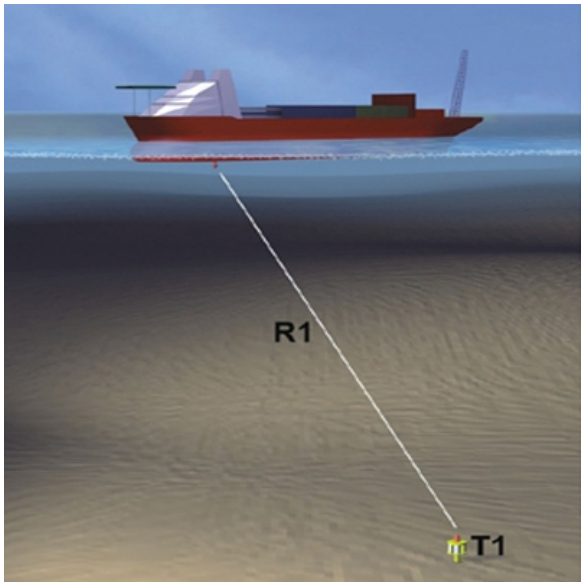

Figure 2.4: Computer generated rendering of an ultrashort baseline underwater acoustic positioning system (reproduced from [13]).

The USBL system triangulates the position of the underwater target, relative to the transceiver, using a range and bearing measurement. The bearing is calculated using the phase difference between the received acoustic signal on each of the acoustic elements of the transceiver and the known geometry of the acoustic elements in the transceiver. The range is calculated using the two-way travel-time between the transceiver and the transponder.

USBL systems typically operate in responder or transponder mode. When the USBL system is operating in transponder mode, the transceiver starts the tracking process by emitting an acoustic signal. Upon reception of this signal at the transponder, an acoustic reply is sent back to the transceiver. In responder mode, the transponder is electrically connected to the transceiver, generally through the tether of an ROV or tow fish. Instead of the transceiver starting the tracking process by sending an acoustic signal, the transceiver starts the tracking process by sending an electrical signal to the transponder through the tether. The advantages and disadvantages of USBL systems are summarized in Table 2.3.

Most USBL systems now use spread spectrum coded acoustic signals. This allows for more objects to be tracked simultaneously as well as providing a better range measurement without increasing the amplitude of the acoustic signals.

Many USBL systems are currently available. Linkquest and ORE both manufacture USBL systems priced under $25000. Although these entry level systems are

Table 2.3: Advantages and disadvantages of a USBL positioning system.

Advantages	**Disadvantages**
• minimal components making USBL systems easy to use • good range accuracy • quick to deploy since there is only a single ship mounted transceiver	• ship based transceiver can be large making, repeatable mounting difficult • accuracy is proportional to slant range, so accuracy decreases with distance to the target • absolute position accuracy depends on additional sensors (gyro, VRU) that can be expensive • minimal redundancy in most USBL systems compared with LBL systems

limited in their accuracy, and do not include sensors to relate the USBL measurements to an absolute frame of reference, they provide a user with cost effective basic positioning. Several of the more expensive systems, e.g. Sonardyne, include integrated heading, pitch, and roll sensors in the transceiver. IxSea goes one step further and includes a full inertial navigation system within the transceiver [21] [22]. The addition of an external GPS unit, provides absolute positioning of the underwater tracked targets. The addition of the internal sensors also makes these systems "calibration free"; i.e. the user can start tracking underwater objects immediately after deployment of the transceiver.

Linkquest and Sonardyne have recently released inverted versions of their USBL systems. These inverted systems are designed with pressure rated transceivers which can be mounted on the underwater vehicle. Employing an inverted USBL system, the vehicle can track and home in on transponders [23]. This enables applications such as AUV docking, where the vehicle uses its onboard USBL system to home in on the underwater dock [24].

Augmenting a USBL transponder with a combination of Doppler velocity logger

(that measures the velocity of the vehicle relative to the seafloor or particles suspended in the water) and inertial navigation system (INS) data is being explored. Using an onboard Doppler velocity logger on an underwater vehicle, the noise of the tracking data can be reduced, thereby providing a better positioning solution [25]. Coupling an INS with a USBL system has been used to enhance error estimation for low cost INS systems [26].

2.2.4 Combined LBL/USBL

Positioning systems that amalgamate two of the previously discussed acoustic positioning schemes are called Combined systems. Although these systems are not commonly used for underwater vehicle tracking, they are used when tracking is absolutely essential, such as dynamic positioning of oil rigs and support vessels. USBL and LBL systems are most commonly combined into a single LUSBL system. These systems combine the high accuracy of LBL systems with the quick deployment of USBL systems. The combination of two independent systems provides an additional redundancy of the acoustic tracking results. The primary disadvantage of Combined systems is their high cost.

2.2.5 Comparison of Underwater Acoustic Positioning Systems

The three classes of underwater acoustic positioning systems, not including Combined systems, are summarized in Table 2.4.

Table 2.4: Comparison of Underwater Acoustic Positioning Systems.

	LBL	**SBL**	**USBL**
Baseline	Several kilometers	20-50m	$<$ 10 cm
Minimum Quantity and Location of Fixed Acoustic Element(s)	$\geq$ 3 on sea floor	$\geq$ 3 on vessel hull	1 on vessel hull
Positioning	Relative to sea floor	Relative to vessel	Relative to vessel
Relative Accuracy	Best	Worst	Medium
Ease of Set-Up	Difficult. Requires precise position calibration of moored transponders on ocean floor	Difficult. Requires precise position calibration of transceivers onboard support vessel	Simple. Single transceiver mounted on vessel.
Size	Large	Medium	Small
Target knows its location	Possible	No	No

2.3 Proposed Underwater Global Positioning System (UGPS)

The proposed UGPS system provides the accurate positioning of a LBL system with the quick and easy "calibration-free" setup of a USBL system. It relays GPS data to receivers on mobile targets in an underwater workspace, allowing the receivers to calculate their positions.

The UGPS concept is illustrated in Figure 2.5. It employs a minimum of three

transmitter buoys, termed satellites, and one or more underwater receivers. The UGPS only transmits signals from the satellites to the receivers; therefore, individual receivers do not add acoustic signals to the water. Hence, an unlimited number of receivers can be used. The UGPS satellites are deployed with a triangular baseline separation of up to 1.5 km (similar to a LBL system). Conceptually, the satellites can be autonomous vehicles, boats, or free floating or moored buoys.

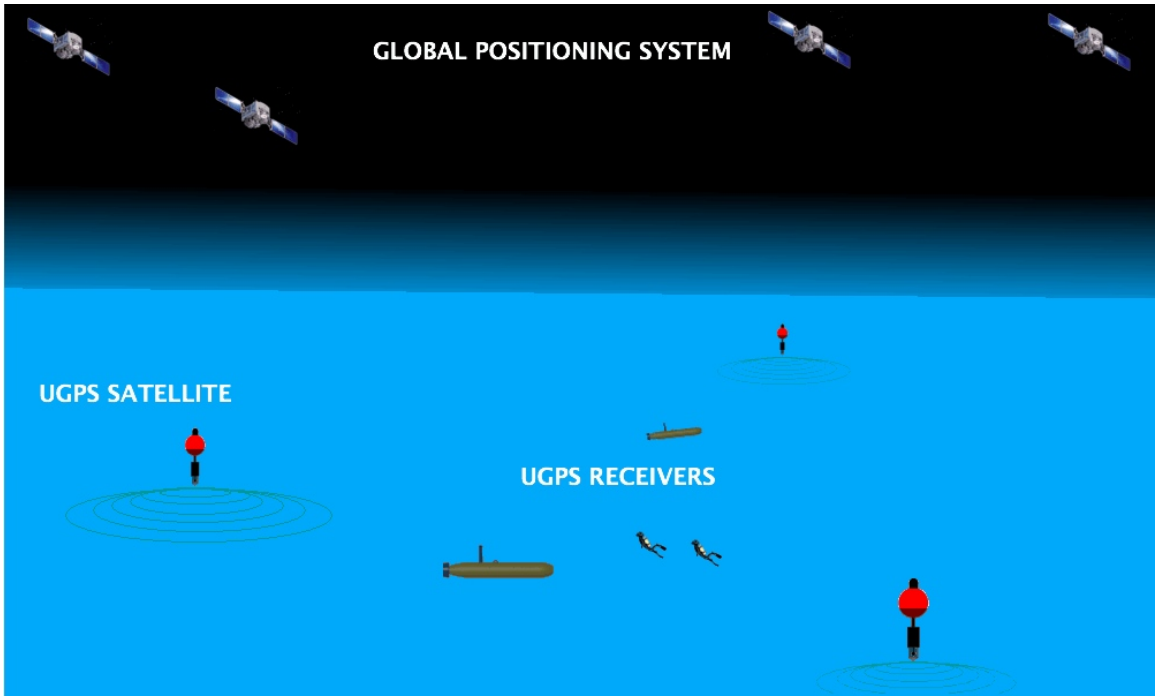

Figure 2.5: Concept drawing of the UGPS with the receivers mounted on autonomous underwater vehicles and divers (not to scale).

Each UGPS satellite consists of:

- A GPS receiver, which provides the position of the UGPS satellite. The precise time signal, also available from the GPS receiver, is used to synchronize all of the UGPS satellites.
- An onboard computer, which formats and compresses the GPS position data and then modulates it for acoustic transmission to the UGPS receivers. The digital form of the signal is converted to an analog voltage signal, by a digital to analog converter, which is applied to the acoustic transmitter.
- An acoustic transmitter which converts the voltage signal from the onboard computer to an acoustic wave that propagates through the water to the UGPS receiver.

The UGPS satellites use the precision timing of the GPS network to simultaneously emit unique acoustic signals. The acoustic signal from each satellite is comprised of a series of modulated acoustic data packets with two portions: time synchronization and data. The time synchronization portion is used to calculate the travel-time of the acoustic signal between the UGPS satellite and the UGPS receiver. The data portion contains the position of the UGPS satellite. The data in these packets is encrypted and a spreading code, known only by the UGPS satellite and all UGPS receivers, is applied. Spread spectrum techniques provide many advantages over narrow band signals, such as the ability to simultaneously transmit data from multiple transmitters using the same frequency band. In addition, spread spectrum techniques are used to increase the signal-to-noise ratio (SNR) of the signal by applying a coding gain. Increasing the SNR allows the system to operate in acoustically noisy environments, e.g. environments with ships, rain, or sea life. The spreading of the data packet also allows the network to only allow verified users to access the UGPS position and timing information. Spread spectrum communication is very difficult to decode without the spreading code.

The UGPS receiver acquires the acoustic signals sent from each UGPS satellite and, using these signals, calculates the position of the UGPS receiver. Each UGPS receiver consists of:

- an acoustic receiver (hydrophone) which converts the sound pressure in the water into an electrical signal.
- a variable gain amplifier and filter which amplifies the small voltage from the hydrophone prior to digitization. A variable gain amplifier is required because as the UGPS receiver travels further from a UGPS satellite, the amplitude of the acoustic signal will decrease. The gain of the variable gain amplifier can be adjusted to enable the reception of small and large amplitude signals. A filter is used to eliminate acoustic signals falling outside of the frequency band of interest.
- a micro-controller which interprets the received acoustic signals and calculates the position of the UGPS receiver.
- a pressure transducer, providing the receiver a precise depth measurement independent of the acoustic system.

The UGPS receiver employs a geometric multilateration technique, similar to that used by the GPS, to calculate its position. The UGPS receiver acquires the acoustic

signals from the UGPS satellites and calculates the difference in arrival time of each acoustic signal relative to the first received signal. Because each acoustic signal is unique and also includes the position of the UGPS transmitter, the receiver knows which UGPS satellite sent each acoustic signal. The UGPS receiver is able to calculate its position using the time difference of arrivals, the position of each of the UGPS satellites, and the depth of the UGPS receiver (from the onboard pressure sensor),. The intended UGPS receiver position accuracy is 5m 68% of the time, using low-cost terrestrial GPS receivers in each satellite. If the GPS units in each satellite were upgraded to survey grade GPS units, sub-meter accuracy could be attained.

The advantages of the proposed UGPS are:

- A continuously updated, absolute position measurement available to the underwater receiver.
- The UGPS provides a finite position error independent of the operational time. In comparison, inertial navigation systems are subject to error accumulation the longer the unit is operational.
- An unlimited number of underwater receivers can be used because the UGPS data is uni-directional. Therefore, communications traffic is minimal and the underwater asset does not reveal its position.
- Unlike many acoustic systems, an external acoustic modem is not required to transmit the position of the vehicle from the surface tracking system to the underwater target. This reduces the cost, bulk, and power requirements of the UGPS receiver.
- Compared to other long baseline systems, setup time is minimal because the UGPS satellites do not have to be surveyed when deployed. Once the buoys have been deployed the systems is operational.
- The UGPS is highly cost effective compared with USBL systems. USBL requires high cost sensors to relate the relative tracked position of the underwater asset to an absolute position.

2.4 Chapter Summary

In this chapter, the GPS and four classes of underwater acoustic positioning systems were presented. The underwater acoustic positioning classes (LBL, SBL, USBL, and

Combined) were examined so that the favorable qualities of each system could be incorporated into the UGPS concept. LBL systems are the most accurate, however they are complex and require a time-consuming calibration process prior to use. SBL systems use small transducers mounted to the support vessel; unfortunately a dry dock is generally required to install the transceivers. USBL systems are rapidly deployable, but are expensive and require precise sensors to relate the tracked position of the target to an absolute frame of reference.

The design of the UGPS was presented. The proposed UGPS incorporates many of the features of the LBL, SBL, and USBL acoustic positioning systems. The UGPS is an accurate LBL system that can be deployed rapidly, much like a USBL system. Unlike any of the other systems, however, the UGPS allows an unlimited number of receivers to operate within the acoustic workspace. This feature of the UGPS is inherited from the GPS.

In the next chapter, the theory required to implement the UGPS concept will be discussed. In addition, the sources of error that contribute to the overall accuracy of the UGPS will be presented.

Chapter 3

Theory of Operation of the Proposed UGPS

In this chapter, the background theory related to the UGPS will be discussed. Specifically, the techniques utilized by the UGPS to calculate the position of the receiver using acoustic signals generated by the satellites.

In the sections below, the following topics will be discussed:

- Positioning Using Time-of-Flight Techniques. Trilateration and multilateration are methods of calculating the position of an object; these methods will be discussed. In addition, the matched filter will be described as a method of identifying the time at which an acoustic signal is received. Finally, pulse compression signals are presented because they produce excellent distance measurement results when used in sonar and radar applications.

- Analysis of System Error. The errors affecting the accuracy of the proposed UGPS are discussed. The errors sources are presented in three separate categories: travel-time measurement, distance calculation and geometric.

3.1 Positioning Using Time-of-Flight Techniques

Triangulation is a term frequently used to describe any type of positioning system that determines the position of an object using distances or angles. Triangulation is, in fact, a specific method of determining the position of an object using the angles between that object and two reference objects, with known positions. In the 18th Century, the sextant was regularly used to triangulate the position of a vessel based on angle measurements from objects with known locations, such as the sun and moon. Basic navigation courses still train mariners to determine their location from a series of bearings from objects at known locations. In Chapter 2, a class of underwater positing systems (USBL) was described that employs angle measurements to determine the position of underwater assets. Although USBL systems are widely used, they have limited accuracy due to the difficult task of accurately measuring the angle from which an acoustic signal is received.

A more accurate technique of determining the position of an underwater object is to measure the distances between that object and several fixed reference objects. Trilateration (spherical positioning) and multilateration (hyperbolic positioning) are two methods that use distance measurements to calculate the position of an object. A positioning system employing trilateration uses the time-of-flight of each signal traveling between a transmitter and a receiver to determine the position of the receiver. These time-of-flight measurements are calculated from the time of arrivals (TOAs) of the received signals and the time at which each transmitter emitted its signal. Multilateration, however, uses the time difference of arrivals (TDOA) of the transmitted signals and requires no knowledge of the time at which each transmitter emitted its signal; this is the defining difference between trilateration and multilateration. In the next section, these two positioning techniques will be discussed.

3.1.1 Trilateration

Trilateration is a technique used to solve for the position of an object given the distance between that object and several reference objects, whose positions are known. Trilateration is often referred to as spherical positioning because, in three dimensions, each distance measurement defines a sphere on which the position of the receiver must lie.

Trilateration can be explained using the following two dimensional example. The position of a target (T) can be determined in two dimensions by measuring the distance between T and three fixed objects (S1, S2, and S3), whose positions are known.

The three fixed objects in this example are called satellites. The distances are calculated using the travel-times of acoustic signals traveling between the satellites and target. These measured travel-times are converted to distances by multiplying the travel-times by the speed of sound in the medium in which they travel (in this case, water).

Given the distance between T and S1, then T must be located on a circle centered at S1 with a radius equal to the distance between T and S1, as illustrated in Figure 3.1.

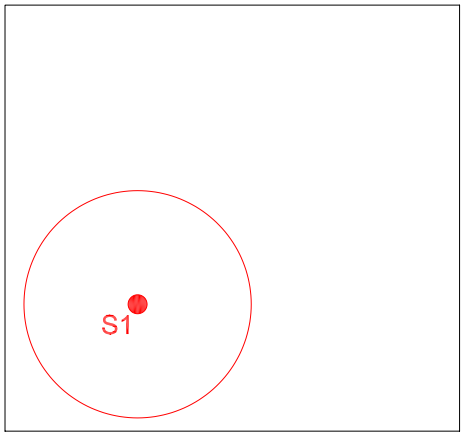

Figure 3.1: Trilateration with one reference object. The location of T is somewhere on the circle.

The equation of a circle is the same as the equation for the distance between two points, one point being the center of the circle and the other somewhere on the circle itself. Equation 3.1 represents the circle on which the object T is located.

$$\rho_1 = \sqrt{(x_T - x_{S1})^2 + (y_T - y_{S1})^2} \tag{3.1}$$

In Equation 3.1, ρ_1 is the distance between S1 and T; x_T and y_T are the cartesian coordinates of the position of T; and, x_{S1} and y_{S1} are the coordinates of S1. The position of T can be further discerned using the distance between T and a second satellite (S2). From this second piece of information, T must lie on a circle centered at S2, with radius equal to the distance between T and S2. Figure 3.2(a) shows that the two circles, centered at S1 and S2, intersect at two locations; therefore, T must be located at one of these two locations. As shown in Figure 3.2(b), using the distance between T and a third satellite (S3), the position of T is uniquely determined.

This example illustrates that the position of a target can be calculated using the distances between the target and 3 reference objects, whose positions are known. This

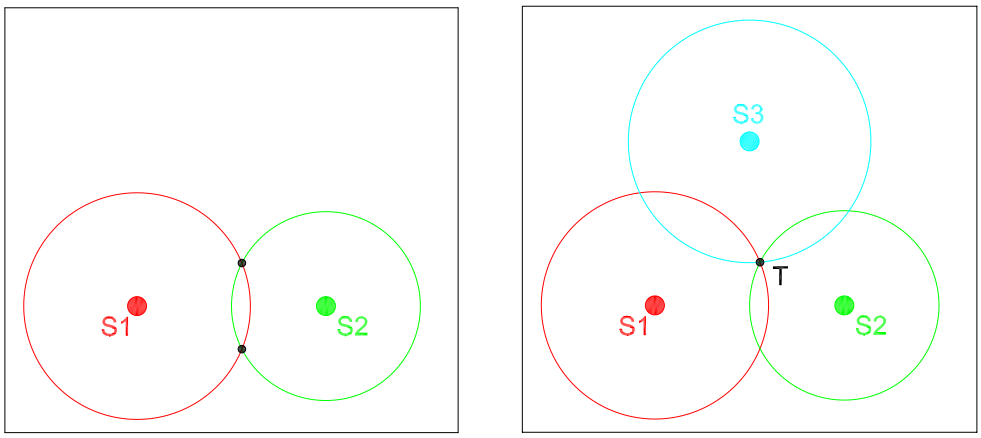

(a) Two satellites (b) Three satellites

Figure 3.2: Graphic depicting trilateration with two satellites and three satellites.

graphical example can be described mathematically using the equations of the three circles shown in Figure 3.2. The equations of the three circles are shown in Equation 3.2.

$$\begin{aligned} \rho_1 &= \sqrt{(x_T - x_{S1})^2 + (y_T - y_{S1})^2} \\ \rho_2 &= \sqrt{(x_T - x_{S2})^2 + (y_T - y_{S2})^2} \\ \rho_3 &= \sqrt{(x_T - x_{S3})^2 + (y_T - y_{S3})^2} \end{aligned} \tag{3.2}$$

Solving these non-linear equations for the location of the target can be accomplished by linearizing the equations and solving iteratively. A rigorous treatment of this process is presented in [27], [28], and [9]. An overdetermined system exists when more than three reference objects are present. A least squares approach using all of these equations can be used to solve for the position of T. Using all of the equations to calculate the position of T generally produces a better result than solving for the position of T with only the least number of equations required [9].

Challenges Associated with Trilateration

Trilateration is used to calculate the 2-D position of a target given three distance measurements. Under water, acoustic ranging is employed to measure these distances. The distances are calculated using the acoustic signal travel-times and the speed of sound in water, which can be measured directly. A LBL system, which was discussed in Section 2.2.1, uses trilateration to calculate the position of the underwater target.

LBL systems require bidirectional data transmission between the transceiver, which is mounted on the tracked target, and multiple transponders, which are moored to the sea floor, to calculate the position of the target. The proposed UGPS employs unidirection data transmission, therefore, the method used by LBL systems to calculate the distances cannot be applied.

Distance measurement without using bi-directional acoustic data transmission requires the receiver to be time synchronized with the satellites. The satellites and receiver are separate pieces of hardware; therefore, it is difficult to keep these units synchronized over time. The clock in the receiver is analogous to a wristwatch that runs a bit fast and, therefore, drifts over time. The receiver clock can be fast or slow, thereby losing synchronization with the satellites. A typical inexpensive crystal oscillator has a 20 parts per million (ppm) error. For example, a 10MHz crystal, which is a common reference crystal for timing applications, with a 20ppm error could actually oscillate at 10.0002MHz. Even though the frequency of the receiver clock is off by only a small amount, it is the integration of this error over time that causes the receiver and satellite to lose synchronization. If the two clocks were started at the same time, after a period of only 50s, the clocks will be out of synchronization by 1ms. Since the speed of sound in water is approximately 1500ms^{-1}, a synchronization error of 1ms equates to a range measurement error of 1.5m. Over a period of a day the receiver will be out of synchronization by as much as 1.7 seconds, equating to a range error of 2.61km.

An additional satellite can be added to the system to compensate for the clock synchronization error, which is also called clock bias. This additional satellite adds an equation to the positioning solution enabling the calculation of the clock bias from the positioning solution. However, adding another satellite to a three-satellite system increases the cost of the system by 1/3 and, therefore, is not an ideal solution.

Another method of eliminating the effect of clock bias is to measure the time difference of arrivals (TDOAs) of the acoustic signals at the receiver, rather than the TOAs. The TDOAs are the difference in arrival times between the first received acoustic signal and all subsequent acoustic signals. Two advantages of using TDOAs are: only small times have to be measured and the clocks in the satellites and receivers do not have to be synchronized. In a three-satellite system, where the satellites are spaced 1.5km apart, the maximum TDOA is 1 second (assuming a sound speed of 1500ms^{-1}). A 20ppm error in the receiver's clock will yield a TDOA timing error of only 20μs, or a range error of only 3cm. This method of calculating the receiver position based on TDOAs is called multilateration and will be discussed in the next

section.

3.1.2 Multilateration

A receiver employing multilateration measures the times between the first received signal and all subsequent signals. All of the transmitters must transmit simultaneously, or with known delays between them, to measure the TDOAs of the acoustic signals.

Multilateration is often referred to as hyperbolic positioning because each TDOA defines a hyperbola on which the position of the receiver must lie. This concept will be explained using the following example. Three satellites (S1, S2, and S3), whose positions are known, simultaneously transmit uniquely identifiable ranging signals. A target (T) receiving these signals measures the times between receiving the first signal and all subsequent signals. For a three satellite system, two times are measured: the time between receiving the first and second signals ($TDOA_{12}$) and the time between receiving the first and third signals ($TDOA_{13}$). In this example $TDOA_{12}$ is 2 seconds while $TDOA_{13}$ is 1.89 seconds.

The TDOAs are the difference of the travel-times of the acoustic signals traveling between the satellites and the target; therefore, many travel-times exist that will yield a $TDOA_{12}$ of 2 seconds, Table 3.1 shows just a few.

Table 3.1: Examples of travel-times of acoustic signals propagating from S1 and S2 to T, that yield a TDOA of 2s.

$\mathbf{t_2}$ Travel-time of acoustic signal from S2 to T (s)	$\mathbf{t_1}$ Travel-time of acoustic signal from S1 to T (s)	$\mathbf{TDOA_{12}}$ (s)
6	4	2
8	6	2
10	8	2
12	10	2

Each travel-time from Table 3.1 is converted to a distance, by multiplying it by the propagation speed of the signals, and plotted in Figure 3.3. For the two travel-times in each row of Table 3.1, the position of T could be at two points. These points are the intersection points of two circles centered at S1 and S2 with radii equal to the travel-times of the signals from S1 and S2 to T. In Figure 3.3, the satellites are shown

as black circles and labeled S1 and S2. The intersection of each pair of travel-times is marked with a small black circle.

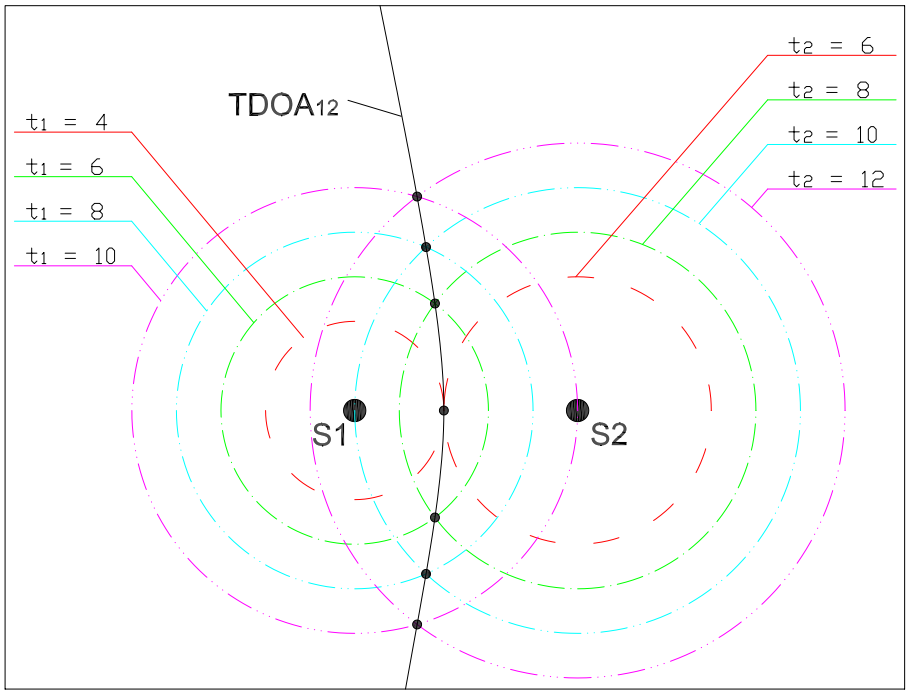

Figure 3.3: Multilateration with one TDOA.

For each pair of travel-times yielding a TDOA of 2, the target can be at two possible locations. If a line is drawn through all of the possible locations for the target T, a hyperbola is formed. This hyperbola defines all of the possible locations of the target T given a TDOA of 2 seconds between the signals received from S1 and S2.

If a third satellite (S3) is introduced, and therefore another TDOA, the position of the target T must also lie on the hyperbola formed using this TDOA. Figure 3.4 shows the hyperbola from the first TDOA ($TDOA_{12}$) and a second hyperbola that is generated from the second TDOA ($TDOA_{13}$). These hyperbolas intersect at a single location within the workspace, therefore, a unique solution for the position of T exists.

In this example, it is assumed that the target is able to distinguish between the ranging signals sent from S1, S2, and S3. In other words the target knows that the signal from S1 is received first and the signal from S2 is received second. This extra piece of information means the position of the receiver can be uniquely determined using only three satellites. If the transmitter signals are not uniquely identifiable, then the second half of each of the hyperbolas is also a possible solution, therefore,

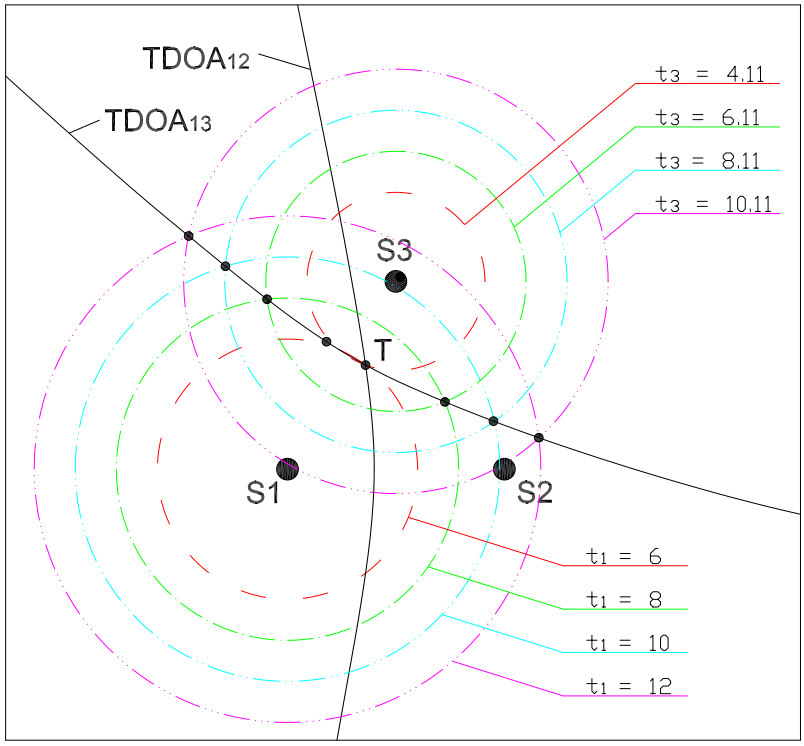

Figure 3.4: Multilateration with two TDOAs.

with three satellites, four solutions to the position of T are possible.

Unlike trilateration, which requires a means of synchronizing the satellites and receiver, multilateration requires no synchronization. This feature of multilateration, however, comes at a cost. The accuracy of the position calculation using trilateration is more accurate than multilateration [31]. Even though trilateration produces a more accurate result, the ability to operate a 3 satellite system without synchronizing the satellites and receiver makes multilateration a better choice for the proposed UGPS.

The proposed UGPS uses multilateration to calculate the position of the underwater receiver using the TDOAs of the transmitted acoustic signals. In the next section, the method used by the receiver to identify the arrival times of signals will be discussed.

3.1.3 Signal Identification and Timing

In the previous section, the location of a target was calculated using either the TOAs or the TDOAs of received acoustic signals. In order to determine the TOAs or TDOAs, a receiver must first be able to identify the origin and time of reception of each received signal. In this section, the process of identifying a received signal

and assigning it a time will be discussed.

3.1.3.1 The Matched Filter

A common technique used in radar and sonar applications to identify a received signal is the matched filter. A matched filter uses the transmitted signal as a template to which the received signal is compared. The better the match between the template and the received signal, the greater the amplitude of the matched filter's output. The comparison between the template and the received signal is accomplished using correlation. Correlation is like sliding the transmitted signal (template) along the x-axis of the received signal and assigning a value to that offset representing the quality of the match.

The simplest method of acoustically measuring the distance between two objects is to measure the time it takes an acoustic signal to travel between the two objects. For this measurement, one object transmits the acoustic signal while the other receives the signal. An appropriate signal used for this application is a short, gated signal of a constant frequency. For example, several periods of a sine wave of constant amplitude and frequency, as shown in the top plot of Figure 3.5. Typically, the received signal will be an attenuated and time-shifted version of the original signal, as shown in the middle plot of Figure 3.5. For underwater acoustic positioning, the attenuation is primarily a result of the geometric spreading of the transmitted acoustic signal while the time shift is a result of the travel-time of the transmitted signal propagating from the transmitter to the receiver. The bottom plot of Figure 3.5 is the output of the matched filter, which compares the received signal with the transmitted signal. The matched filter's output has been scaled such that the reception of a signal with amplitude equal to the transmitted signal would result in an amplitude of ± 1.

The peak of the matched filter's output denotes the time at which the match between the template and the received signal is maximum. The time at which the maximum signal occurs is used to estimate the travel-time of the signal; using this time, the distance is calculated by multiplying the travel-time by the speed of sound in water.

This example illustrated the concept of using a matched filter to measure the distance between two objects using a simple transmitted signal. Although a gated sine wave has been used frequently in sonar and underwater positioning systems, there are many problems inherent in this type of signal:

- Distance measurement resolution depends on the duration of the transmitted

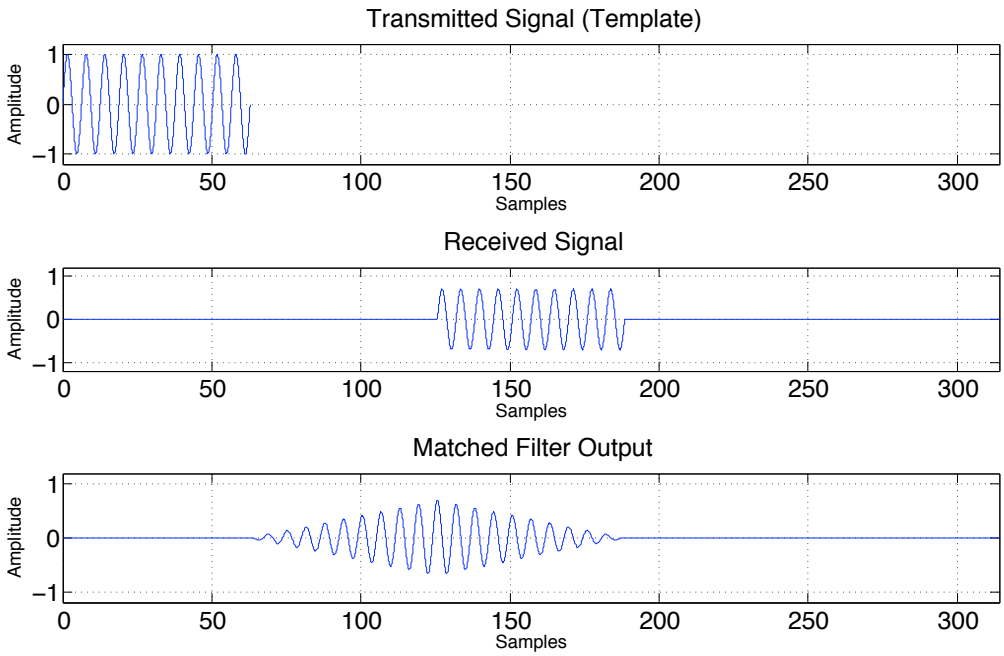

Figure 3.5: Example of a matched filter used to identify a sine wave signal within a received signal.

signal. The distance resolution, ρ_{RES}, for a sine wave is calculated as $\rho_{RES} = c \cdot \tau$, where c is the speed of sound in water and τ is the duration of the transmitted signal. The range resolution is the length (in meters) of the acoustic signal, therefore, a smaller pulse duration results in a better resolution.

- Amplitude of the matched filter is dependent on the duration and the amplitude of the compared signals. Therefore, to obtain a large amplitude from the matched filter, the signal has to have a large amplitude, a long duration, or both. Since the signal duration also affects the resolution of the time measurement, there is a tradeoff between range resolution and matched filter amplitude.

- Resistance to the effect of multi-path signals is low because the maximum output of the matched filter is not significantly different than other points in the matched filter's output.

Multi-path Signals

For an underwater positioning system to operate over a wide area, the transmitter must sends acoustic signals in all directions (omni-directional). As a result, a receiver can be situated in any direction, relative to the transmitter, and still receive the

signals. The path length that is used by a positioning system to calculated its position is called the direct path, which is a straight line between the transmitter and receiver. It is also possible for a part of the transmitted signal, which normally would not have reached the transmitter, to reflect off an object and be redirected towards the receiver. This is known as a multi-path signal and is a copy of the transmitted signal acquired by the receiver. A receiver can have trouble distinguishing between a direct path signal and a multi-path signal. Figure 3.6 illustrates an example where a multi-path signal (displayed in red) is received immediately after the direct path signal. The multi-path signal is generally smaller than the direct path signal because it travelled a longer path and as such attenuates more.

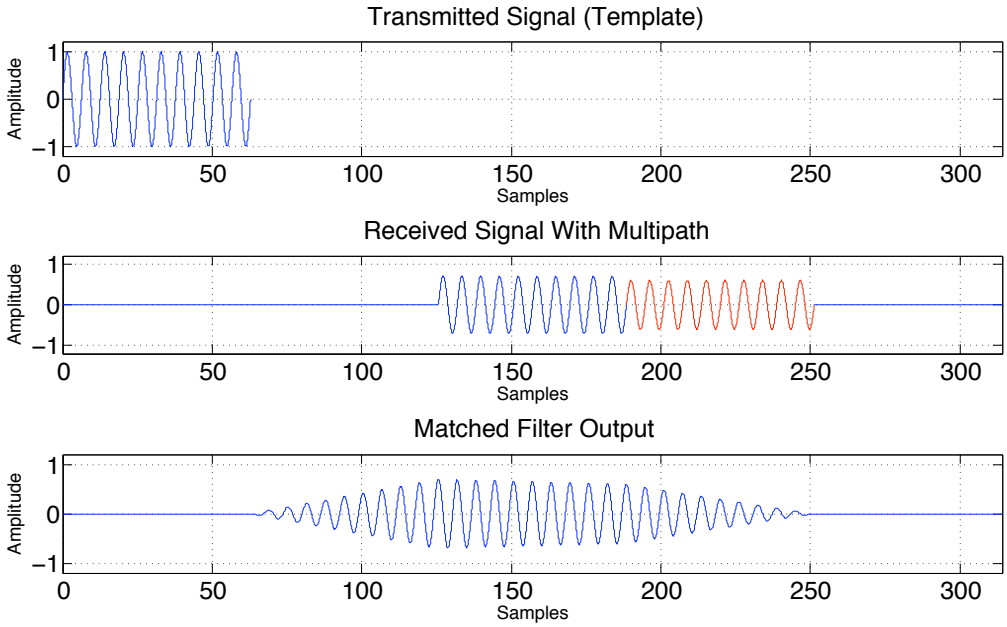

Figure 3.6: Example of a matched filter used to identify a sine wave signal within a received signal which contains direct path and multi-path signals.

The output of the matched filter is a blending of the direct path and multi-path signals. The maximum is no longer obvious because it is not significantly different than other points in the matched filter's output. With the addition of noise, the location of the maximum could change considerably.

3.1.3.2 Pulse Compression

The example in the last section illustrated the power of a matched filter for comparing a received signal with a template as a means of measuring their similarity. This section describes a technique called pulse compression which is used in radar and

sonar applications to address the problems associated with using a simple sine wave as the transmitted signal.

Pulse compression makes use of a class of signals that generate narrower and more distinct cross-correlation peaks after matched filtering. Unlike a traditional sine wave signal, the transmitted signal can have a much longer duration without reducing the resolution of the matched filter's output. The pulse compression technique produces a narrower, or compressed, cross-correlation peak; hence the term pulse compression. Pulse compression is achieved by increasing the bandwidth of the transmitted signal. The increased bandwidth allows the resolution to remain high, even when the duration of the signal is increased.

The effect of pulse compression can be observed by examining the autocorrelation of the transmitted signal. Autocorrelation is a special case of cross correlation when the two signals being compared are the same, i.e. they are both the template signal. Autocorrelation is a measure of how well a signal matches a time shifted version of itself. Ideally a signal used for underwater positioning would have a cross correlation of 1 only when it is perfectly aligned with itself, but 0 everywhere else. This type of signal would be ideal for a positioning system because there would be a single point that would clearly define the time when the signal is received. In addition, the signal would be virtually immune to multi-path interference because it would not interact with the multi-path copy of itself.

Figure 3.7 shows the autocorrelation of two different signals. The signal on the left is the 10 cycle sine wave presented in the last section. The autocorrelation of the signal is shown below. The output of the autocorrelation has been scaled to an amplitude of ± 1. During autocorrelation a copy of the signal is translated across the signal to determine how well they match. When the copy of the signal is offset by one cycle of the sine wave and compared to the original signal, 9 of the 10 cycles still line up, and the correlation is high. This results in an autocorrelation that does not have one unique maximum with an amplitude noticeably higher than the rest. Instead, as each cycle of the sine wave interacts with the time shifted version of itself, it produces a local maximum proportional to the number of cycles that overlap. The signal on the right of Figure 3.7 is a linear frequency chirp; i.e. the frequency of the signal increases linearly with time. This signal generates a sharply peaked time compressed output. This signal has the same duration as the original signal, but has a very different autocorrelation. The autocorrelation yields a unique maximum, so the chirp is an effective signal for pulse compression.

Features of the pulse compression technique are:

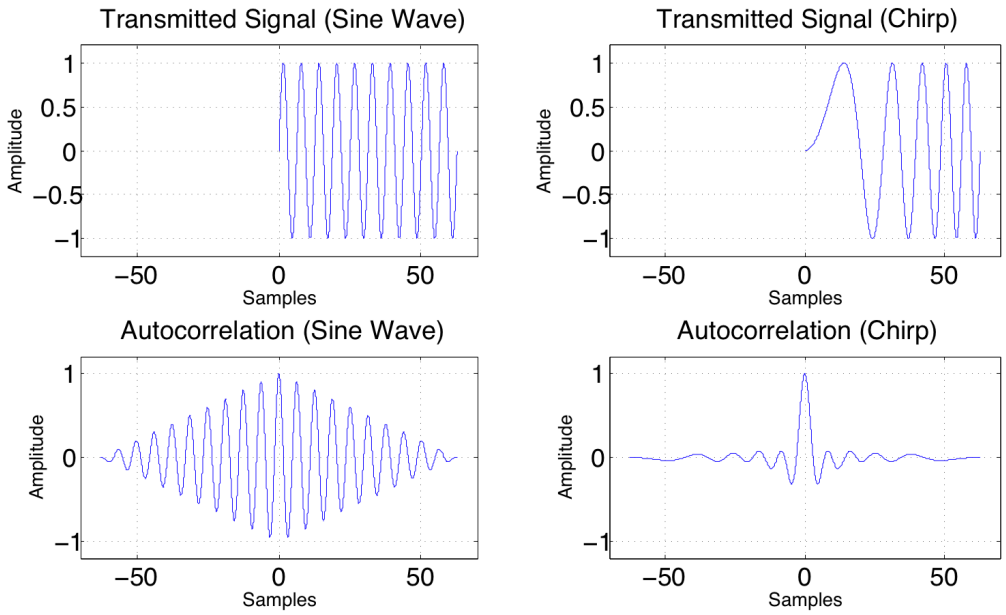

Figure 3.7: Autocorrelation of a sine wave and a linear frequency chirp.

- The range resolution is increased by using greater bandwidth. The range resolution, ρ_{RES}, for a linear frequency chirp is calculated as $\rho_{RES} = \frac{c}{\beta}$, where c is the speed of sound in water and β is the bandwidth of the transmitted signal [29]. A larger bandwidth produces a better resolution.

- The amplitude of the cross-correlation can be increased by using a signal with a longer duration without effecting the range resolution. This means that the amplitude of the signal does not have to increase in order to obtain a higher signal to noise ratio. Producing large amplitude signals requires large transmitter circuitry, pulse compression eliminates the need for large amplitude signals, leading to cheaper drive electronics.

- Resistant to multi-path because the autocorrelation of the signal yields a single distinct peak.

In the previous section, a plot was presented showing the matched filter's output for a 10 cycle sine wave with a multi-path signal received immediately after. The correlation of the template with the direct path and multi-path signals produced a cross correlation that did not produce a unique maximum that clearly showed the time at which the signal was received. The same example is presented in Figure 3.8, but this time using a linear frequency chirp as the transmitted signal. The top plot,

in Figure 3.8, is the transmitted signal, which acts as the template for the matched filter. The middle plot is the received signal, which consists of a direct path signal as well as the muti-path signal (displayed in red). The bottom plot in Figure 3.8 shows the output from the matched filter. The matched filter output has been scaled such that the reception of a signal with amplitude equal to the transmitted signal would result in an amplitude of ± 1. The multi-path signal is easily resolved from the direct path signal, resulting in a very clear indication of the time at which the direct path signal is received.

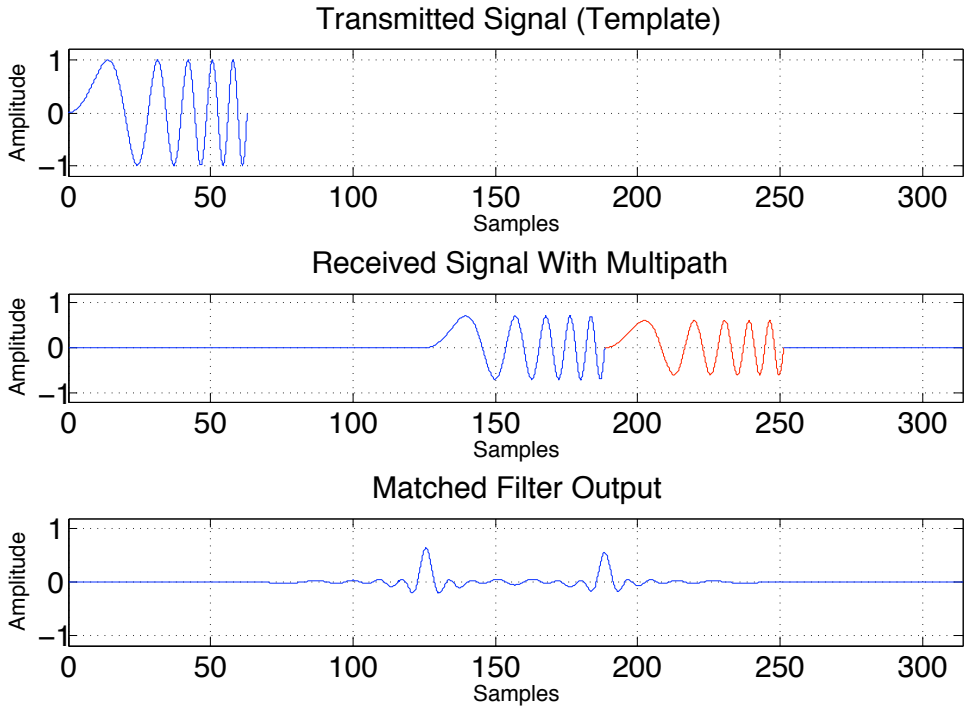

Figure 3.8: Example of a matched filter used to identify a linear frequency chirp signal within a received signal which contains a direct path and a multi-path signal.

The one limitation of employing pulse compression signals is that the electronics required to generate and analyze the signal are more complicated than those required for a simple sine wave. This was a major limitation in the past, but with the advent of digital signal processing and high power micro controllers, these barriers have been removed.

3.2 Analysis of the System Error

The position of the underwater receiver, in the UGPS, is calculated directly from the TDOAs using multilateration. However, for the purpose of describing the errors, the position calculation is separated into three parts. The sources of error, in the position calculation of the receiver, are:

1. Travel-Time Measurement. Errors measuring the precise time at which a signal is received. This error affects the accuracy of the TDOA measurements.

2. Distance Calculation. Errors converting the travel-times, calculated from the TDOAs, into distances.

3. Geometric. Inaccuracy of the calculated receiver position due to the location of the UGPS satellites.

Each of these three factors has an associated error that will degrade the overall system performance. In this section, each error is discussed and quantified in order that the overall performance can be assessed.

3.2.1 Travel-Time Measurement Errors

The travel-time measurement errors affect the TDOA measurement accuracy. The four specific error sources that degrade the travel-time measurement are discussed below. Throughout this section a transmitted signal with a center frequency of 30kHz and a bandwidth of 20kHz will be used to quantify the travel-time measurement errors.

3.2.1.1 Resolving Accuracy of the Matched Filter

The resolving accuracy of a matched filter is the ability to detect the time at which an acoustic signal is acquired at the receiver. As discussed in the previous section, this is related to the bandwidth of the transmitted signal. The accuracy can be explained using direct path and multi-path signals. When the sound travels between the UGPS satellite and the UGPS receiver it will take several paths, as shown in Figure 3.9. The most direct path is a line between the satellite and receiver. Sound, however, is also able to reflect off objects with different densities than the water, for example, the ocean floor or ocean surface. These signals combine at the receiver and affect the resultant travel-time measurement.

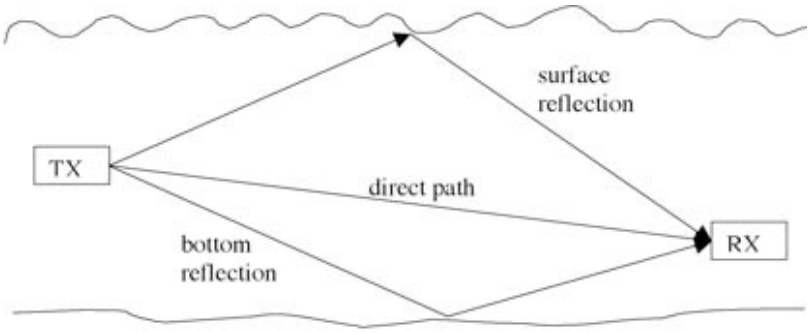

Figure 3.9: Acoustic signals from a transmitter reflect off objects to creating multiple acoustic signals at the receiver (reproduced from [30]).

The matched filter is better able to resolve a direct path signal from a multi-path signal when the signal utilizes more bandwidth; therefore yields a narrower cross-correlation peak. Based on the resolving formula for pulse compression radar, the ability to resolve two signals is equal to the sound velocity divided by the bandwidth of the signal. A signal with a 20kHz bandwidth traveling through water with a sound velocity of $1500 ms^{-1}$ results in a resolution of 7.5cm. This means that the receiver can identify a direct path signal from a multi-path signal if their path lengths are greater than 7.5cm. If the difference in path lengths is less that 7.5cm, then the direct path and multi-path signals are indistinguishable. The resolution of the matched filter will be used as the error estimate.

3.2.1.2 Bias Between satellites and Receiver Clocks

Each of the UGPS satellites are synchronized to Coordinated Universal Time (UTC) using their GPS receivers; therefore, the satellites are synchronized to within $1\mu s$ of each other. It is only the receiver that is not synchronized with the rest of the UGPS. This lack of synchronization would generally be a problem, but because the UGPS uses multilateration to calculate the position of the underwater receiver, the receiver does not have to be synchronized with the satellites. However, Deffenbaugh [31] shows that even though no synchronization is required for multilateration, a time synchronization estimate can improve the accuracy of a multilateration systems. Time synchronization as a means of reducing the error of the UGPS will not be presented in this thesis.

3.2.1.3 Frequency Shift

In a wireless system, it is common for a received signal to experience a frequency shift. In other words, the received signal is a frequency shifted version of the transmitted signal. Sources of frequency error are:

- Doppler shift. Equation 3.3 is used to calculate the magnitude of a Doppler shift.

$$f_{Doppler} = f_0 \left(1 - \frac{v_{s,r}}{c + v_{s,r}}\right) \tag{3.3}$$

  In Equation 3.3, f_0 is the frequency of the transmission, $v_{s,r}$ is the velocity of the source relative to the receiver and c is the velocity of sound in water. Doppler shift occurs when the transmitter and receiver move relative to one another. For example, the Doppler shift for a REMUS 100 AUV traveling at its maximum speed of 2.6ms^{-1} away from a transmitter, emitting a 30KHz acoustic signal, is 52Hz. Sources of Doppler shift are:

  - Relative motion of the receiver and transmitter. Only the component of the velocity of the transmitter in the direction of the receiver contributes to the Doppler shift.
  - Water moving relative to the transmitter and receiver. Since water is the medium in which sound propagates, when the water moves relative to the transmitter and receiver it will produce a Doppler shift.

- Transmitter and receiver clock frequency errors. Crystal oscillators are used as timing sources for the UGPS satellites and receiver. The frequency error of crystal oscillators varies substantially. A worst case estimate of 200 parts per million of error for each of the crystals will be used. Assuming crystal oscillators with 200 parts per million error, the frequency shift of the transmitted 30kHz signal between the transmitter and receiver is 12Hz. This means that when the receiver acquires the 30kHz acoustic signal, it could appear as low as 29988Hz and as high as 30012Hz.

Both the clock error and the Doppler shift produce a frequency shift of the received signal. This frequency shift affects the ability of the matched filter to correctly identify the time at which the signal is received. The Doppler error will be quantified using the following example. The output of a matched filter for a chirp signal with 20kHz bandwidth is shown as the blue line in Figure 3.10. The waveform shown in red is the output of the matched filter when the received signal experiences a Doppler shift.

This frequency shift moves the peak of the matched filter by 18μs. This equates to a distance error of 2.7cm for a sound velocity of 1500ms^{-1}.

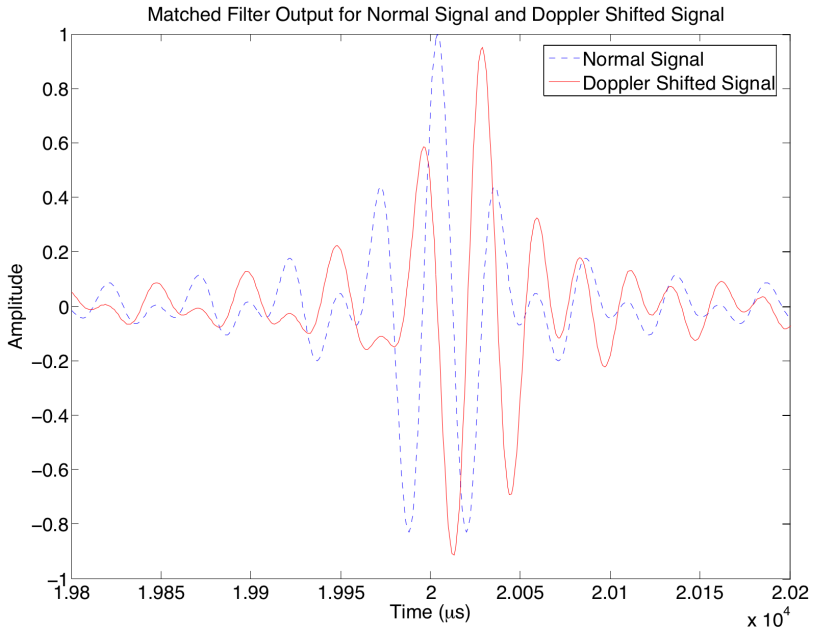

Figure 3.10: The output of a matched filter for a normally received signal (dashed-blue) and a Doppler shifter signal (red).

3.2.1.4 No Signal Reception

Signal loss does not necessarily introduce an error into the system, but it is an important topic for discussion. There are several factors that occasionally make it impossible to measure the travel-time of the acoustic signal. This occurs when the transmitted signal does not reach the receiver due to:

- Burst errors. These are errors due to large acoustic noise sources in the vicinity of the receiver that drown out part, or all, of the transmitted acoustic signal. This type of error can occur because of ships in the area; weather phenomenon such as rain and wind; and ocean phenomenon such as waves and marine life.

- Signal fading. Signal fading primarily occurs in two ways: multi-path signal interaction and shadow zones (caustics). Multi-path signals can interact with the direct path signal in a way that they destructively interfere with each other. The result is a cancellation of the transmitted signal, thereby leaving no signal for the receiver to acquire. Signal fading also occurs because of shadow zones,

which are a result of the environment in which the acoustic signal travels. Varying sound velocities in a water channel cause sound wave refraction. In some cases the sound refracts in such a way that no acoustic signal travels from the transmitter to the receiver. Figure 3.11 shows a submarine in the shadow zone of the surface vessel.

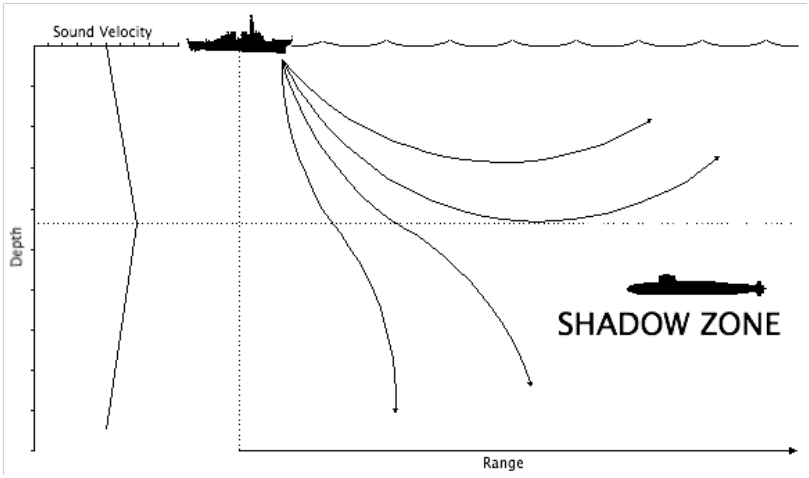

Figure 3.11: Sound refraction causing a shadow zone (reproduced from [32]).

3.2.2 Distance Calculation Errors

The travel-times of the acoustic signals must be converted to distances in order to calculate the position of the receiver. In the conversion from travel-time to distance, several sources of error are present that can ultimately affect the accuracy of the final calculated position of the underwater receiver. Even if the travel-time of the acoustic signal is measured perfectly, the position estimate of the underwater receiver will have some error because the properties of the water are not uniform.

A property of a material is the velocity at which sound will propagate. For example, sound propagates through 20°C dry air at 343.6ms^{-1} and mild steel at ≈5900ms^{-1}. The sound velocity of water changes with the temperature, salinity and pressure, therefore, the sound velocity in a lake or ocean is not constant. As sound travels through water, which has varying sound velocity, the sound is refracted, much like light is refracted as it passes through mediums with different indices of refraction. Because the shortest length between two points is a straight line, when the sound is redirected the path length increases. This increases the path length that the acoustic signal travels. Figure 3.12 shows an exaggerated version of sound refracting as it propagates through water with a positive and negative sound velocity profile

gradient. A positive gradient means that the sound velocity increases with depth.

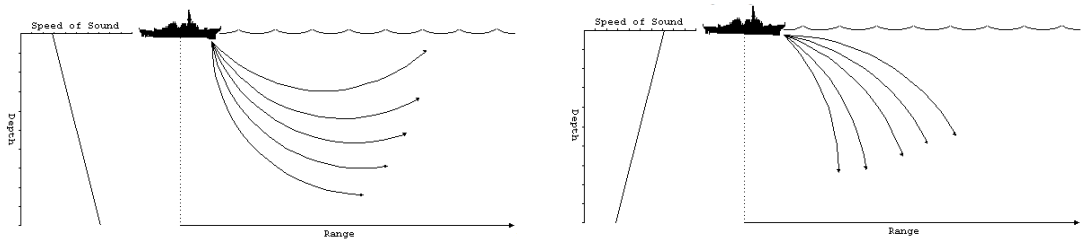

(a) Positive sound velocity profile gradient (b) Negative sound velocity profile gradient

Figure 3.12: Ray bending with positive and negative sound velocity profile gradients (reproduced from [32]).

Errors associated with converting the travel-time of the acoustic signals to distances are related to an accurate knowledge of the sound velocity profile. In general, a sound velocity profile is measured using one of two instruments. The first method directly measures the sound velocity by measuring the time-of-flight of a high frequency acoustic signal over a short distance. The second method indirectly calculates the sound velocity using the pressure, conductivity, and temperature (CTD) of the water. Each manufacturer claims their respective instrument is better, however, in recent years direct-measurement sound velocimeters have become more popular. These sensors measure the sound velocity directly, and have a response time on the order of tens of microseconds. In comparison, the response time of CTDs are in the order of hundreds of milliseconds. The faster response time means that the sensor responds to sharp differences in sound velocity that occur at thermoclines. Thus, the faster response gives a more accurate sound velocity profile.

The following factors affect the accuracy of the sound velocity profile:

- Poor accuracy and resolution of the sound velocity measurement.
- Slow response time in sound velocity and depth sensors.
- Vertical shift of profile (due to incorrect depth measurements).
- Incorrect knowledge of sound velocity (either from old data, or no sound velocity profile).

The following example illustrates the magnitude of the error between a straight line path, which is calculated using the average sound velocity, and a curved path, which is a result of the variation in sound speed. In this example, the sound velocity

profile is a linear positive gradient sound velocity profile starting at the surface with a sound velocity of 1480ms^{-1} and increasing to 1500ms^{-1} at 100m. The two endpoint values are taken from a sound velocity profile of Saanich Inlet in April 2001. Figure 3.13 shows the direct path and curved path for a signal with a time-of-flight of 1 second. For the direct path signal, the average sound velocity was used to calculate the range. The curved path is calculated using a Bellhop model as implemented in the Acoustic Toolbox, written by HLS Research [33]. Note that the scales for the x-axis and y-axis on the graph are different, therefore, the curved path appears exaggerated.

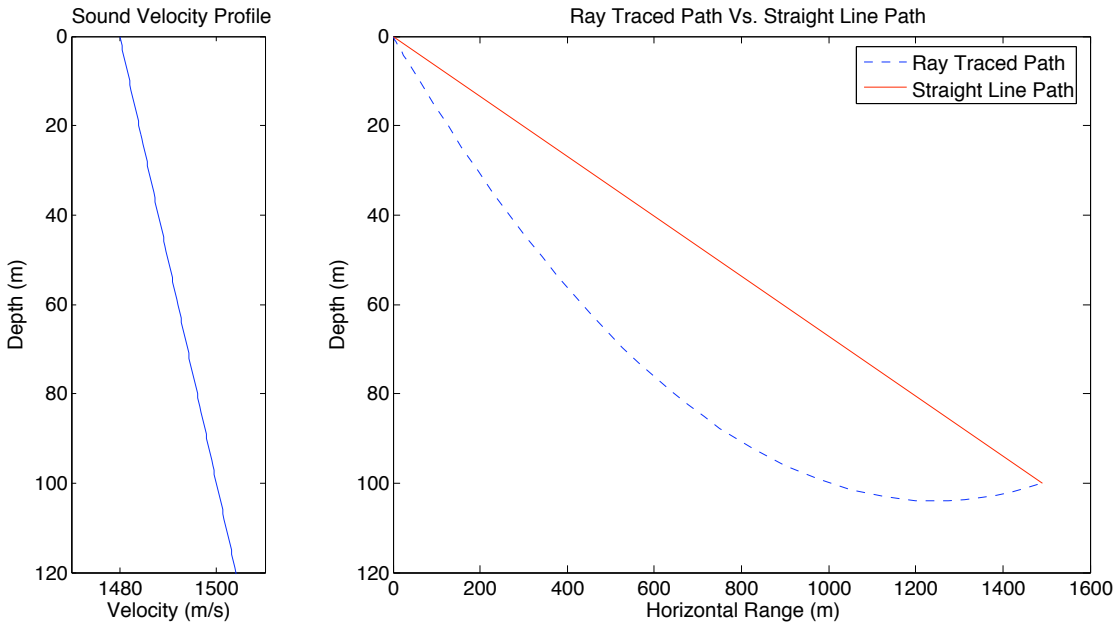

Figure 3.13: Curved path due to the variation in sound speed vs. a straight line path calculated using the average sound speed.

For a time-of-flight of 1 second, the position error between the direct path and the curved path due to the change in sound velocity is 2.46 meters, or 0.16% of the slant range.

3.2.3 Geometric Error

3.2.3.1 Transmitter Position Error

The position error of each satellite in the UGPS directly affects the position calculation of the UGPS receiver. The position of the UGPS satellites are measured using Garmin brand GPS units with position accuracies of <3m 95% of the time, when a fix with the Wide Area Augmentation System (WAAS) is available. An error of 3m

95% of the time means that the output of the GPS unit will be accurate to within 3m 95% (2 standard deviations) or 1.5m 68% (1 standard deviation) of the time.

3.2.3.2 Dilution of Precision

The geometric error is not a product of errors in timing measurement or converting that time to distance. Geometric errors are a result of the physical locations of the UGPS satellites relative to the receiver. The best horizontal position solution is present when the distance between the UGPS satellites is maximized. This holds true for terrestrial GPS systems as well. Dilution of precision (DOP) is a term used to describe the error due to the geometry of the system. In the terrestrial GPS, the DOP is separated into horizontal dilution of precision (HDOP), vertical dilution of precision (VDOP), position dilution of precision (PDOP) which combines HDOP and VDOP, and time dilution of precision (TDOP). Most handheld GPS units provide the DOP information to the user so that they can determine how favorable the satellite geometry is at any time.

For the UGPS, DOP will be used to show the standard deviation of the position solution for the various locations of the receiver within the vicinity of the UGPS satellites. Alcover [34] and Deffenbaugh [31] present a means of calculating the lower bound of the position error for trilateration and multilateration problems using the Cramér-Rao bounds. This method has been sufficiently covered in these two sources, and will not be repeated in this thesis. The method discussed by Deffenbaugh will be used in the following example to show the lower bound of the horizontal position error (HDOP) of the UGPS receiver. A UGPS system is established with three satellites placed 1500m apart. The distance calculation errors between each UGPS satellite and the UGPS receiver are assumed to be independently identically distributed Gaussian random variables with zero means and standard deviations equal to 1m. The map of the HDOP, for a receiver at a depth of 100m, is shown in Figure 3.14. The black circles indicate the location of the UGPS satellites. The figure shows contour lines labelled with the standard deviations. For example, on the contour lines labelled 1, the standard deviation of the error is 1m. That is, the accuracy of the calculated position of the UGPS receiver is within 1m 68% of the time.

Figure 3.14 shows the error of the position calculation given a distance error of 1m. A value of 1m was chosen so that the HDOP can be used as a scaling factor for the actual distance calculation error. For example, if the distance calculation error is 0.5m then the calculated receiver position error will be 0.5m when the receiver is at a location where the HDOP from Figure 3.14 is 1.

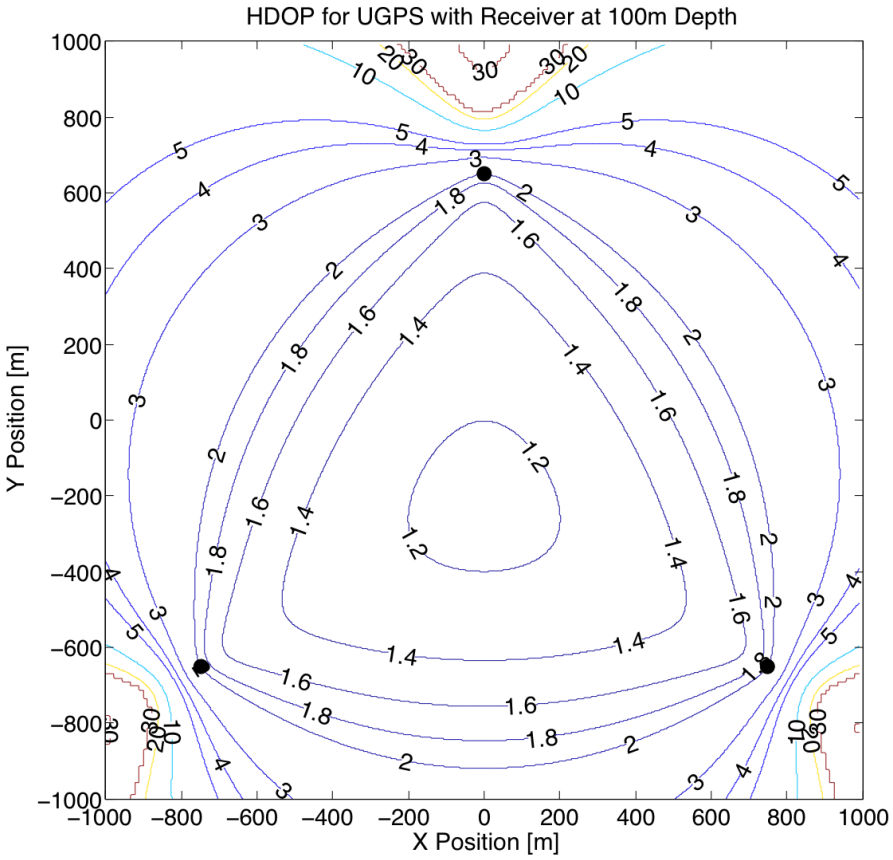

Figure 3.14: Horizontal dilution of precision as a function of receiver location.

The operating area of the UGPS will be limited to the area outlined by the baselines of the three satellites. From Figure 3.14, the HDOP within this area is less than 2.

3.2.4 Summary of Error Sources

In section 3.2, the errors that contribute to the overall accuracy of the UGPS are identified. These errors were separated into three categories: travel-time measurement, distance calculation, and geometric. The errors were discussed as a means of determining the largest sources of errors in the UGPS, so that these errors can be minimized. Table 3.2 summarizes the error sources discussed.

The calculated position error sources, in order of largest to smallest, are:

- Distance calculation error, which is the error introduced by assuming that the sound travels in a straight path between the satellite and the receiver. This error can be reduced using a sound velocity meter to measure the sound velocity

Table 3.2: Summary of UGPS error sources.

Error Source	Description of Error	Magnitude
Travel-Time Measurement Errors	Resolving Accuracy of Matched Filter	0.075 m
	Bias Between satellite and Receiver Clocks	-
	Frequency Shift	0.027m
	No Signal Reception	-
Distance Calculation Errors	Assumption that the sound velocity is constant	2.46 m
Geometric Errors	Satellite Position Error	1.5m (1σ)
	Dilution of Precision	total distance error x 2 (1σ)

profile and applying a ray tracing algorithm to calculate the propagation path.

- The geometry of the UGPS satellites produces a dilution of precision. This error could be decreased by applying a time synchronization technique, as described by Deffenbaugh [31]. Additional UGPS satellites could also be added to provide redundancy to the position solution and thereby reduce the position error.

- The position of the UGPS satellites. The position is determined using a consumer grade GPS module with a position accuracy of 1.5m. To decrease this, a survey grade GPS could be used to reduce the position error to <0.5m.

- Travel-time measurement errors. These errors are an order of magnitude less than the other errors, therefore, they are negligible relative to the other errors. These errors could be reduced by increasing the bandwidth of the transmitted signal, purchasing higher quality clock sources with less frequency deviation, and applying an algorithm in the receiver to correct for a doppler shift in the signal.

3.3 Chapter Summary

Trilateration and multilateration were presented as methods of calculating the position of an underwater receiver, given distances between the receiver and several acoustic satellites. Trilateration is widely used in positioning systems; unfortunately,

it either requires bidirectional data transmission or time synchronization between the satellites and receiver. Multilateration was presented as an alternative method of calculating the position of a receiver, without requiring bidirectional data transmission or time synchronization between the satellites and receiver; however, receiver position accuracy is not as good as with trilateration.

The matched filter was used to identify the received signals from the satellites and assign a time of reception to these signals. Pulse compression was presented as a technique that reduces the impact of multi-path interference, generates high signal-to-noise ratios, and provides good range resolution.

The sources of error that degrade the accuracy of the UGPS position calculation were presented. These errors were separated into three groups: travel-time measurement, distance calculation, and geometric errors. The largest error source of the proposed UGPS is the distance calculation error resulting from incomplete knowledge of the water's sound velocity profile. This could be virtually eliminated using a sound velocity meter to measure the sound velocity profile and applying a ray tracing algorithm to calculate the propagation path. Another significant error that could be reduced is the satellite position error. This error is a result of using low-cost GPS receivers in each satellite. The error could be reduced from 1.5m to <0.5m by upgrading to survey-grade GPS receivers.

In the next chapter, a test system will be presented that was built to quantify the theoretical errors that were calculated in this chapter. A model of the test system was also developed to simulate the results of experimental test thereby reducing the time and cost of performing experimental tests.

Chapter 4

Description of the UGPS Model and Experimental Apparatus

A test system has been designed and implemented to experimentally evaluate the efficacy of the UGPS concept. In addition, a model of the experimental system has been developed. A model of the test system affords the following benefits:

- Prediction of acoustic signal behavior.
- Testing of alternative signals and, as an extension, processing algorithms for those signals.
- Algorithm comparison under identical operating conditions; something that is very difficult to achieve in a real-world environment.
- Inexpensive method of testing a complex system.

One disadvantage of the model, however, is the inability to completely represent real ocean environments. An ocean is a complex and dynamic environment; therefore, the best way to fully evaluate a system is to experimentally test that system in a real-world environment.

In this chapter, both the experimental apparatus and model are presented.

4.1 Description of the Experimental Apparatus

The test system was designed and built to verify the UGPS concept. The main components of the test system, and their functionality, are described below and illustrated in Figure 4.1:

1. UGPS satellite. Emits an acoustic signal that has been preprogrammed into the satellite's computer. This can be any signal within the 18-55kHz frequency band.

2. UGPS receiver. Acquires the acoustic signal transmitted by the UGPS satellite and converts this signal to a voltage.

3. Surface station. Digitizes the voltage from the UGPS receiver and logs this data for post-processing.

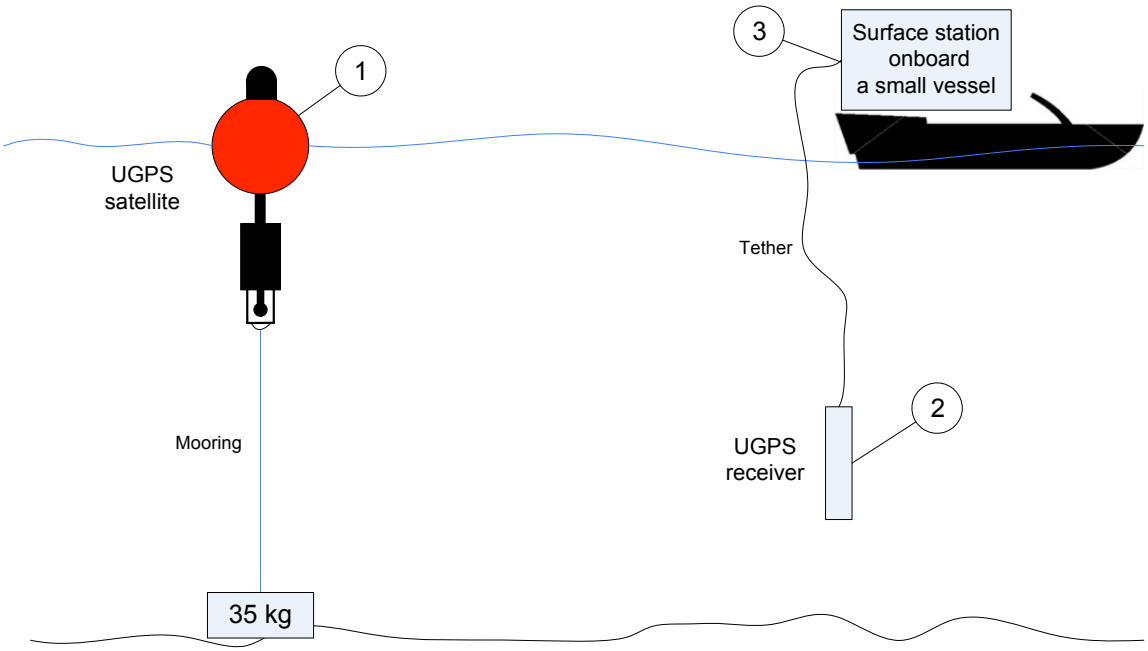

Figure 4.1: Test setup showing the UGPS satellite (1), UGPS receiver (2) and the surface station (3).

4.1.1 UGPS Satellite

The UGPS satellite was designed to fulfill the following criteria:

- Flexibility: ability to transmit a variety of preprogrammed acoustic signals within the 18-55kHz frequency band. This frequency band was chosen because it encompasses two commonly used bands in USBL and LBL positioning system.
- Synchronization: synchronization of the UGPS satellite with the UGPS receiver so that ranging can be performed.
- Physical Size: sufficiently compact and light weight (<20kg) to be easily deployed by one person from a small vessel.
- Deployment: quickly and easily deployable, with minimal setup in the field. Have the ability to float freely, but also be moored when required.
- Range: projector amplitude large enough to allow the acoustic signal to be received 1km away.
- Positioning: able to determine and log its position within 3 meters at the moment the acoustic signal is emitted.
- Battery Life: 5 hour run time.

The above specifications led to the design of the UGPS satellite. The external and internal design of the satellite is shown in Figures 4.2 and 4.3 respectively. These figures show the location and functionality of the major components. Additional photographs of the UGPS satellite are included in Appendix A.1.1.

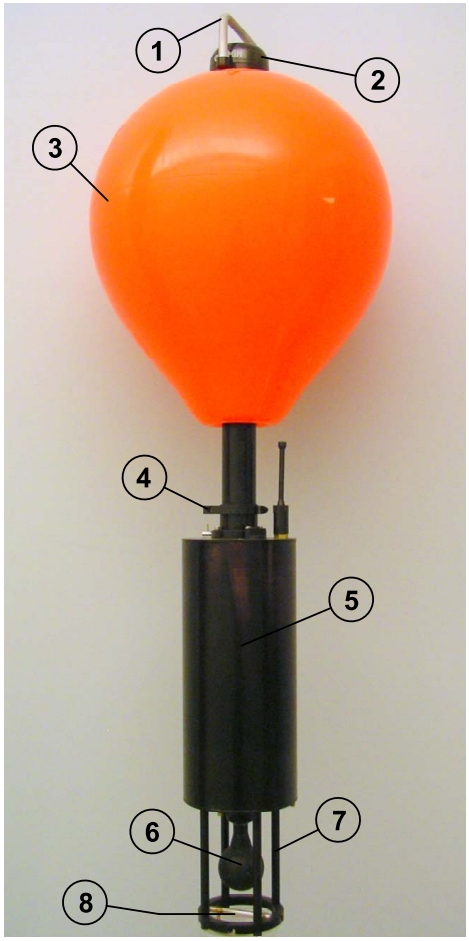

	Description	Function
1	Recovery handle	A convenient location above the water line to grasp when recovering and deploying the satellite.
2	Garmin GPS 16-HVS	Provides position and timing information to the computer inside the satellite. The GPS is electrically connected to the pressure housing with an 8 pin Subconn MCBH8F connector inside the float.
3	Float	Provides 55kg of buoyancy. Bright color is visible on the water making recovery of the satellite easier.
4	Quick release handle	Used to separate the float, GPS, and wireless Ethernet adapter from the pressure housing. Separating the upper and lower half of the satellite facilitates transport.
5	Pressure housing	Watertight aluminum housing, with black hardcoat anodizing. The pressure housing is 40cm long and 17cm in diameter.
6	Acoustic projector	ITC-1032 omnidirectional piezoelectric acoustic transducer.
7	Projector cage	Protects the projector from damage.
8	D-ring	Provides an attachment point at the bottom of the satellite that can be used for mooring.

Figure 4.2: Photograph of the UGPS satellite in its fully assembled pre-deployment state.

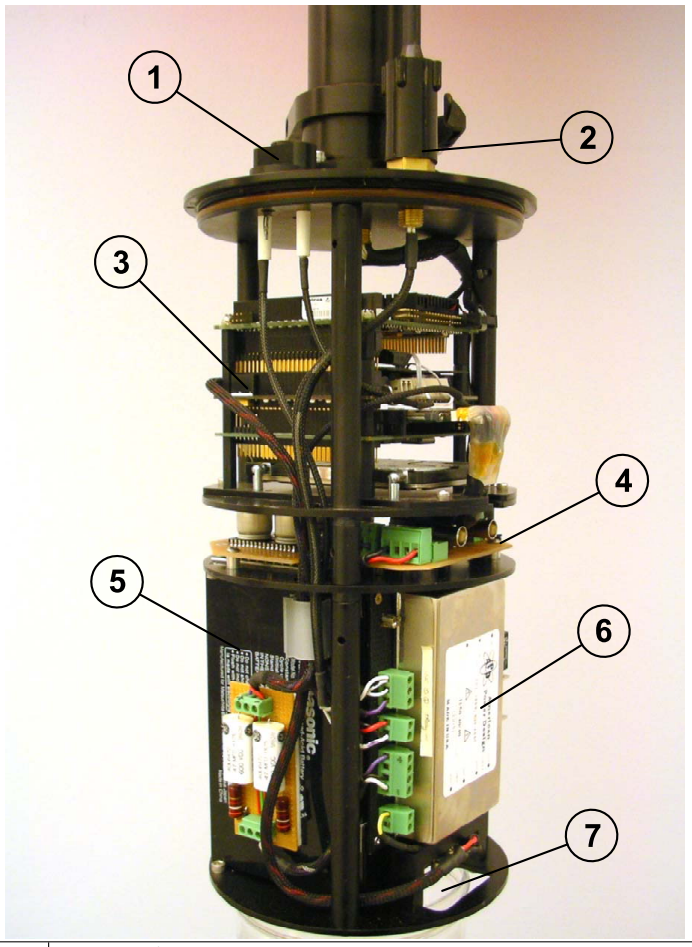

	Description	Function
1	ON/OFF Switch	Magnetically coupled switch used to turn the satellite on and off.
2	Charging connector (Subconn MCBH2F)	Wetmate underwater connector for charging the battery in the satellite. The charging circuit is contained inside the satellite so an applied voltage between 6-40VDC will both power the satellite and charge the battery.
3	Computer	PC-104 computer with NI DAQ card used to acquire and log the GPS position of the satellite and received acoustic signals. See Appendix A.1.2 for a detailed list of components.
4	Projector amplifier board	Custom amplifier used to drive the acoustic projector. The analog voltage output from the DAQ card is input to this board where it is amplified to drive the acoustic projector.
5	Battery (LC-RA1212P)	12V, 12Ahr lead acid battery used to power the satellite.
6	DCDC	Converts the 12V battery voltage to ±40VDC used to drive the acoustic projector.
7	Projector chassis connector	Blind mate connector allowing the projector to remain mounted to the pressure housing while the internal chassis is removed.

Figure 4.3: Photograph of the interior of the UGPS satellite chassis and system components.

4.1.1.1 UGPS Satellite Software

The functionality of the UGPS satellite is controlled with the graphical user interface (GUI) software running on the computer in the satellite. This software was written in LabVIEW because of its inherent ability to control data acquisition hardware, visually display information, and easily analyze acquired data.

Using the GUI, a user can load a file into memory containing the signal the user wants to transmit. The software synchronizes the computer with UTC time provided by the GPS unit and, at the requested time, outputs the loaded signal, via the analog output card to the projector amplifier. The signal is then amplified and transformed into an acoustic wave by the projector. At the instant the acoustic wave is generated, the software also logs the GPS position of the satellite.

The graphical user interface, shown in Figure 4.4, has 5 interfaces(tabs) with the following functions:

- Communication Setup: setup the EIA-232 communications interface for the Garmin GPS unit.
- Log File Setup: setup the names and location to save the log files created for the GPS position data. The position data from the GPS is constantly logged so that the position of the satellite is known at the instant an acoustic signal is transmitted.
- Waveform Setup: allows a user to load a voltage waveform from a file. This waveform is the signal that the user wishes to transmit acoustically.
- DAQ Setup: setup the data acquisition card functions. The DAQ card is used to output the voltage waveform to the projector amplifier, which in turn drives the acoustic projector.
- GPS Status: displays the real time position of the satellite.

Additional screen shots showing more detail of the graphical user interface are included in Appendix A.1.3.

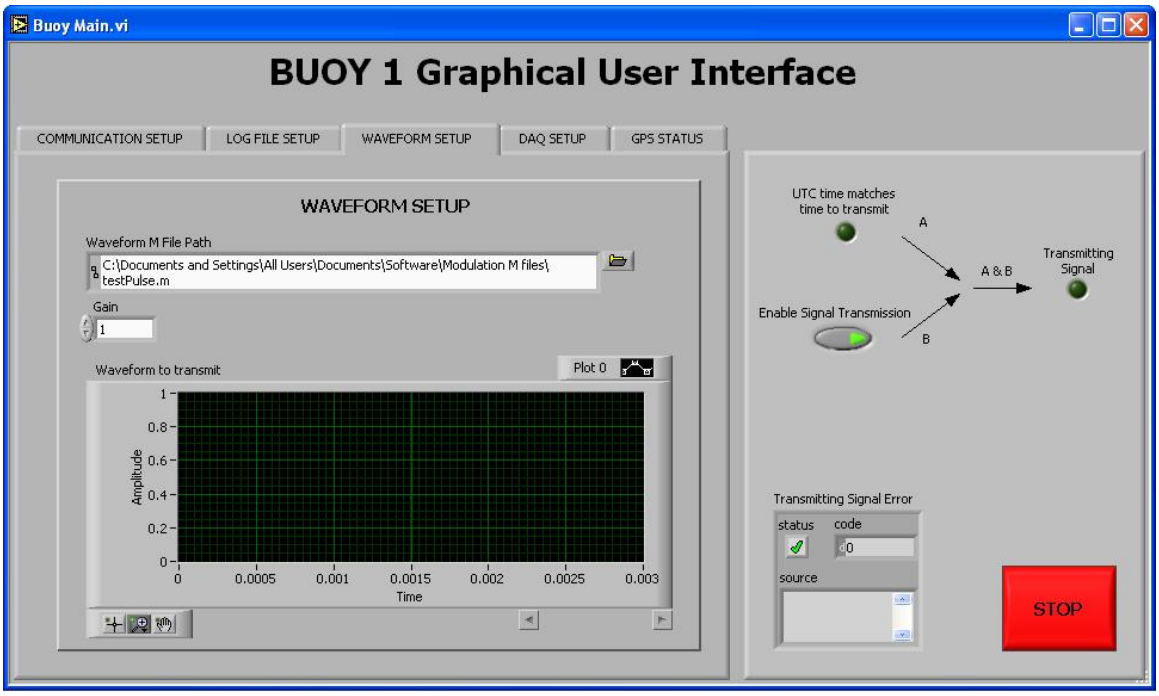

Figure 4.4: Graphical user interface of the UGPS satellite.

4.1.2 UGPS Receiver

The UGPS receiver was designed to fulfill the following criteria:

- Receive Acoustic Signals: convert acoustic pressure waves transmitted by the UGPS satellite into electrical signals that can be digitized and logged using a standard computer.
- Amplify: amplify a received signal to a large enough level to be digitized using off the shelf data acquisition hardware.
- Synchronization: synchronization of the UGPS receiver with the UGPS satellite so that ranging can be performed.
- Positioning: ability to sense its depth in the water column to within ±10cm.
- Physical Size: easily manageable from onboard a small vessel.
- Deployment: mounting hardware to hang the receiver from a lift line.
- Depth rating: able to operate at a depth of 30m.
- Battery Life: 5 hour run time.

The specification led to the design of the UGPS receiver. The external and internal design of the receiver is shown in Figures 4.5 and 4.6 respectively. These figures show the location and functionality of the major components.

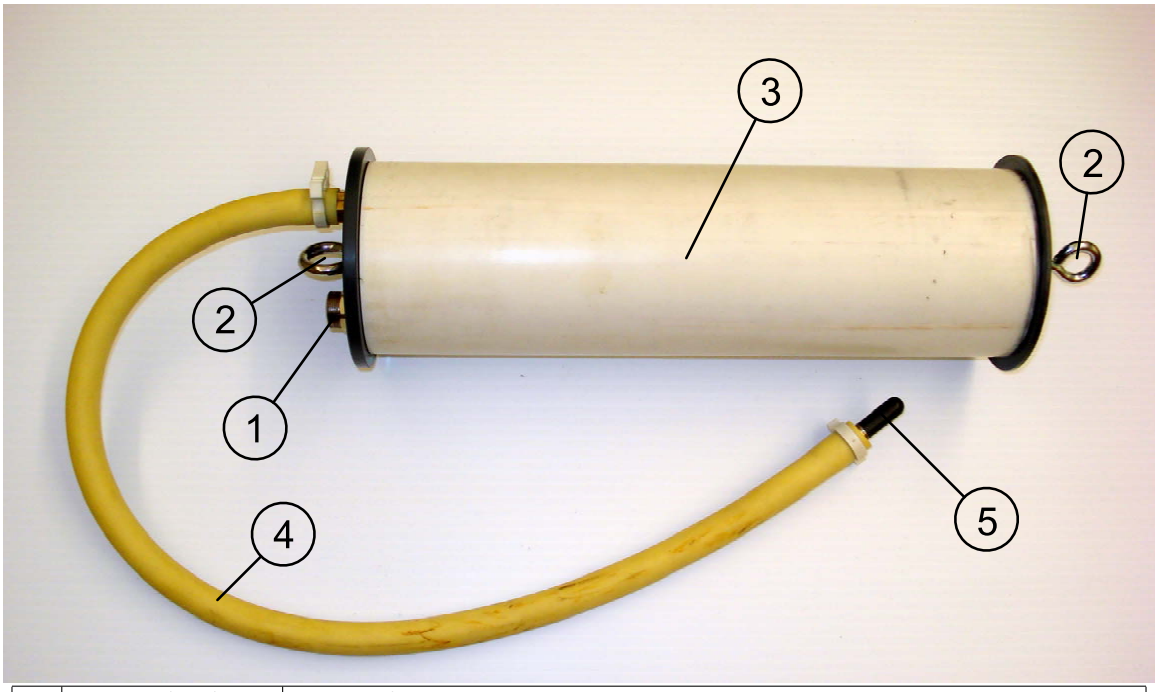

	Description	Function
1	Underwater connector	Connects the UGPS receiver to the surface support station via a 30 meter 4 conductor tether. The four conductors are used to transmit the amplified hydrophone voltage as well as the analog voltage from the pressure sensor.
2	Tether mounting hardware	Provides attachment points to strain relief the tether and also attach lift lines.
3	Enclosure	Depth rated to 30m and made of PVC for its low cost and ease of manufacturing. The enclosure is 30cm long and 10cm in diameter.
4	Hydrophone extension	Extends the hydrophone away from the flat surfaces on the enclosure. In early tests it was noted that when the hydrophone was mounted directly in the flat endcap an acoustic signal would reflect off the endcap and create noisier data. The addition of the extension eliminated this problem.
5	Hydrophone	Reson TC4013 miniature hydrophone. This reference hydrophone was chosen for its flat frequency response over the frequency range used for this test system.

Figure 4.5: Photograph of the exterior of the UGPS receiver.

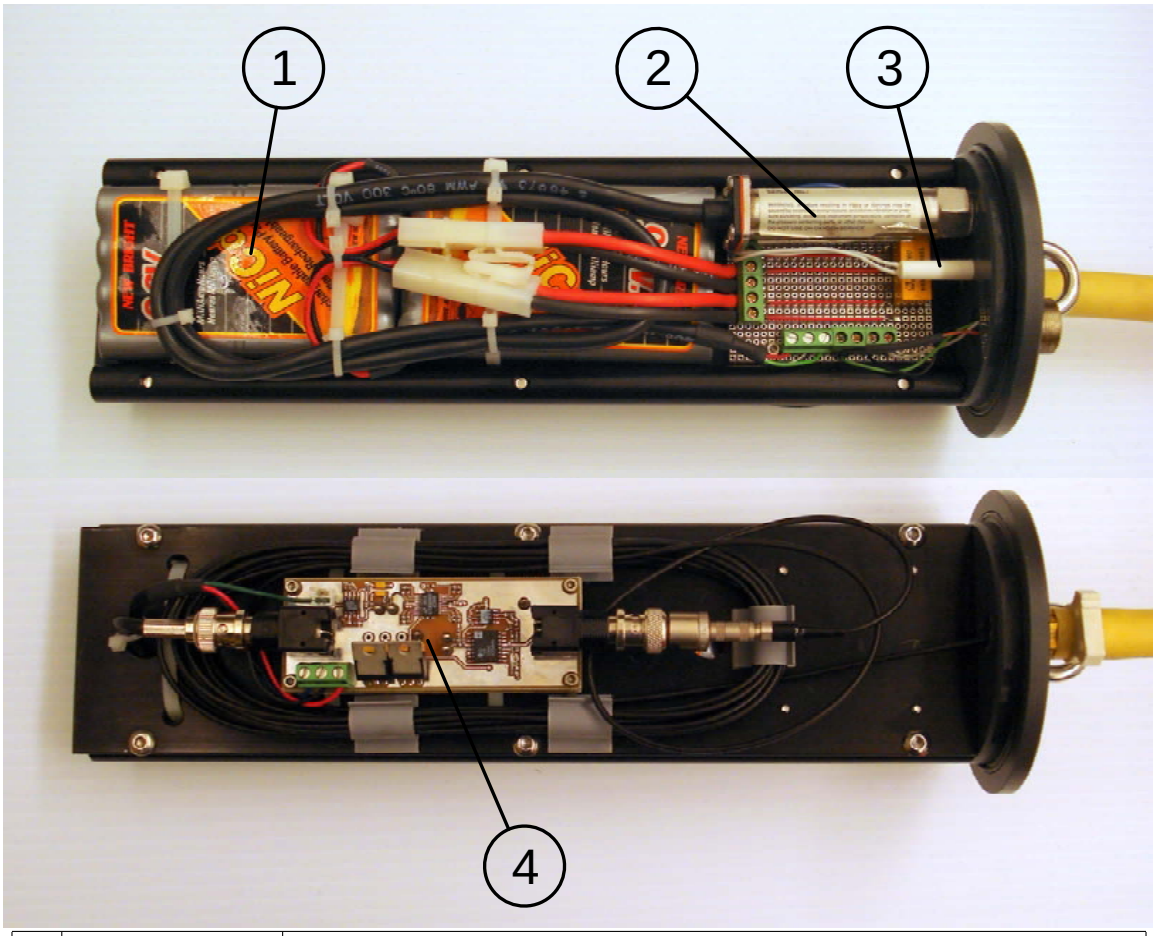

	Description	Function
1	Batteries	Two 9V NiMH batteries used to provide ±9V to power the hydrophone amplifier and pressure sensor.
2	Pressure sensor	Omega PX603 analog output pressure sensor. This pressure sensor measures the depth of the UGPS receiver.
3	Magnetic reed switch	Magnetically coupled switch used to turn the UGPS receiver on and off.
4	Hydrophone amplifier/filter	Custom hydrophone amplifier and filter module. Amplifies the very small charge output from the piezo hydrophone so that it can be transmitted through the tether and digitized by the surface support computer.

Figure 4.6: Photograph of the UGPS receiver chassis. The top picture shows one side of the chassis tray and the bottom picture shows the other side.

4.1.2.1 UGPS Receiver Hydrophone Amplifier

The UGPS receiver uses a hydrophone to convert the pressure waves (sound) in the water into a voltage that can be digitized and input to a computer for analysis. A pressure is converted by the hydrophone to a small electrical charge. This small charge is applied to the hydrophone amplifier which both amplifies the signal and filters out unwanted frequencies. Figure 4.7 illustrates the functional blocks of the custom hydrophone amplifier in the UGPS receiver.

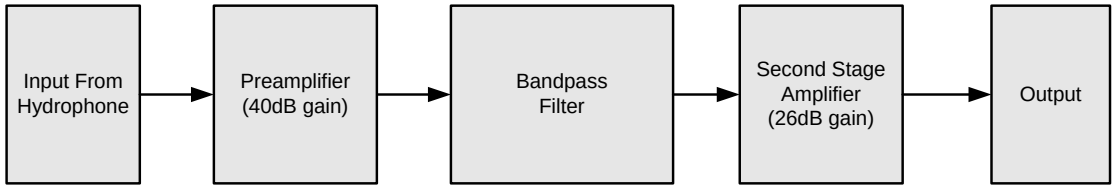

Figure 4.7: Block diagram showing the flow of an analog signal through the hydrophone amplifier.

The hydrophone is a piezo electric device and, therefore, outputs a charge proportional to the strain applied to the piezo electric element. A high-impedance voltage amplifier is used as a pre-amplifier to boost the hydrophone signal by 40dB. A high-impedance amplifier is required because a hydrophone has a high output impedance which, if connected to an amplifier with a lower impedance, would result in an attenuated signal. Typically, a charge amplifier is used to amplify the output of a piezo electric element, however, it is more common to use voltage amplifiers with hydrophones. The calibration data provided by a hydrophone manufacturer is stated in dB referenced to 1V/uPa; this means the voltage produced by the hydrophone is directly related to the applied pressure. A voltage amplifier preserves the pressure to voltage relationship, therefore, even after amplifying the hydrophone signal with a voltage amplifier, the signal still relates directly to the pressure applied to the hydrophone.

After the pre-amplification, the signal is filtered, using a bandpass filter. The filter removes the low frequency audible signals, that are not of interest in this system, and the high frequency signals that cause aliasing when digitizing the signal. Finally, the voltage signal is amplified a further 26dB before it is output. The combination of the pre-amplifier, filter and second amplifier result in an output with the frequency response shown in Figure 4.8.

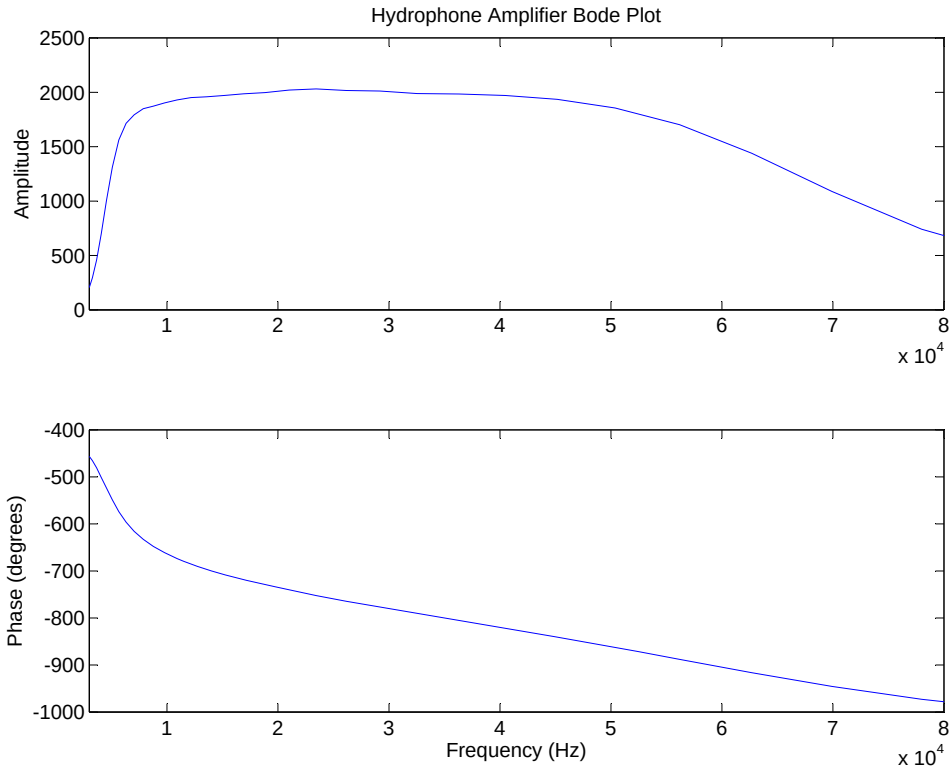

Figure 4.8: Frequency response of the hydrophone amplifier depicted in a Bode plot.

4.1.3 Surface Station

The surface station is comprised of a PC computer, residing on the boat, that is electrically attached to the UGPS receiver via a tether. The surface station digitizes the analog voltages from the UGPS receiver and logs these voltages for post-processing. Employing a GPS receiver, the surface station is synchronized to UTC. The UGPS satellite and surface station are synchronized to UTC using GPS receivers, therefore the logged data from the UGPS receiver and satellite are time synchronized.

The surface station computer is a Shuttle brand PC, with a National Instruments PCI-6251 data acquisition card and a Garmin 16-HVS GPS receiver. As with the UGPS satellite, the surface station runs Windows XP with a LabVIEW application for its graphical user interface.

4.1.3.1 Surface Station Software

The surface station GUI is used to control the data acquisition card and to log the incoming signals from the UGPS receiver. The graphical user interface, shown in Figure 4.4, has 8 interfaces(tabs) with the following functions:

- Communication Setup: setup the EIA-232 communications interface for the Garmin GPS unit.
- Log File Setup: setup the names and location to save the log files created for the GPS position data, pressure sensor voltage, and hydrophone amplifier voltage.
- DAQ Setup: setup the data acquisition card functions. The DAQ card is used to digitize the two voltages from the UGPS receiver, ie. the pressure sensor voltage and the voltage from the hydrophone amplifier.
- Pressure Setup: setup the scale and offset of the voltage received from the pressure sensor in the UGPS receiver to convert the raw voltage into a depth.
- GPS Status: displays the real time position of the GPS unit connected to the computer.
- Received Signal: a graph of the received signal which provides the operator with visual confirmation that a signal has been received.
- Cross Correlation: cross correlates the received signal with a template of the transmitted signal that is loaded from a file. This allows the operator to verify, in real time, that not only has a signal been received, but that it is the expected signal.
- Frequency Analysis: displays the power spectrum of the received signal. This was used to monitor the frequency components of other sources of noise present in the received signal.

Additional screen shots showing more detail of the graphical user interface are included in Appendix A.2.1.

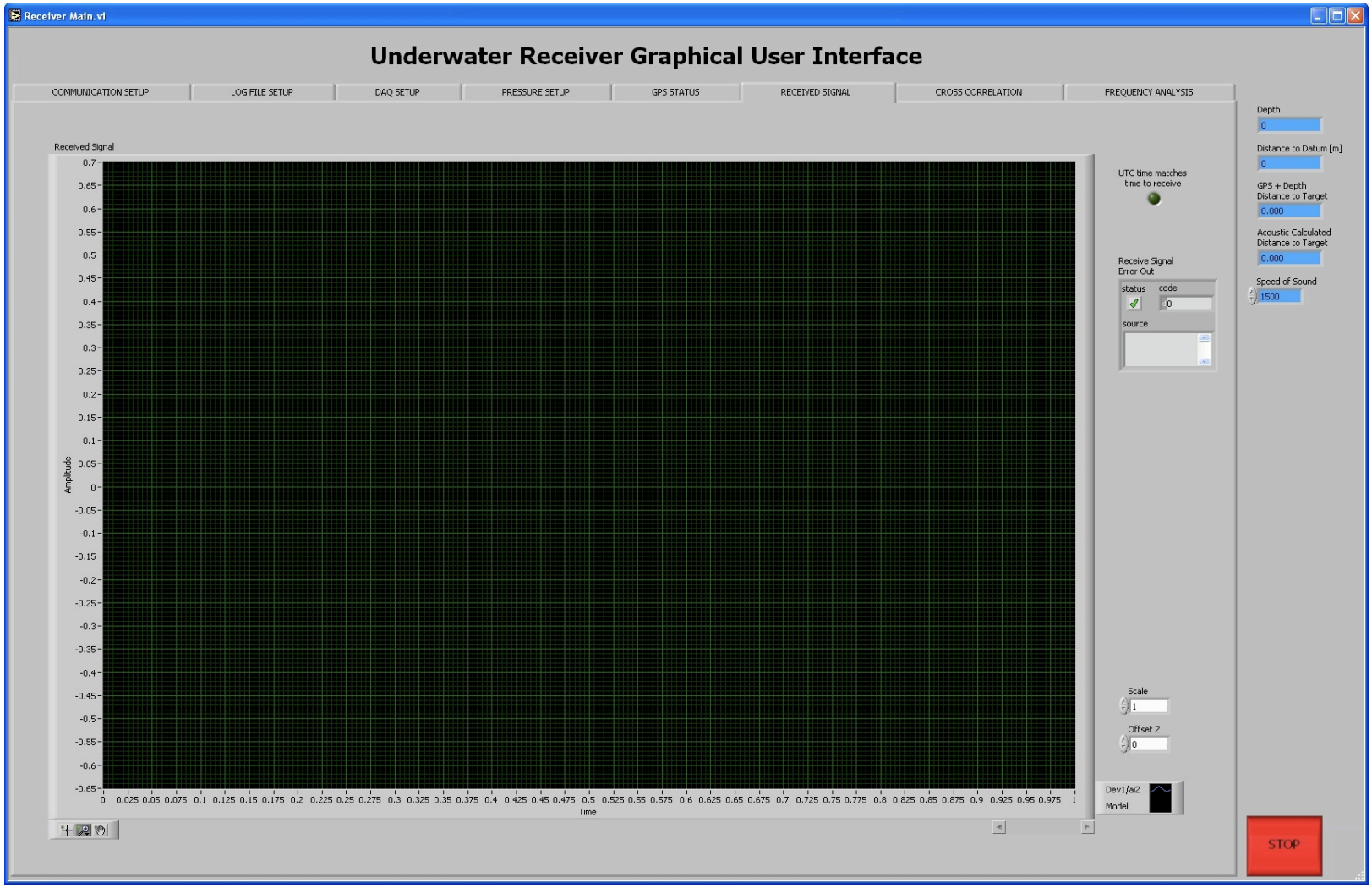

Figure 4.9: Graphical user interface of the surface support computer. Through the use of this GUI, a user controls the functions of the UGPS receiver.

4.2 Modeling the UGPS

An analytical model of the UGPS test system was created and employed to perform an initial assessment of the system's behavior. The model has 9 components; each component representing a key functional element. The propagation of signals through the 9 components of model, illustrated in Figure 4.10, recreates the flow of signals through the UGPS test system.

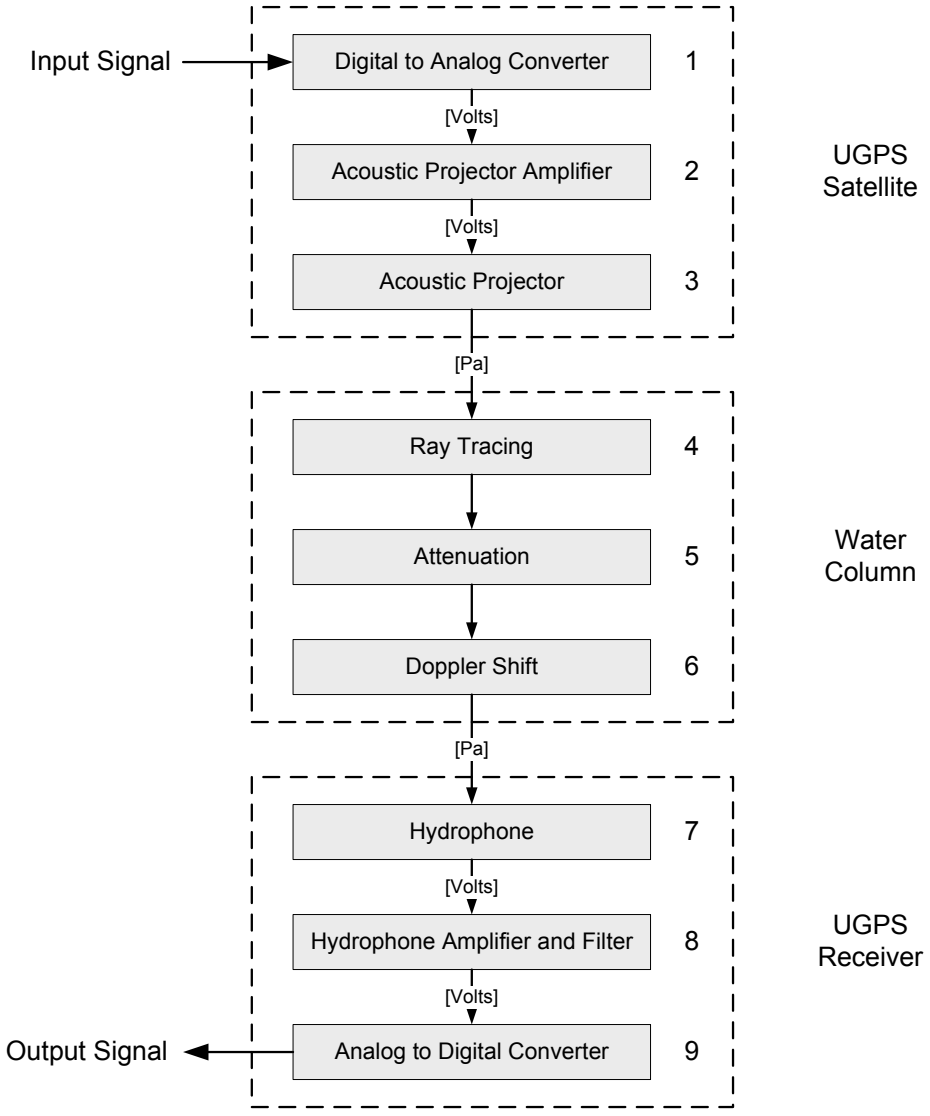

Figure 4.10: Diagram of signal propagation in the model.

The first three elements of the model represent the key components of the UGPS satellite, which transmits acoustic signals to the underwater receiver. The next three

components model the interaction of the acoustic waves with the water. Finally, the last three components model the UGPS receiver. The 9 blocks in Figure 4.10 are each modeled independently and then combined to make a complete model of the system. By modeling each component separately the model is generic and, therefore, still useful if any of the components are replaced. In this section, the generation of the 9 model components will be discussed. The sub-section title for each of the 9 components is labelled with the component number. For example, the digital to analog converter in the UGPS satellite is the first of the nine modeled components, therefore it is labelled (1 of 9). All of the model code is included in Appendix D.

4.2.1 UGPS Satellite

The satellite is the surface component of the UGPS and transmits acoustic signals to the underwater receiver. The model of the satellite is presented in three parts:

- Digital to analog converter (D/A). Converts the digital representation of the transmitted signal to an analog voltage.
- Acoustic projector amplifier. Amplifies the analog voltage from the D/A to drive the acoustic projector.
- Acoustic projector. The amplified voltage is applied to the acoustic projector which converts the amplified voltage waveform into a pressure wave.

4.2.1.1 Digital to Analog Converter (Model Component 1 of 9)

The first component of the UGPS model is the digital to analog converter (D/A) in the UGPS satellite. The D/A converts the digital representation of the transmitted signal to an analog voltage. There are two parts of the D/A converter that must be modeled: the sampling rate and the quantization. The sampling rate is the rate at which the digital to analog converter can output different voltages. Sampling rate is usually expressed in terms of the number of samples per second (S/s) that can be output. Quantization is a measure of the smallest voltage change that the digital to analog converter can produce.

It is important to note that there are other variables affecting the digital to analog conversion process that could be modeled such as the system noise, accuracy due to temperature drift, settling time, gain error, and clock drift. Assuming the D/A has been calibrated within the last year, these variables only contribute several hundred μV of error to the system [35]. These errors are small in comparison to the error from

the sampling rate and quantization. Therefore, the contribution to the D/A error from these factors will not be modeled.

Sampling Rate

The D/A model resamples the input waveform to the sampling frequency of the D/A. This is done using the MATLAB resample function. The resample function uses a weighted sum of points from the input signal to generate data at the output sampling rate. Figure 4.11 shows a linear frequency sweep from 0Hz to 100kHz that has been sampled at 2MS/s and then resampled at 200kS/s.

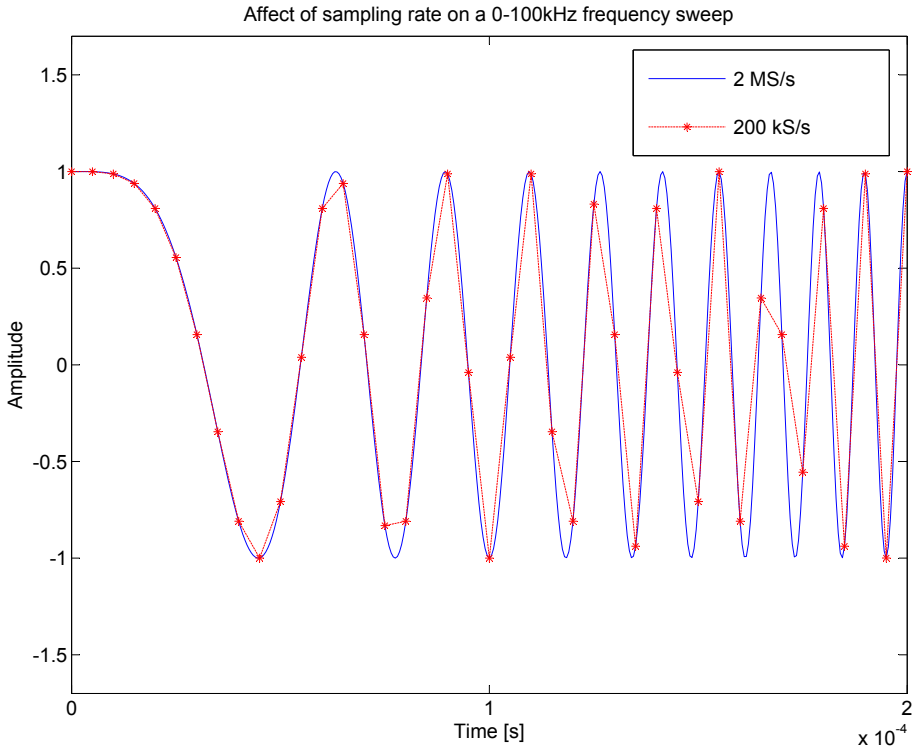

Figure 4.11: Affect of sampling rate on a 0-100kHz frequency sweep.

The sampling rate of the digital to analog converter has a dramatic effect on the output signal. Although the basic waveform is still present, a low sampling rate distorts the waveform. A sampling frequency that is less than one half the highest frequency within the transmitted signal violates the Nyquist-Shannon sampling criteria. This results in aliasing of the signal. The sampling frequency, therefore, sets a limit for the frequency of the transmitted signal. For this model, the signal is sampled at 200kS/s, therefore, the frequency limit of the transmitted signal is 100kHz.

Quantization

Quantization, of the resampled signal, by the D/A converter results in discrete output voltage steps. The model quantizes the signal by first limiting the input signal to the upper and lower limits of the D/A converter and then rounding the input signal to the closest multiple of the resolution. The resolution of the D/A in the test system is 12 bits over the voltage range of ± 10V. The resolution is calculated using Equation 4.1. In Equation 4.1, maxVoltage and minVoltage are the maximum and minimum voltage limits of the D/A converter. N is equal to the resolution of the D/A converter (in bits) and is calculated as 4.884mV.

$$resolution = \frac{maxVoltage - minVoltage}{2^N - 1} \tag{4.1}$$

Figure 4.12 shows a linear frequency sweep from 0-50kHz that has been quantized using the upper and lower limits and the resolution of the D/A.

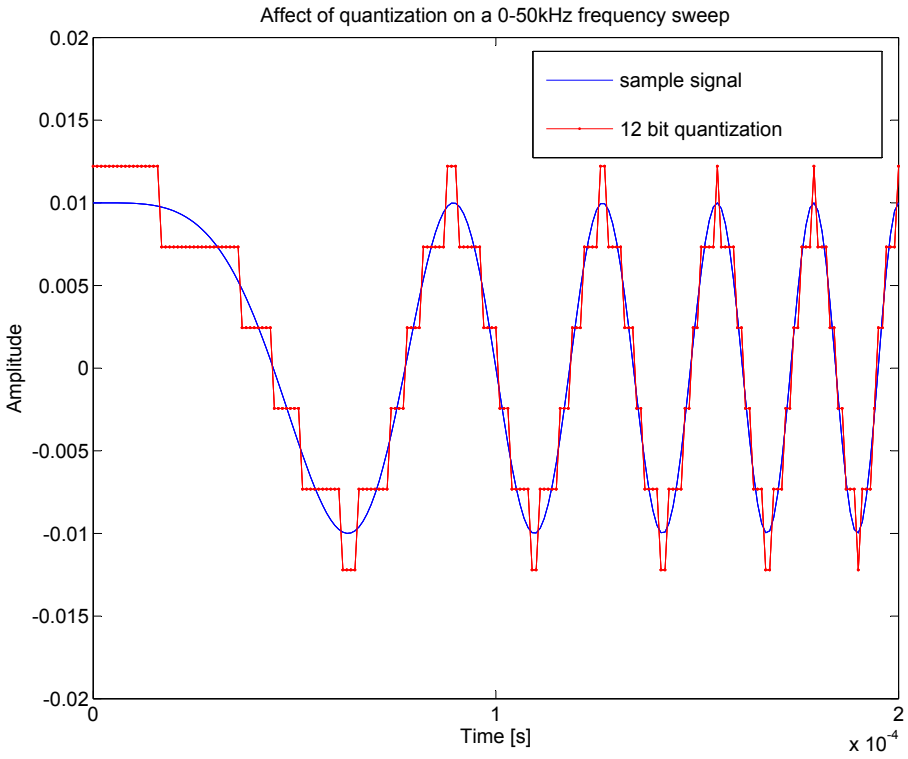

Figure 4.12: Affect of quantization on a 0-50kHz frequency sweep.

Unlike the sampling rate, which affects large and small amplitude signals equally, the negative effect of quantization is most noticeable on signals with an amplitude close to the resolution.

4.2.1.2 Acoustic Projector Amplifier (Model Component 2 of 9)

The second component of the UGPS model is the acoustic projector amplifier in the UGPS satellite. The amplifier boosts the signal generated by the D/A converter to drive the acoustic projector.

The acoustic projector amplifier is modeled using experimental data illustrating the relationship between the amplifier's output and input signals. Generally, an amplifier model is based on the specification provided by the manufacturer of the amplifier. Although manufacturer's specifications are usually very accurate, they cannot take into account the circuitry that is required to integrate their product into a user's custom design. This additional circuitry can significantly affect both the amplitude and frequency response of a system. By modeling the system using the input and output data directly, a mathematical model that very closely matches the physical system is achieved.

The MATAB System Identification Toolbox was used to generate the model for the acoustic projector amplifier. This toolbox uses measured data from the real system to generate a mathematical model which represents that system. The System Identification Toolbox requires two pieces of information to generate a model: working data and validation data. The working data and validation data both consist of two signals: the input signal to the amplifier and the output signal from the amplifier. The working data is used to generate the model while the validation data is used to measure how well the model approximates the response of the real system given a different input signal.

A test was set up to generate the working and validation data. The test setup, illustrated in Figure 4.13, consisted of a National Instruments PCI-6251 data acquisition card and its appropriate breakout box (SCB-69). An analog output port on the SCB-68 was connected to the input port on the acoustic projector amplifier. The output of the acoustic projector amplifier was fed back into an analog input port on the SCB-68.

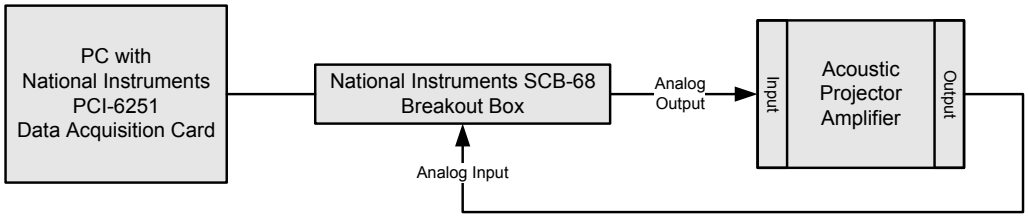

Figure 4.13: Diagram of the projector amplifier test setup.

Using this test setup, the working and validation data were generated. The working signal used to generate the model was a square wave with an amplitude of 0.5V, a frequency of 500Hz, and a duration of 0.01s. The validation signal was a sine wave with a constant amplitude of 0.5V and a frequency that increased linearly from 0Hz to 100kHz over a period of 0.1s.

Within the System Identification Toolbox, an ARX model was used to model the projector amplifier. ARX is a parametric model that is specified by the order of the polynomials which represent the modeled transfer function. The ARX parametric model is defined by the polynomials A and B, and the delay. The ARX model is an overdetermined system and uses a least squares fit to determine the coefficients of the polynomials that define the model.

Using the System Identification Toolbox an ARX model with polynomial orders of A = 1, B = 2, and delay of 0 was generated from the working data. The model was then run with the validation data and yielded a 99.88% fit with the validation data. The fit calculation is performed by the System Identification Toolbox using Equation 4.2, where Y is the measured output and $\hat{Y}$ is the simulated/predicted model output.

$$FIT = \frac{1 - NORM(Y - \hat{Y})}{NORM(Y - MEAN(Y))} * 100 \tag{4.2}$$

4.2.1.3 Acoustic Projector (Model Component 3 of 9)

The third component of the UGPS model is the acoustic projector in the UGPS satellite. The acoustic projector converts the voltage from the acoustic projector amplifier to a pressure. The pressure generated from the projector produces the acoustic waves that propagate through the water to the receiver.

Projector Specifications

The manufacturer of an acoustic projector typically provides three calibration graphs that summarize the properties of the projector. The information from these three graphs can be used to model the acoustic projector. The graphs provided by International Transducer Corporation (ITC), for the ITC-1032 projector used in the UGPS satellite, are included in Appendix B.

The first graph specifies the directivity of the projector. This is a measure of the pressure amplitude produced by the transducer as a function of the polar angle. Generally, plots are provided for the two planes of the transducer, the XY and XZ. The XZ plane is parallel to the axis of the cable protruding from the transducer. The

ITC-1032 transducer is a spherical transducer with an omnidirectional response. The directivity graphs show that the transducer amplitude is within 0.67 dB referenced to 1μPa @ 1m at 25kHz for all angles in both the XY and XZ planes.

The second graph is the water admittance. This graph shows the relationship between the frequency of the input signal and the complex admittance of the projector. Admittance, which is the reciprocal of impedance, is a measure of how easily AC current can flow through a circuit. The admittance data is used to design the amplifier electronics required to drive an acoustic projector. The admittance can also be used to model the transient response of the projector to an input signal.

The third graph is the transmit voltage response (TVR). The transmit voltage response is a measure of the steady state pressure produced by the transducer when 1V RMS is applied across the transducer leads at a specific frequency. Transmit voltage response, measured in dB referenced to 1μPa/V @ 1m, can be converted to a sound pressure level (SPL) (which is the pressure produced by the projector). SPL, measured in decibels referenced to 1μPa, is defined in Equation 4.3 and is a function of the transmit voltage response and the voltage applied to the transducer.

$$SPL = TVR + 20 \cdot \log_{10} V_{in} \tag{4.3}$$

Modeling the Projector

Using the three calibration graphs, the acoustic projector can be completely modeled. In this work, the directivity will not be modeled because the ITC-1032 is a spherical projector, and has an omnidirectional response. In addition, the transient response of the transducer is not modeled. The transmitted signals for the test system consist of 100's of cycles of a sine wave. The transient response of the transducer only affects the first 2 or 3 cycles, and adds 2 or 3 extra cycles to the end of the signal. This is insignificant when compared to the length of the entire signal. Because the transient portion minimally effects the overall signal shape, it is not modeled.

The steady state response of the projector is modeled. The steady state response, described by the TVR, is a measure of the pressure amplitude as a function of frequency. The TVR for the ITC-1032 changes by as much as 10dB in the 20-40kHz frequency range. This means that for an input signal with a constant amplitude and a variable frequency between 20 and 40kHz, the amplitude of the generated pressure wave changes by a factor of 3, simply due to the frequency of the input signal.

The first step in modeling the projector is to calculate the frequency of the input signal. The frequency of the input signal will likely change throughout a transmission,

therefore, the frequency will be calculated for each sample. The per-sample frequency calculation is known as the instantaneous frequency.

The instantaneous frequency of the input signal is calculated using the Hilbert transform. The Hilbert transform generates a signal whose frequency components are shifted by -90 degrees relative to the input signal. The Hilbert function, in MATLAB, computes the Hilbert transform of an input signal and returns a complex result. The real component of the result is the original signal and the imaginary part is the Hilbert transform of the original signal. The instantaneous frequency is calculated by taking the derivative of the instantaneous phase angle, which is the angle between the real and imaginary components.

The instantaneous frequency of the input signal is used to apply the correct TVR value for each sample of the signal. Using Equation 4.3, the sound pressure level is calculated from the TVR and the input voltage. Figure 4.14 shows the response of the projector model to an input signal with 1V RMS amplitude and varying in frequency from 20 to 50kHz.

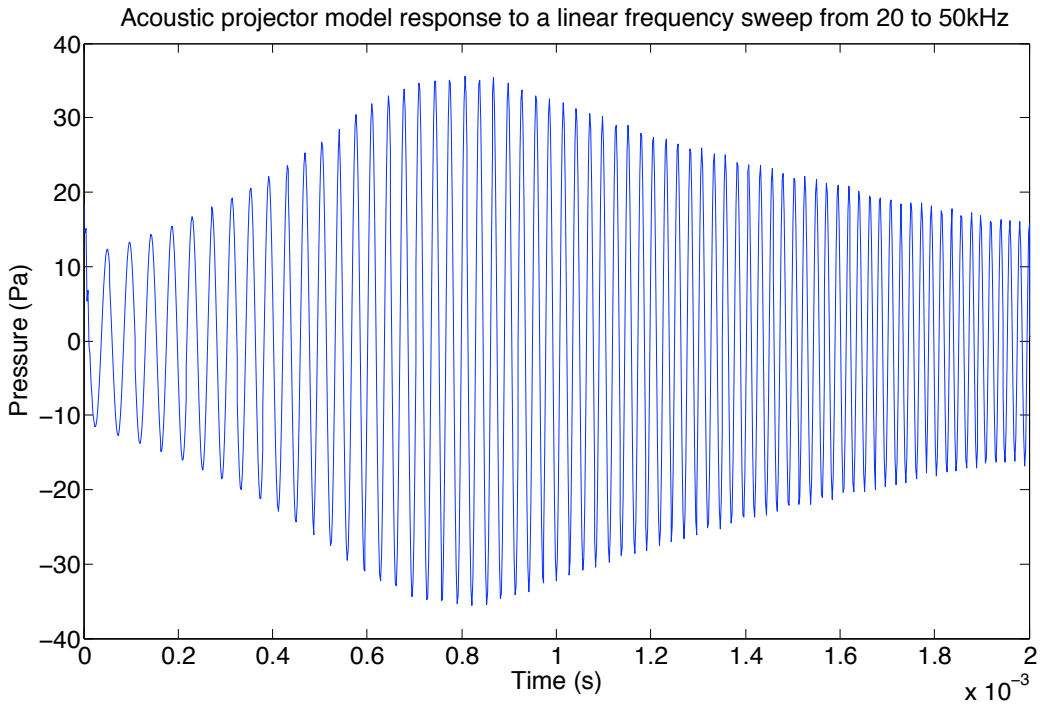

Figure 4.14: Response of the acoustic projector model for an input signal with constant amplitude and sweeping a frequency from 20 to 50kHz.

4.2.2 Water Column

The acoustic signals emitted by the UGPS satellite propagate through water to reach the UGPS receiver. In this section, the effect of the water on the acoustic signal will be modeled. There are three components of the water column model, which are the fourth, fifth and sixth components of the overall UGPS model:

- Ray Tracing. The direct path and two multi-path signals are modeled. Multi-path signals are a result of the acoustic signal reflecting from the water surface and ocean/lake bottom.
- Attenuation. As the acoustic signal propagates through the water it attenuates. This model accounts for the geometric spreading of the acoustic signal as well as the viscous and chemical absorption.
- Doppler Shift. The frequency of the acoustic signal increases or decreases due to the motion of the UGPS receiver relative to the UGPS satellite. The change in frequency due to the Doppler shift is modeled.

Throughout the water column model, water properties such as the sound velocity, salinity, pH and temperature are assumed constant.

4.2.2.1 Ray Tracing (Model Component 4 of 9)

The fourth component of the UGPS model simulates the different paths that the acoustic signal travels from the UGPS satellite to the UGPS receiver. The most direct path is a straight line between the transmitter and receiver. Sound, however, is able to reflect off objects with different densities than the water, for example, the ocean floor or ocean surface. Therefore, the UGPS receiver acquires the direct path signal as well as reflected signals from the ocean surface and floor. The ray tracing portion of the model produces an output signal that is a combination of the direct path and two multi-path signals.

The model calculates the length of three acoustic paths: direct, surface reflection and bottom reflection. These three paths are assumed to be straight lines and are defined by the position of the transmitter and receiver. Figure 4.15 illustrates a test setup with the relevant parameters labelled. In Figure 4.15, z_r is the depth of the receiver, z_t is the depth of the transmitter, z_b is the depth of the bottom, and x_{r-t} is the horizontal distance between the transmitter and receiver.

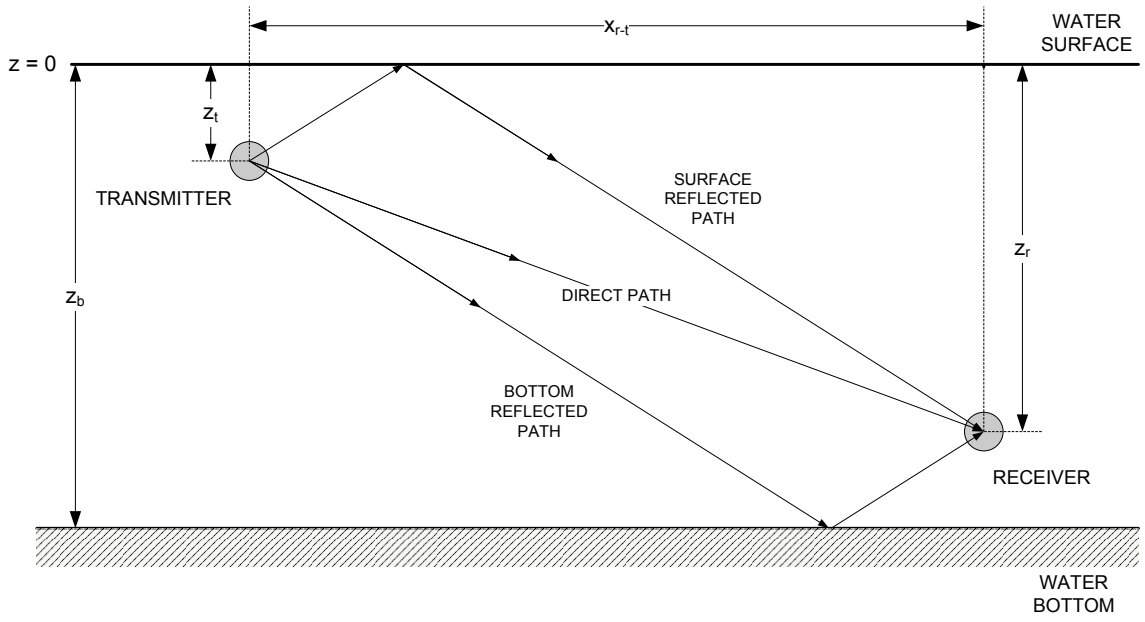

Figure 4.15: Illustration depicting the geometry and key parameters of the ray tracing portion of the UGPS model.

From the geometry, the three path lengths are calculated. The three path lengths and the sound velocity are used to calculate the travel-time of the acoustic signal for each path. The input signal and knowledge of the geometry, are used to generate three independent output signals, delayed by the travel-times of the acoustic signal traversing the three paths.

In the model, the two multi-path signals are multiplied by -1 because the amplitude of a reflected acoustic signal is inverted. In addition, each multi-path signal is multiplied by a reflection coefficient to account for the portion of the signal lost due to the reflection. The signals from the three paths are added together to produce the output signal.

4.2.2.2 Attenuation (Model Component 5 of 9)

The fifth component of the UGPS model simulates the attenuation of the acoustic signals as they propagate through the water column. Sound attenuates in water because of absorption and geometric spreading of the acoustic signal. These two mechanisms are modeled so as to accurately represent the transmission loss (TL) of the acoustic signal.

Attenuation Due to Absorption

Absorption of sound in water is described in detail by Ainslie and McColm [36]. The absorption is divided into two separate categories: viscous absorption and absorption by specific chemicals. Equation 4.4 is presented by Ainslie and McColm to calculate the absorption coefficient. The first two terms in the Equation 4.4 represent the absorption due to specific chemicals and the last term represents viscous absorption.

$$\begin{aligned}\alpha &= 0.106\frac{f_1 f^2}{f_1^2+f^2}e^{\frac{pH-8}{0.56}} + \\ &\quad 0.52\left(1+\frac{T}{43}\right)\left(\frac{S}{35}\right)\frac{f_2 f^2}{f_2^2+f^2}e^{-(D/6)} + \\ &\quad 0.00049 f^2 e^{(-(T/27)+(D/17))} \quad \text{dB/km}\end{aligned} \tag{4.4}$$

Where:

$$f_1 = \left(0.78\sqrt{(S/35)}e^{(T/26)}\right) \quad \text{kHz} \tag{4.5}$$

$$f_2 = \left(42e^{(T/17)}\right) \quad \text{kHz} \tag{4.6}$$

Equation 4.4 is valid for the following ocean conditions:

$$\begin{aligned}-6 < T < 35°\text{C} \quad & (S = 35\text{ppt}, pH = 8, D = 0\text{km}) \\ 7.7 < pH < 8.3 \quad & (T = 10°\text{C}, S = 35\text{ppt}, D = 0\text{km}) \\ 5 < S < 5050 \quad & (T = 10°\text{C}, pH = 8, D = 0\text{km}) \\ 0 < D < 7\text{km} \quad & (T = 10°\text{C}, S = 35\text{ppt}, pH = 8)\end{aligned}$$

In Equation 4.4, f is the frequency at which the absorption coefficient is calculated, D is the depth of the measurement in km, pH is the acidity of the water, S is the salinity of the water in parts per thousand, and T is the temperature of the water in degrees Celsius.

Attenuation Due to Geometric Spreading

In addition to the signal attenuation due to absorption, an acoustic signal also attenuates because of the geometry of the acoustic signal. For example, a spherical projector transmits the acoustic signal in all directions equally, i.e. in a spherical pattern around the projector. The energy of the wavefront is spread over the surface of a sphere; therefore, as the sphere expands the energy per unit area of the pressure

wave decreases. The decreased amplitude is quantified in Equation 4.7. R is the distance from the receiver in km.

$$SpreadingLoss = 20 \cdot \log_{10} R \quad \text{dB re. 1m} \tag{4.7}$$

The attenuation due to absorption and spherical spreading are summed to produce the total attenuation due to the propagation of the acoustic signal through the water. In the UGPS model, the instantaneous frequency of the signal is used to calculate the attenuation at each sample of the signal.

4.2.2.3 Doppler Shift (Model Component 6 of 9)

The sixth component of the UGPS model simulates the Doppler shift that occurs when the UGPS receiver moves relative to the UGPS transmitter.

The Doppler shift is modeled by resampling the input signal. Resampling the signal has the effect of stretching or compressing the signal, depending on the resampling ratio. Resampling an input signal, as a means of producing a Doppler shift, is described using the following example. Three cycles of a sine wave are represented by 1500 sample points. The three cycles are resampled by a factor of 2/3; as a result, 1000 samples now represent the same three cycles. If the sample frequency of both waveforms is assumed to be 1500 samples/second, the first signal represents a 3Hz signal, while the resampled signal represents a 4.5Hz signal.

The resampling ratio used to model a Doppler shift was defined by the Doppler equation (Equation 3.3). In Equation 3.3, the output frequency is a ratio of the sound velocity to the sound velocity plus the velocity of the receiver, relative to the transmitter. In the model, the output signal is resampled by the same ratio defined by the Doppler formula. The result is a Doppler shifted version of the input signal.

4.2.3 UGPS Receiver

The receiver is the subsea component of the UGPS. The receiver converts acoustic pressure waves to digital signals so they can be interpreted by a computer. The underwater receiver model is described in three parts. These three parts are the seventh, eight, and ninth components of the overall UGPS model:

- Hydrophone. The hydrophone converts the acoustic pressure waves to analog voltage.
- Hydrophone amplifier. The analog voltage is amplified and filtered.

- Analog to digital converter. The amplified signal is converted to a digital representation of the analog voltage.

4.2.3.1 Hydrophone (Model Component 7 of 9)

The seventh component of the UGPS model is the hydrophone in the UGPS receiver. The hydrophone converts pressure to an analog voltage proportional to that pressure.

Hydrophone Specifications

Hydrophones are supplied with calibration graphs that summarize their properties. Projectors and hydrophones are both piezoelectric devices that convert between a mechanical pressure and electrical charge. In most cases, a projector can be used as a hydrophone and vice versa. Hence, the calibration graphs provided by a manufacturer for a projector and a hydrophone are almost identical. The one exception is that instead of the transmit voltage response graph, the steady state response is described by the hydrophone sensitivity. The hydrophone sensitivity, also known as the open circuit voltage (OCV), is the voltage produced by the hydrophone for 1uPa of applied pressure. The OCV, measured in dB referenced to V/μPa, is the steady state response to a pressure input. The OCV plot for the hydrophone used in the test system is included in Appendix C

Hydrophone Model

Only the steady state response of the hydrophone will be modeled. The directivity will not be modeled because the TC4013 is a spherical hydrophone, and has an omnidirectional response. The admittance will also not be modeled because, just like the projector, the signals transmitted consist of 100's of cycles of a sine wave, so the transient response does not significantly affect the shape of the received waveform.

The steady state response of the hydrophone will be modeled using the OCV and the instantaneous frequency of the received signal. The instantaneous frequency is calculated using the Hilbert transform. The OCV, read from the hydrophone sensitivity graph at every instance of the received signal, is used in Equation 4.8 to calculate the voltage output from the hydrophone for 1μPa of applied pressure.

$$OutputVoltage = 10^{\frac{OCV}{20}} \tag{4.8}$$

Figure 4.16 shows the response of the hydrophone model to an input pressure with 1μPa RMS amplitude and varying in frequency from 20 to 50kHz.

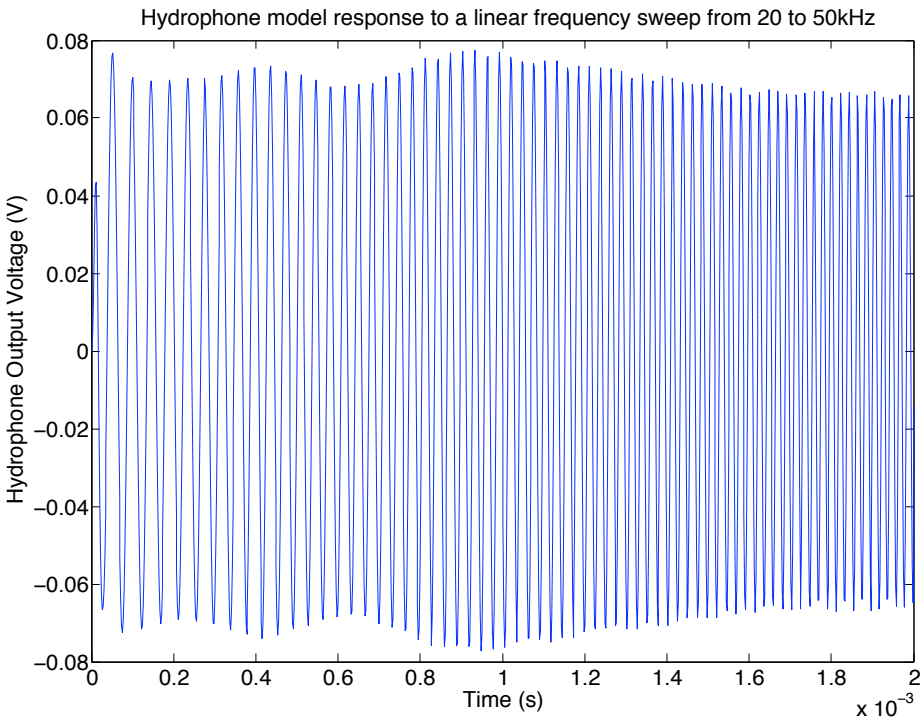

Figure 4.16: Response of the hydrophone model for an input signal with constant amplitude and sweeping a frequency from 20 to 50kHz.

4.2.3.2 Hydrophone Amplifier (Model Component 8 of 9)

The eighth component of the UGPS model is the hydrophone amplifier in the UGPS receiver. The hydrophone amplifier filters and amplifies the small voltage that is produced by the hydrophone.

The System Identification Toolbox was used to generate a model of the hydrophone amplifier from experimental data. The test setup used to measure the response of the projector, as described in Section 4.2.1.2, was used to generate the working and validation data for the hydrophone amplifier. The hydrophone amplifier was connected to a PCI-6251 data acquisition card through the SCB-68 breakout box, as shown in Figure 4.17.

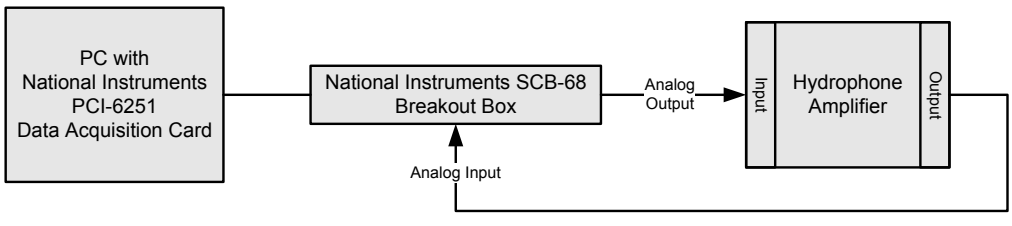

Figure 4.17: Diagram of the hydrophone amplifier test setup.

Using this test setup, two voltage waveforms were applied to the hydrophone amplifier. The first voltage waveform, which was used as the working data for the model, was a square wave with an amplitude of 0.0019V, a frequency of 500Hz, and a duration of 0.01s. The second data set, used as the validation data, was a sine wave with a constant amplitude of 0.0019V and a frequency that increased linearly from 0Hz to 100kHz over a period of 0.1s. Figure 4.18 shows 50ms of the output voltage measured from the hydrophone amplifier for the validation data set.

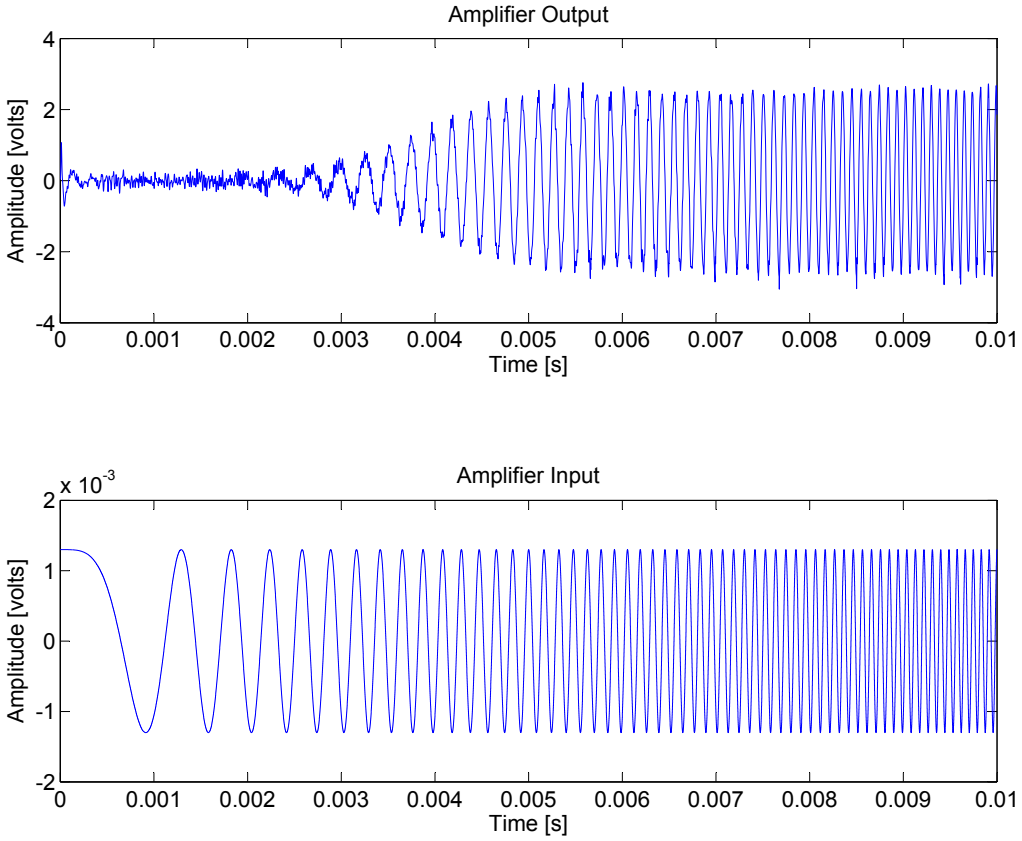

Figure 4.18: Hydrophone amplifier model input and output signals for the validation data.

Unlike the projector, which has a nominal gain of 6.1, the hydrophone amplifier has a nominal gain of 2100. This means that an input voltage of 1.9mV is amplified to 4V. As a consequence of the higher gain, the small amount of noise in the system is also amplified along with the voltage signal from the hydrophone. This higher order noise that is "sitting" on top of the signal will not be modeled.

Using the relationship between the amplifier input signal and the output signal, a mathematical model was generated. Using the System Identification Toolbox and the two data sets generated from the test setup, an AMX8883 model was generated

to approximate the hydrophone amplifier. Figure 4.19 shows the response of the hydrophone amplifier and the model, to a step input.

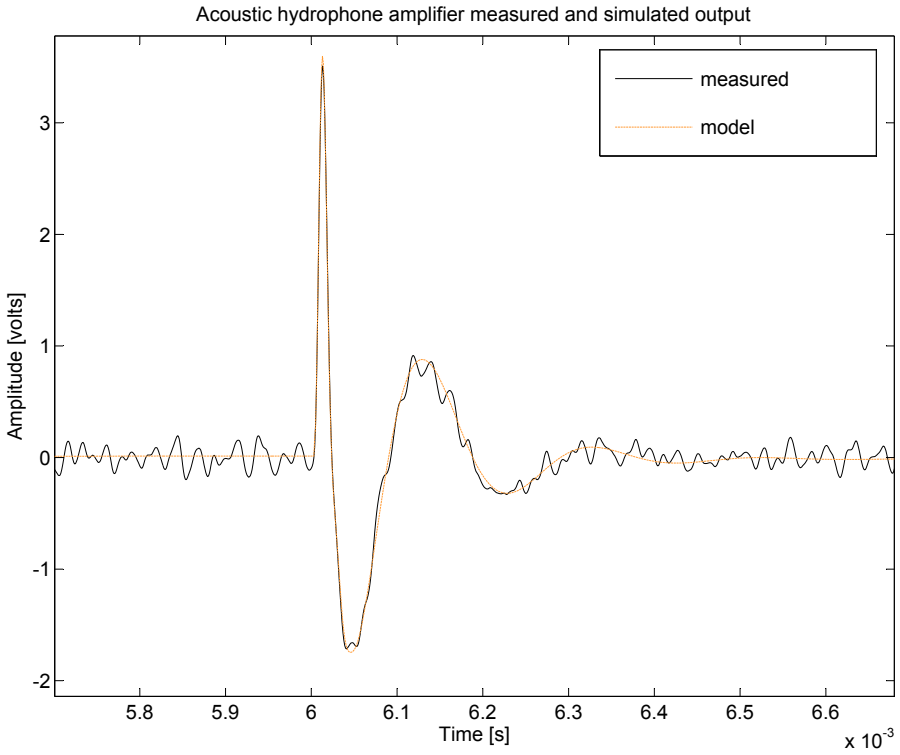

Figure 4.19: Acoustic hydrophone amplifier measured and simulated output.

The solid black line in Figure 4.19 is the measured response of the hydrophone amplifier and the dotted orange line is the modeled response. Note that the measured data has a lot of noise, as opposed to the model. Although some of this noise is likely emanating from the hydrophone amplifier, it is more likely that the noise is being injected into the system from the test setup itself.

Even though the system noise is not modeled, the model yielded a 91.22% fit as compared to the output from the hydrophone amplifier.

4.2.3.3 Analog to Digital Converter (Model Component 9 of 9)

The ninth, and final, component of the UGPS model is the analog to digital converter (A/D) in the UGPS receiver. The A/D converter digitizes the analog voltage from the hydrophone amplifier.

The A/D converter is modeled using the same methods used for the D/A converter in the UGPS satellite (Section 4.2.1.1). The input signal from the hydrophone

amplifier is resampled to the sampling rate of the A/D converter and then quantized to the resolution of the A/D.

The A/D converter not technically part of the UGPS receiver in the test system, rather it is part of the surface station, described in Section 4.1.3. For the purpose of this model, however, the A/D converter is associated with the UGPS receiver because it will become part of the UGPS receiver in subsequent test systems.

The A/D converter model is based on the National Instruments PCI-6251 data acquisition card in the surface station. The surface station samples the hydrophone voltage at a sampled rate of 500kS/sec and a resolution of 16 bits over a range of $\pm$ 5V. Using Equation 4.1 from Section 4.2.1.1, the resolution of the A/D is calculated to be 0.153 mV.

4.3 Chapter Summary

This chapter presented the design of a test system that will experimentally verify the UGPS concept before the design of a complete system. It consists of three components: a satellite, receiver, and surface station.

The satellite floats on the water surface and transmits acoustic signals through the water to the receiver. The amplitude and frequency of the signals can be varied for testing purposes. At the receiver, the signal is acquired using a hydrophone, amplified and finally sent to the surface station where it is digitized and logged for post-processing. Although the complete UGPS requires multiple satellites to synchronize the receiver with the satellites, the test system synchronizes the receiver with the single satellite through the use of a GPS receiver.

This chapter also described a model of the test system. This model consists of nine components, each representing a key function of the UGPS test system. The goal of the model is to simulate the results of an experimental test and thereby reduce the time and cost of performing real-world tests. The model must be verified in order to ensure that it accurately represents the test system.

In the next chapter, the UGPS test system will be evaluated in a series of lake tests. These tests will quantify the test system performance so that a prediction of the overall UGPS performance can be obtained. In addition, the lake tests will be used to verify the model.

Chapter 5

Evaluation of the UGPS Model and Experimental Apparatus

A test system has been developed to evaluate the performance of the overall UGPS. In this chapter, the test system is used to perform four experiments. Each experiment evaluates a key performance metric of the UGPS. The results of each experimental test are also modeled as a means of verifying the model's ability to accurately represent the test system.

This chapter contains four sections:

- Tank-Test Model Verification. The results of an experiment performed in a small test tank are compared to modeled results.
- Field-Test Hardware Evaluation. The experimental apparatus is used to perform four tests. The tests are designed to evaluation key performance metrics of the UGPS.
- Field-Test Model Verification. Three of the four hardware evaluation tests are modeled. The results of the model are compared to the experimental results.
- Discussion of Results. The results of the modeled and experimental tests are discussed.

5.1 Tank-Test Model Verification

The UGPS model, described in Section 4.2, is comprised of 9 separate sub-components, each representing an integral part of the UGPS test system. In this section, the entire UGPS model is verified by comparing experimental results, obtained using the test system, to modeled results.

For this test, the UGPS satellite and receiver were rigidly mounted 0.5m apart inside a small laboratory test tank. Due to the small tank size, the transmitted acoustic signal was a short duration chirp. The short duration chirp was used so the direct path signal reached the receiver, in its entirety, before multi-path signals were received.

Three separate tests were performed using different chirp signals. The frequency range of each chirp signal was: 20-30kHz, 25-35kHz, and 30-40kHz. Overall, the model was verified for the 20-40kHz frequency range. Figure 5.1 shows the three signals acquired by the UGPS receiver. In addition, the model results are plotted on the same graph.

The transient response of the projector and hydrophone have not been modeled, therefore the beginning and end of the waveforms do not match the model. In addition, the TVR and OCV, from the projector and hydrophone respectively, were extracted from the plots provided by the manufacturers. Since this information was read from a graph, the accuracy of the reading is not precise and, therefore, does not perfectly match the experimental results. Even with the above caveats, the modeled data very closely matches the experimental results.

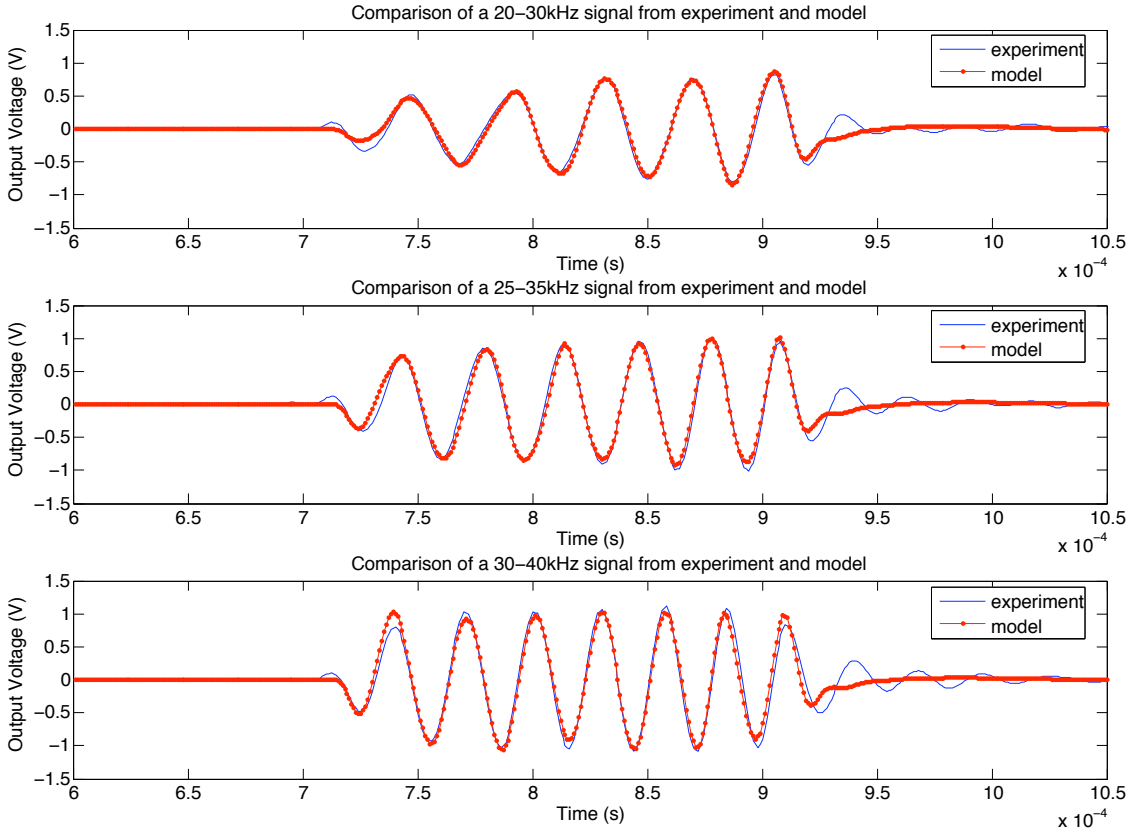

Figure 5.1: Experimental and modeled results for three acoustic chirp signals transmitted in a small laboratory test tank. The frequency range of each chirp signal was: 20-30kHz (top), 25-35kHz (middle) and 30-40kHz (bottom).

5.2 Field-Test Hardware Evaluation

Section 4.1 described a test system that was developed to evaluate the performance of the complete UGPS. In this section, four tests utilizing the system are described. The objective of the tests is to quantify the error sources related to underwater positioning (as discussed in Section 3.2). All the error sources are then combined to determine the accuracy of a full UGPS.

The three main error sources described in Section 3.2 are: travel-time measurement, distance calculation and geometric (due to the position error of the UGPS satellite and dilution of precision). Measuring the contribution of each error allows the accuracy and resolution of the overall system to be deduced. Travel-time error and geometric error, resulting from position error of the UGPS satellite, are quantified using the test setup. The geometric error from the dilution of precision, is a result of the placement of the satellites relative to the receiver. This error source is a measure of geometry and, therefore, can be calculated directly. The distance calculation error, due to ray bending, is not measured in these tests because appropriate equipment (a sound velocity meter) was not available.

The four tests used to quantify travel-time measurement and UGPS satellite position error are:

Test 1: Short-Range Accuracy. The short-range accuracy test is designed to measure the time-of-flight of an acoustic signal over a known distance. The distance is calculated using the time-of-flight and compared to the known distance to determine the ranging accuracy of the system. Furthermore, four different types of ranging signals are tried so as to determine the best signal for accurate ranging.

Test 2: Resolution. The test system's ability to resolve small motions of the UPGS receiver is measured. The UGPS satellite is moored approximately 150m from the UGPS receiver. The receiver is mounted on a tripod and moved in 10cm increments in the direction of the UGPS satellite. The differences of the acoustically measured distances are used to determine the resolution of the system.

Test 3: Long-Range Accuracy. This test evaluates the UGPS test system with respect to its maximum range capability. The accuracy of the acoustic ranging is compared with the range measurements from two GPS units; one at the UGPS satellite and one at the receiver.

Test 4: Transmitter Position Error. This test evaluates the variation in GPS position data from two stationary GPS receivers. Two GPS units are placed

2.41 meters from each other and the data output from the units are logged. The distance between the two units is calculated using the latitude and longitude output from each of the units.

In the following sections, each of the tests are described in detail.

5.2.1 Test 1 - Short-Range Accuracy

There are two objectives of the short-range accuracy test. The first objective is to determine the distance measurement accuracy of the test system over three fixed and known distances. The accuracy is determined by comparing the measured distance between the UGPS satellite and receiver, using a tape measure, with the average distance calculated from the acoustic time-of-flights. The second objective of the vertical test is to observe the cross correlation of 4 different acoustic signals and determine the best signal for use in accurate ranging. The best signal is defined as the one with the highest cross correlation, between the transmitted and received signal, with the smallest side lobes.

5.2.1.1 Test Setup

The UGPS receiver was suspended from the UGPS satellite using a low stretch steel cable. To keep the cable taught, a 5kg cement block was attached to the bottom of the UGPS receiver. Three tests were performed, each using a different length steel cable. The length of each cable was measured to within 5mm using an open reel survey tape measure. Figure 5.2 depicts the test setup for each of the cable lengths.

The UGPS satellite and receiver were setup to transmit and receive the acoustic ranging signal every 10 seconds. At each 10 second interval, 4 different ranging signals were transmitted by the satellite. Each signal had a duration of 3.7ms and a separation of 50ms between signals.

The first of the four transmitted signals was a frequency shift keyed (FSK) modulated message. The message was 18 bits long and spread using a pseudo noise (PN) code of length 126. The carrier frequency of this transmission was 33kHz with a modulation frequency of 20kHz. The second signal was identical to the first except that a binary phase shift keyed (BPSK) modulation was used instead of FSK. The third signal was a linear frequency sweep (chirp) from 25kHz to 45kHz. The fourth signal was a 33kHz continuous sine wave. The amplitude of the transmitted signal, as measured from the output of the projector amplifier, was set to 0.4V. This small amplitude was used so the signal received from the hydrophone would not saturate

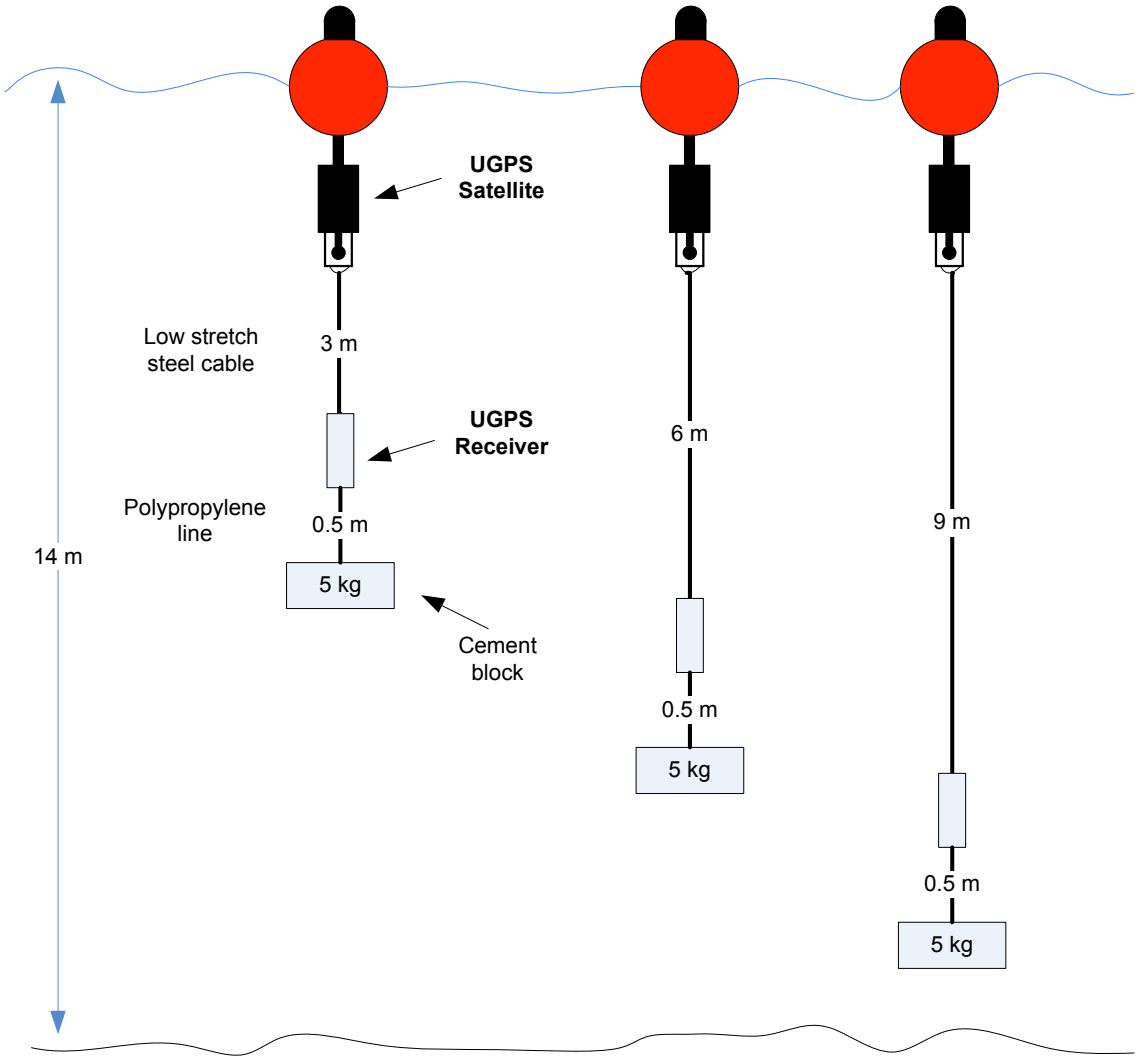

Figure 5.2: Test setup of three separate vertical tests.

the receiver amplifier. Figure 5.3 shows the transmitted signal. Due to the scale of the figure, each of the four signals blends together and appears as a band.

In Figure 5.3, the BPSK signal has a lower amplitude than the other three signals. This lower amplitude is a result of the sampling rate of the analog to digital converter in the UGPS satellite.

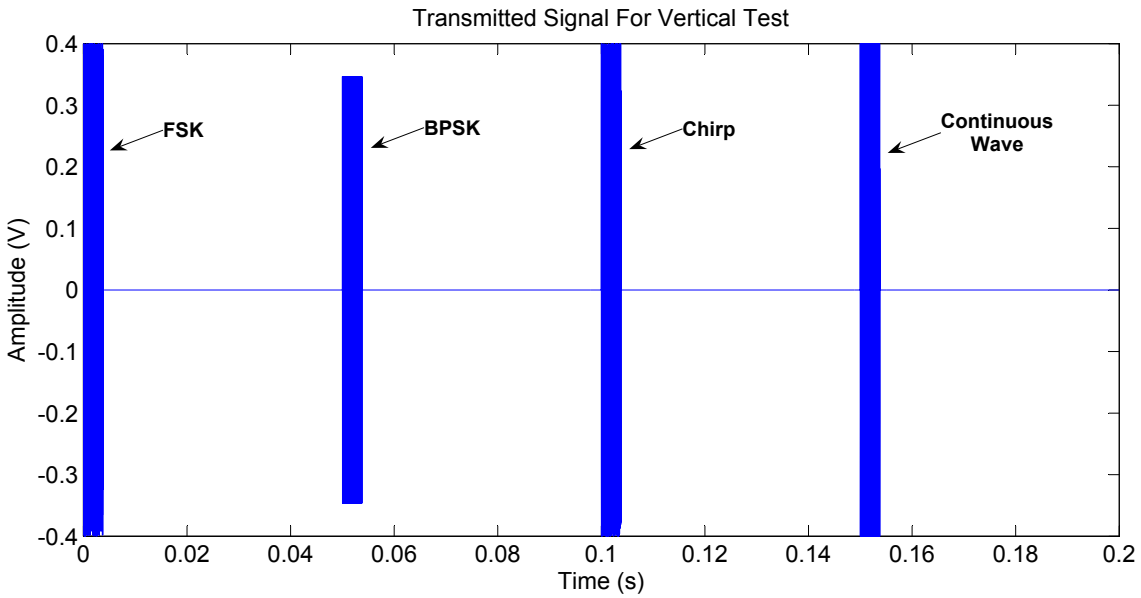

Figure 5.3: Transmitted signal for the short-range accuracy test.

5.2.1.2 Results

The output signal from the UGPS receiver was cross correlated with each of the original transmitted signals. The cross correlation of a single ranging operation for the 9m steel cable is shown in Figure 5.4.

In the first three plots of Figure 5.4, the direct path signal from the UGPS satellite to the receiver is centered at sample 500 (note the minimum peak). The second, smaller signal, centered at approximately 570 is a multi-path signal; it is a replica of the original signal that bounced off the bottom surface of the UGPS satellite and then traveled to the receiver. The distance between these two signals is 0.14ms or approximately 21cm, which is twice the distance between the center of the projector and the bottom surface of the satellite (shown in Figure A.5).

The detection algorithm, used to determine the time of arrival of each signal, utilizes the time of the minimum peak of the cross correlation between the received signal and the transmitted signal as the time of arrival. The time-of-flight was calculated by taking the time between the start of the data acquisition, which was triggered by the GPS pulse per second, and when the detection criteria was met. Using this detection technique, the time-of-flight of each transmitted signal was calculated. The test results are summarized in Table 5.1.

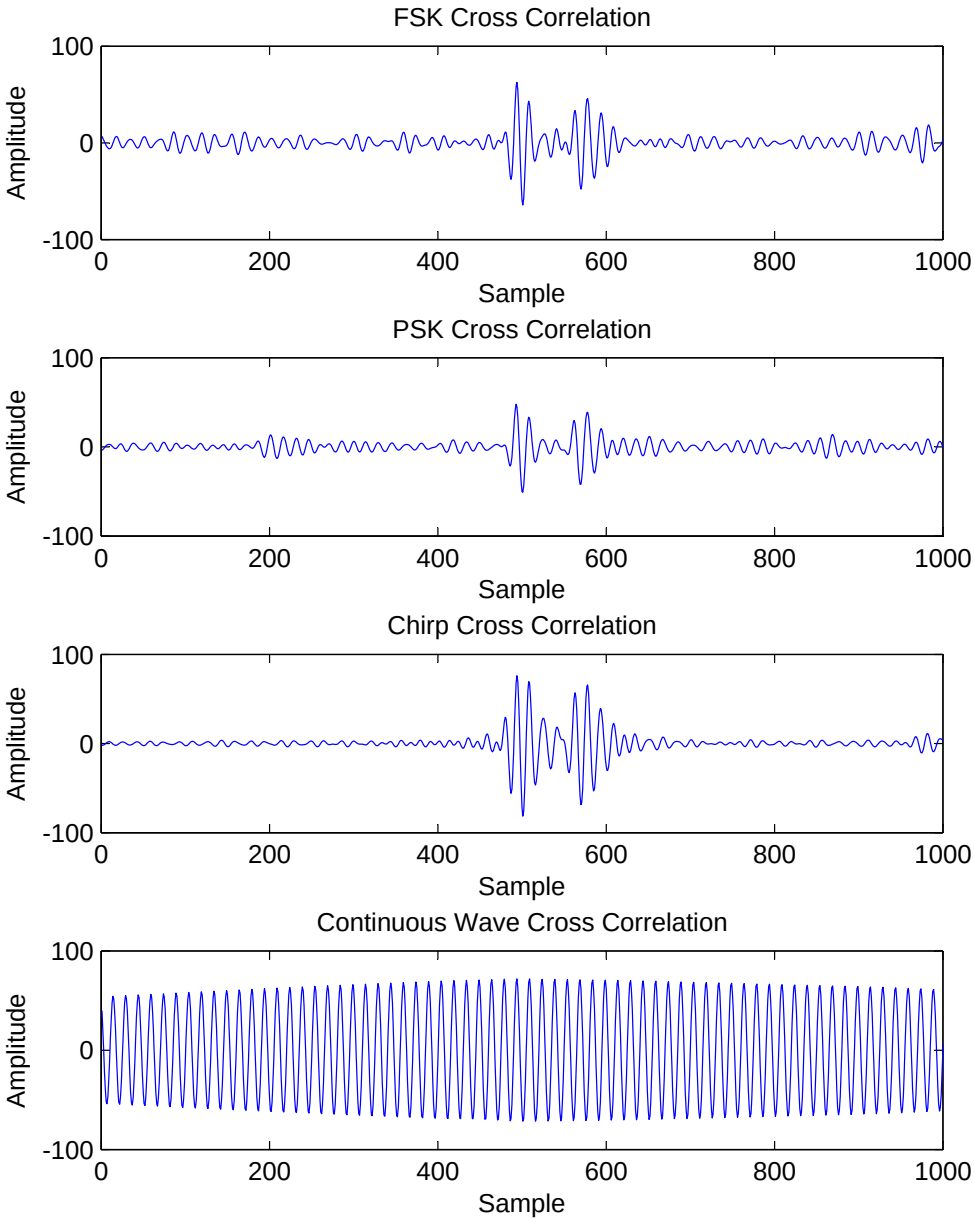

Figure 5.4: Cross correlation between the transmitted signal and the received signal for the 9m steel cable.

Table 5.1: Results of the vertical test. In the table, σ is the standard deviation of the measured travel-time.

Pulse Type	Distance Between Transducers (m)	Measured Travel Time (μs)		Calculated Sound Velocity (ms^{-1})
		mean	σ	
FSK	2.671	1806	0.00	1480.7
BPSK	2.671	1806	0.32	1480.4
Chirp	2.671	1806	0.00	1480.4
CW	2.671	1968	10.40	-
FSK	5.781	3904	0.00	1480.7
BPSK	5.781	3904	0.59	1480.4
Chirp	5.781	3906	0.40	1480.4
CW	5.781	4058	11.60	-
FSK	8.779	5931	4.16	1480.7
BPSK	8.779	5932	3.96	1480.4
Chirp	8.779	5932	4.10	1480.4
CW	8.779	6924	4210	-

In Table 5.1, the sound velocity for each type of signal was calculated by plotting the measured distances against the measured travel-times. A linear fit was then performed for each signal type and the slope of this fit was used as the sound velocity.

5.2.1.3 Discussion

- The time-of-flights and known distances were used to calculate the sound velocity in the water. Ideally a sound velocity sensor would have been used to measure the sound velocity directly, however one was not available.
- The acoustically measured distances were within 3mm of the measured distances using the tape. The estimated accuracy of the measured distance, using the tape measure, was 5mm; therefore, all of the acoustic measurements were within the accuracy of the measured reference lengths.
- The FSK signal was selected for the rest of the tests because of the good cross correlation results. The matched filter output for the FSK signal showed good amplitude with minimal side lobes.

5.2.1.4 Conclusions

- The acoustic distance measurement is accurate over short distances.

5.2.2 Test 2 - Resolution

The resolution test is designed to measure the ability of the test system to resolve small motions of the UGPS receiver. In this test, the resolution is determined by measuring the acoustic travel-time between a moored satellite and a receiver mounted on a translational stage. The receiver is moved by small known amounts (10cm) and the resulting differences in time measured.

5.2.2.1 Test Setup

The UGPS satellite was moored approximately 150m from shore in 14 meters of water. As illustrated in Figure 5.5, the satellite was moored using a 35kg cement block and a mooring line.

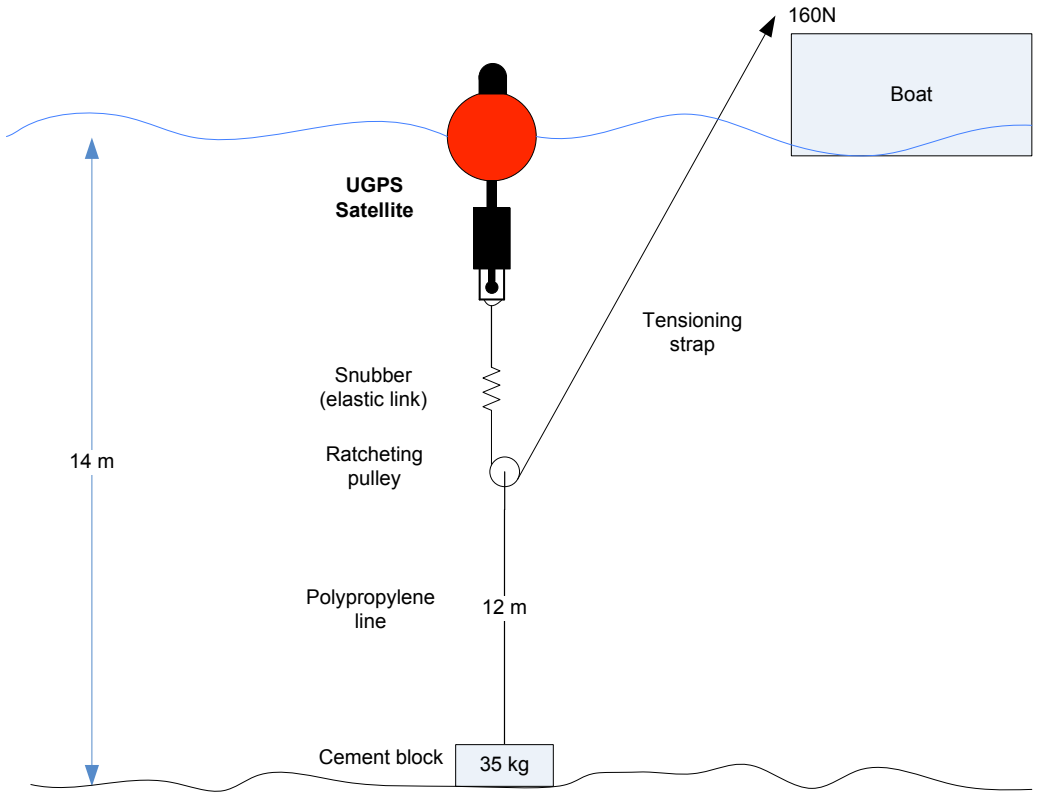

Figure 5.5: Test setup of UGPS satellite for the resolution test.

The mooring line was a polypropylene line in series with a snubber (elastic link) and a tensioning strap with a ratcheting pully. Using the tensioning strap, the mooring line was tightened until 160N of downward force was exerted on the satellite. The

snubber was used so that if a large wave occurred the float would not submerge, because the snubber would stretch allowing the float to stay on the surface. By applying this 160N of downward force, the lateral movement of the satellite was restricted.

The UGPS receiver was mounted on a linear translation stage, as shown in Figure 5.6, which in turn was attached to a tripod. This tripod was setup close to shore in approximately 2 meters of water and was anchored to the bottom using 5kg lead balls on each leg. The translational axis of the linear stage was alined with the direction of the satellite. Using the translation stage the receiver was moved to 5 positions in increments of 10 cm.

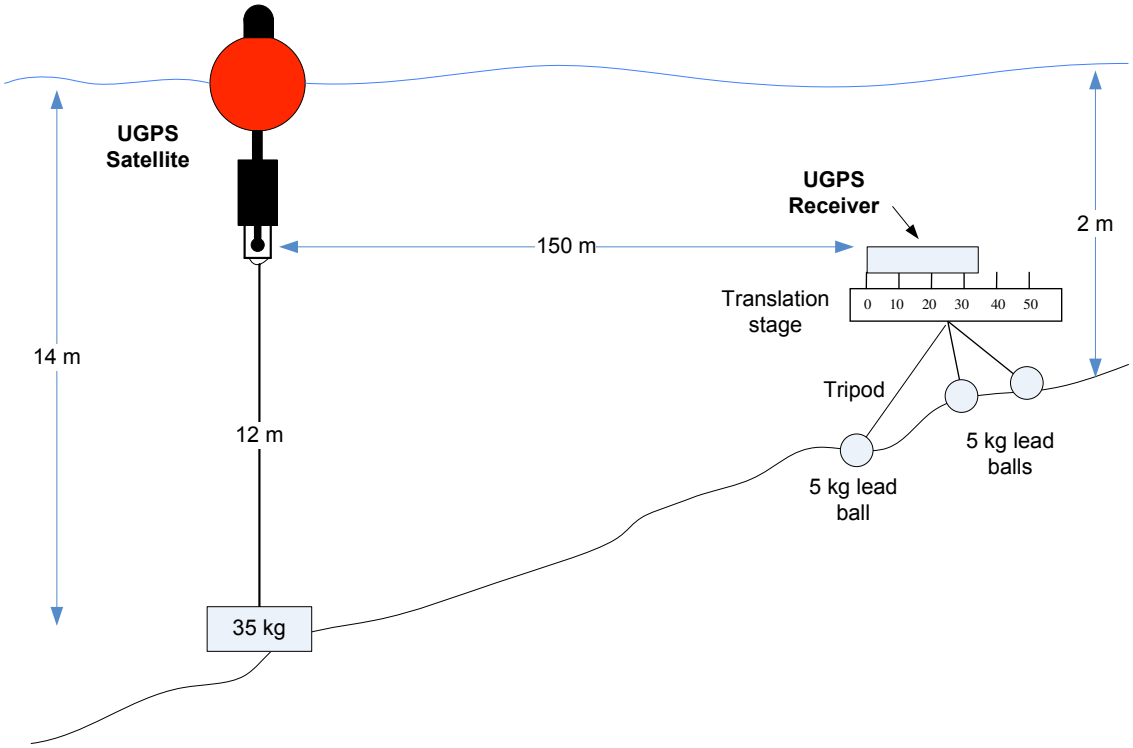

Figure 5.6: Test setup showing the UGPS satellite and UGPS receiver, on a translation stage, for the resolution test.

Although the satellite was moored, the force applied by wind and waves moved the satellite. A spotting scope was setup on shore to monitor the movement of the satellite. Since this test was performed on the shore of a lake, the only available location to setup the spotting scope was in line with the underwater receiver. Therefore, only the lateral movement of the satellite was monitored. It was assumed that the lateral motion of the satellite was representative of the movement of the satellite in the axis defined by the direction between the satellite and the receiver.

Figure 5.7 shows three photographs of the test setup on the lake. The top photo shows the spotting scope setup on the shore looking at the satellite in the distance. The bottom photographs show the receiver setup on the translation stage underwater.

Figure 5.7: Top: Photograph of the spotting scope directed at the UGPS satellite (shown in the center of the red circle) in the distance. Bottom: UGPS receiver mounted on the underwater tripod. The hydrophone is identified by the red circle.

5.2.2.2 Results

The travel-time between the satellite and the receiver was measured using the same technique explained in Test 1. The distance between the satellite and the receiver, for each received signal, was calculated using the measured acoustic travel-time and the speed of sound that was calculated from the results of Test 1 (Section 5.2.1). Table 5.2 shows the measured results for the FSK signal.

Table 5.2: Results of shore test. In the table, σ is the standard deviation of the mean measurement.

Translation Stage Reading (m)	Mean Acoustic Travel-Time (μs)	Acoustic Distance (m)		Relative Acoustic Distance (m)
		mean	σ	
0.0	99694	147.597	0.022	0.023
0.1	99749	147.678	0.033	0.103
0.2	99819	147.782	0.029	0.207
0.3	99869	147.857	0.024	0.282
0.4	99943	147.966	0.025	0.392
0.5	100012	148.068	0.038	0.493

The last column in Table 5.2 was calculated by subtracting the average of the mean acoustic distances from each acoustic distance, and then adding the average of the translation stage readings.

Using the spotting scope, it was observed that the satellite moved less that 10cm during the entire test. When the satellite did move during the test it was because a wave impacted the side of the satellite. When this happened the satellite oscillated around its average position.

5.2.2.3 Discussion

- The largest offset between the average acoustically measured distance and translation stage reading was 2.3cm. This shows that the system is able to repeatably resolve a receiver translation of 10cm.

- The maximum standard deviation for the acoustic measurement was 3.8cm. The magnitude of the standard deviation was most likely from the motion of the UGPS satellite during the test. The UGPS satellite was moored for this test, but it was observed that the position of the satellite oscillated around the

average position with an amplitude of 10cm. This oscillation was observed using a spotting scope located approximately 150m from the satellite.

5.2.2.4 Conclusions

- The accuracy of the matched filter was verified to be on the same order of magnitude as expected from the error analysis section.
- Based on this test, the UPGS test system is able to repeatably resolve a 10cm movement of the receiver.

5.2.3 Test 3 - Long-Range Accuracy

The UGPS uses acoustic signals to calculate the distance between the UGPS satellite and the UGPS receiver. In this test, the distance measured using the acoustic signal is compared with the distance measured using two Garmin GPS units placed directly above the acoustic transmitter and receiver. This long-range accuracy test is designed to quantitatively measure the accuracy of the acoustic distance measurement of the UGPS over distances greater than 200 meters.

5.2.3.1 Test Setup

The UGPS satellite was moored in 14 meters of water using the procedure described for Test 2 (Section 5.2.2). The UGPS receiver was moored at 6 different locations. Each location was at a different distance from the UGPS satellite. Figure 5.8 shows the location of the UPGS satellite and the 6 locations of the UGPS receiver.

The UGPS receiver was moored by tethering the bottom of the receiver to a concrete block using a 0.5m long polypropylene line, as shown in Figure 5.9. The top of the receiver was tethered to a float on the water surface. Using the same equipment and procedure employed to moor the UGPS satellite, the float was tensioned with a downward force of 160N. The buoyant force on the float acts in a vertical direction; therefore, the float naturally positioned itself directly above the UGPS receiver. A GPS receiver (Garmin 16-HVS) was mounted to the top of the float.

The absolute position of the UGPS receiver was determined from its depth (calculated from a pressure sensor in the UGPS receiver) and surface position calculated from the GPS receiver on the float. The complete test setup of the UGPS satellite and UGPS receiver is shown in Figure 5.10.

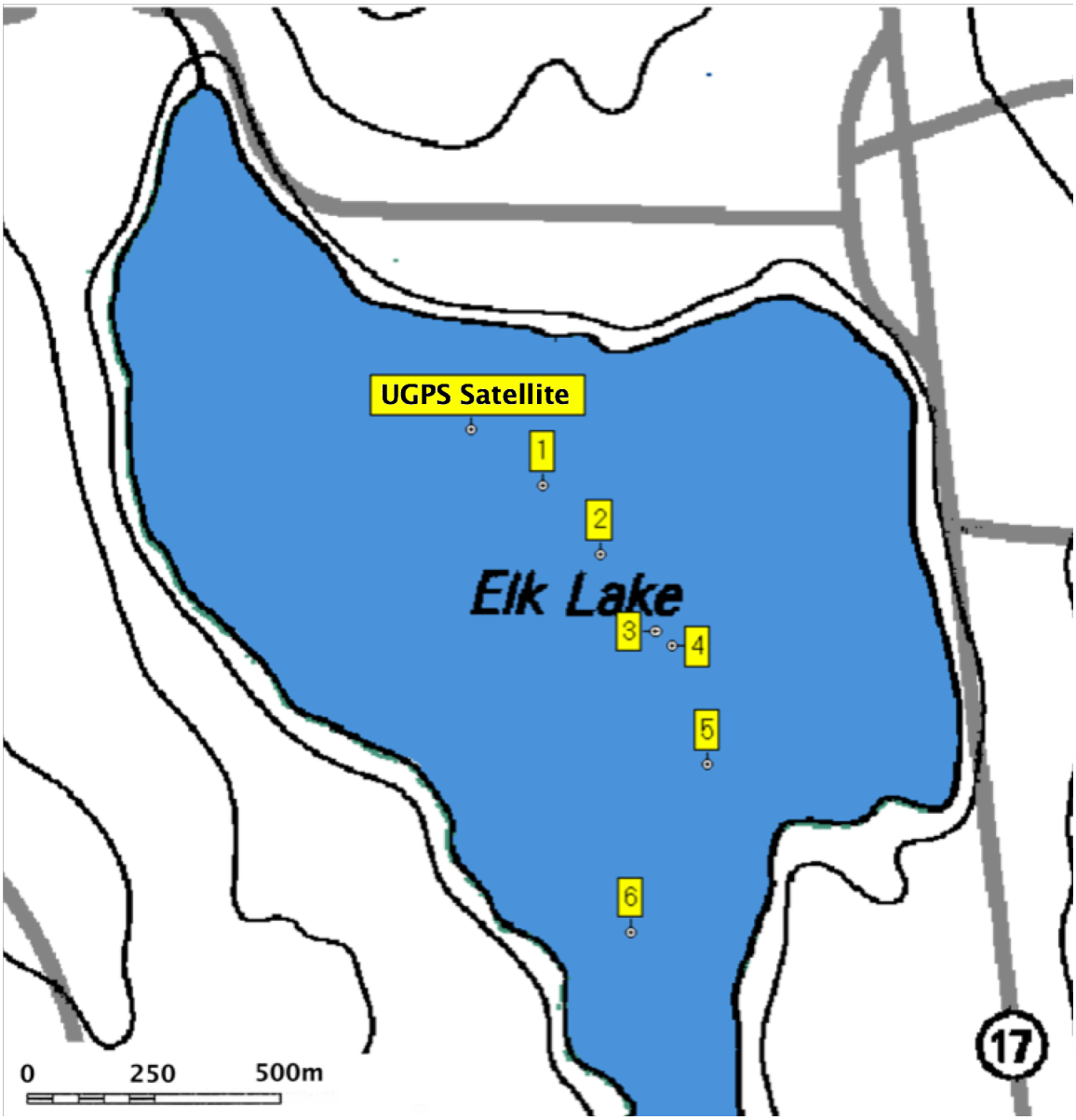

Figure 5.8: Chart showing the position of the UGPS satellite and the six UGPS receiver locations for the long-range accuracy test.

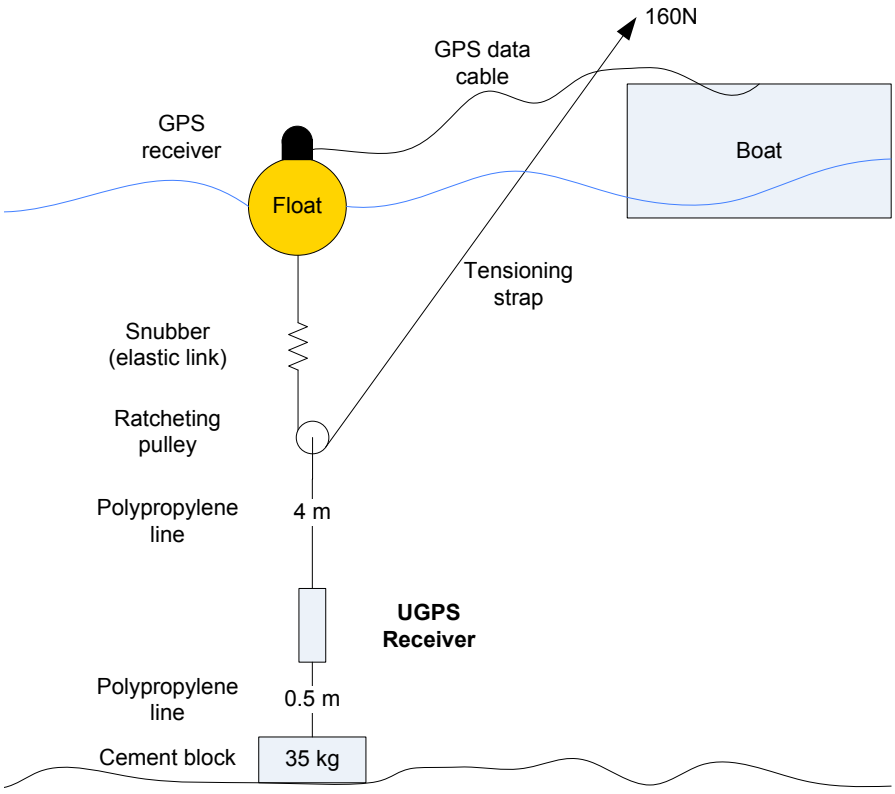

Figure 5.9: Test setup of UGPS receiver for long-range accuracy test.

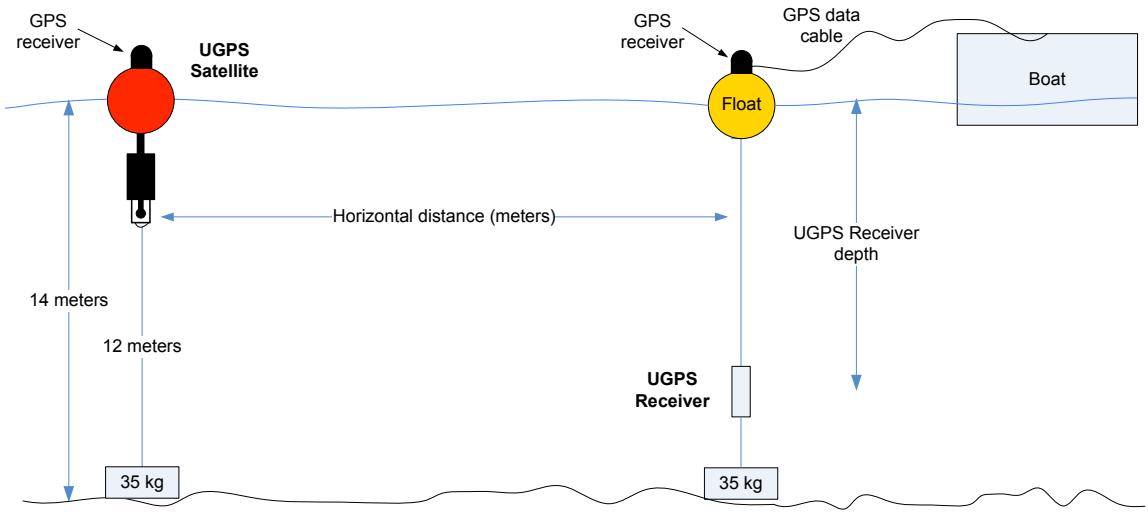

Figure 5.10: Test setup of the UGPS satellite and UGPS receiver for the long-range test.

5.2.3.2 Results

The horizontal distance between the UGPS satellite and the UGPS receiver was measured using two methods. The first method employed the travel-time of an acoustic signal traveling between the UGPS satellite and the receiver. This travel-time was then multiplied by the sound velocity of the water (measured in the short-range accuracy test (Section 5.2.1)) to determine the distance between the UGPS satellite and UGPS receiver. The second method to measure the distance between the UGPS receiver and UGPS satellite used the data output from the GPS receivers. Because the GPS receivers were placed directly above the UGPS satellite's acoustic projector and the UGPS receiver's hydrophone, the distance between the GPS receivers corresponds to the horizontal distance between the UGPS satellite and UGPS receiver.

The satellite and receiver were set up to transmit and receive the acoustic ranging signal, described in detail in Section 5.2.1, every 10 seconds. For each of the 6 UGPS receiver locations, no less than 30 separate signals were received and analyzed. As with Test 2, only the FSK signal was analyzed to produce the acoustic ranging results summarized in Table 5.3.

Table 5.3: Long-Range Test results. In the table, σ is the standard deviation of the mean measurement.

Receiver Location	**Acoustic Distance (m)**		**Receiver Depth (m)**		**Horizontal Acoustic Distance (m)**	**Horiztonal GPS Distance (m)**		**Acoustic and GPS Difference (m)**
	mean	σ	**mean**	σ		**mean**	σ	
1	181.09	0.14	6.79	0.02	180.99	179.39	0.55	1.60
2	353.34	0.05	5.51	0.02	353.31	352.21	0.59	1.10
3	539.56	0.07	5.34	0.02	539.54	539.48	0.53	0.06
4	582.90	0.02	5.61	0.02	582.88	582.47	0.42	0.40
5	810.37	0.03	0.80	0.00	810.37	808.74	0.42	1.63
6	1041.60	0.08	0.30	0.00	1041.60	1041.29	0.54	0.31

The acoustic distances were calculated by multiplying the acoustic travel-times by 1480.5ms^{-1}, which was the speed of sound in the water that was calculated in Test 1. The horizontal acoustic distance was calculated using Pythagoras' Theorem where the hypotenuse is the calculated acoustic distance and the vertical side is the depth of the acoustic receiver.

5.2.3.3 Discussion

- A range of 1041m was achieved with good results.
- Each GPS has an accuracy of 1.5m 68% of the time. The acoustic distance measurements agreed with the distance measurement from the GPS units, within the accuracy of the GPS; therefore, the UGPS range measurements are acceptable over long ranges.

5.2.3.4 Conclusions

- Long range and good accuracy were achieved over a distance of 1km, therefore the UGPS should be able to operate using a 1km baseline between satellites.

5.2.4 Test 4 - Transmitter Position Error

This test is designed to observe the change in output position data from two stationary GPS receivers over a period of time. The position data from the two identical GPS units is used to calculate the distance between the two units.

5.2.4.1 Test Setup

Two GPS receivers were placed 2.41m from each other in an environment free of large obstacles that could possibly generate a multi-path signal at the GPS receivers. The data from each GPS receiver was logged for 15 hours, 26 minutes and 38 seconds. The GPS receivers were identical Garmin GPS 16-HVS units both running the same firmware version.

5.2.4.2 Results

The output data from each GPS were used to calculate the distance between the two units for each data sample. Figure 5.11 is a histogram of the calculated distance between the two GPS units. The average distance between the two GPS receivers, calculated from the GPS data, was 4.47m with a standard deviation of 2.29m.

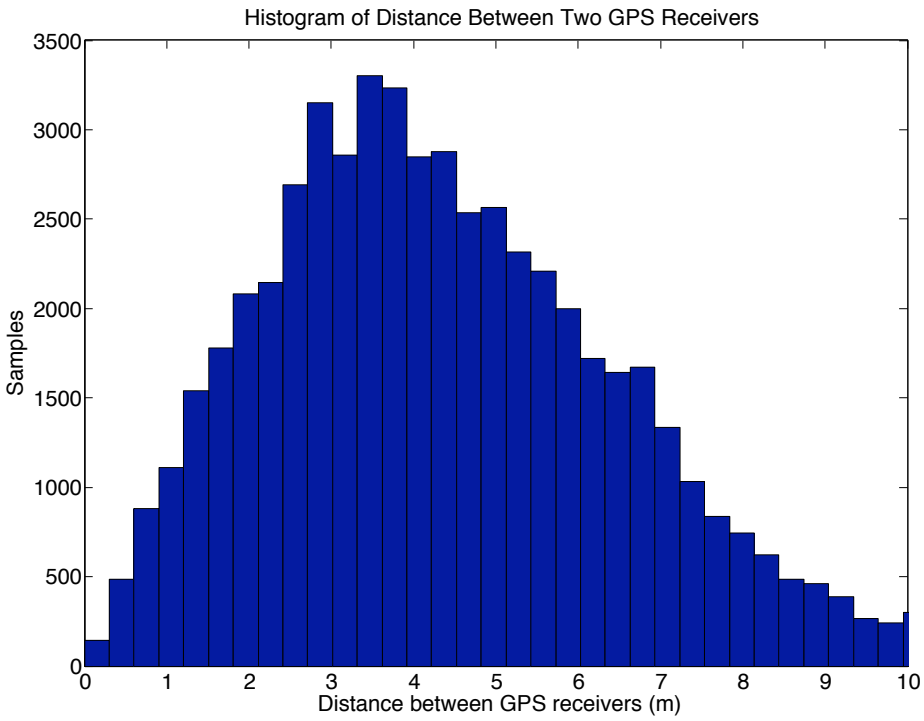

Figure 5.11: Difference in position between GPS receiver 1 and GPS receiver 2.

5.2.4.3 Discussion

- The calculated distance was 4.47m, with a standard deviation of 2.29m. This is a distance error of 2.06m, from the measured value. The published error specification of each GPS unit is 1.5m, therefore, the measured error is within the specification.

- The output from the two GPS units is not correlated. If the data from the two GPS units were correlated, the distance measurement between units would be constant even while the position output from each GPS unit changed. This is not the case, as shown by the large standard deviation of the distance measurement.

5.2.4.4 Conclusions

- The GPS position error was verified, therefore the estimated UGPS satellite error is correct.

5.3 Field-Test Model Verification

The first three tests described in Section 5.2 are modeled. The model is verified by comparing the experimental results to the model's output.

In Section 5.1 the modeled acoustic signal was directly compared to the experimental signal. In this section, the output of the matched filters are compared, rather than the acoustic signals. The tank test described in Section 5.1 was specifically designed so the receiver acquired the direct path signal in its entirety before a multi-path signal was received. For the lake test, the multi-path signals are always received before the direct path is fully received. Therefore, the acoustic signals are difficult to compare directly, because the constructive and destructive interference of the direct and multi-path signals greatly affect the shape of the signal. Even a small change in the multi-path length vastly changes the output signal. The matched filter output is not quite so sensitive, so it is easier to visually compare the modeled and experimental results.

5.3.1 Test 1 - Short-Range Accuracy

In this test, the UGPS receiver was suspended from the UGPS satellite using a low stretch steel cable. The satellite transmitted acoustic signals and the receiver acquired these signals for analysis. The test setup was described in detail in Section 5.2.1

This experimental setup is modeled for the case when the steel cable was 2.671m in length. The model is set up so that the range between the UGPS satellite and receiver is 2.671m. Also, the depth of the acoustic projector is set to 11.5cm, which is the distance between the projector and the bottom of the UGPS satellite. The outputs of the matched filters for the modeled and experimentally measured signals are shown in Figure 5.12.

The reception times of the direct path and multi-path signals for the model and experiment are identical; this is a key result of the modeled signal. This is important because the receiver location is based on the timing information extracted from the matched filter. This simulation shows that the model closely agrees with the experimental test results.

5.3.2 Test 2 - Resolution

The resolution test (Section 5.2.2) is a medium-range test with the satellite and receiver approximately 150m apart. The UGPS satellite is moored in 14m of water

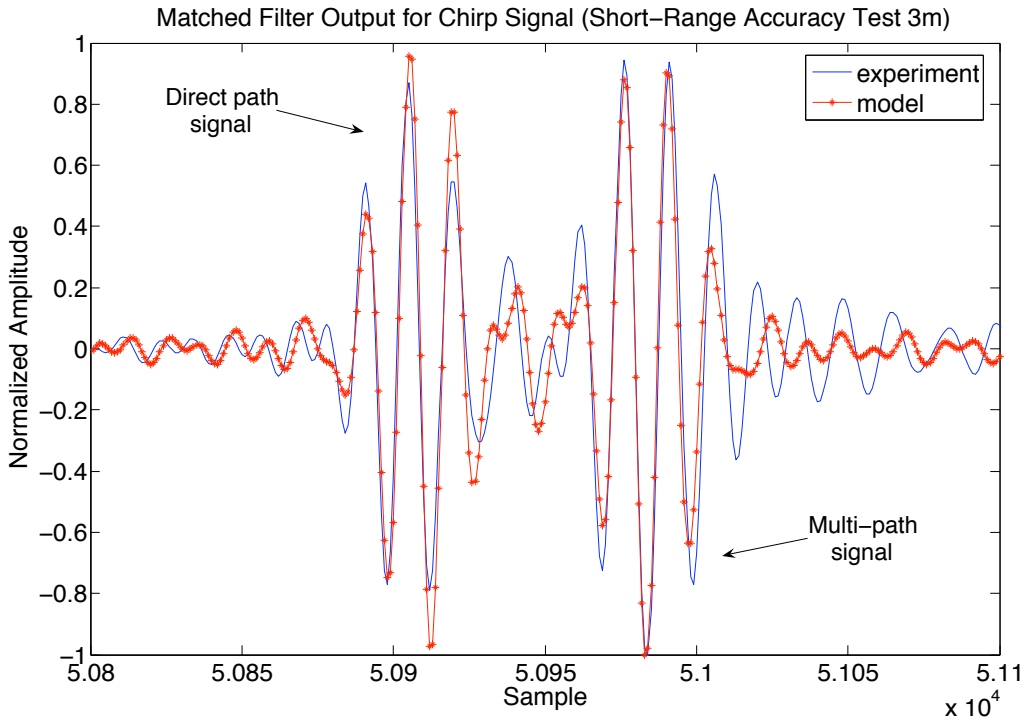

Figure 5.12: Matched filter output comparing the experimental and modeled signals for the short-range accuracy test. The compared matched filter results are for the chirp signal.

and the UGPS receiver is mounted on a translation stage in 2m of water.

The resolution test is modeled when the translation stage is set to 0.3m. The model is set up so that the range between the UGPS satellite and receiver is 147.857m, which was the acoustically measured distance from the resolution test (Section 5.2.2). Also, the depth of the acoustic projector is set to 0.8m and the depth of the receiver at 2m. The outputs of the matched filters for the modeled and experimentally measured signals are shown in Figure 5.13.

Note the direct path and multi-path signals are indistinguishable from one another. This is because the difference between the direct path and multi-path lengths is only 0.027m. The results of the model and experiment are almost identical, therefore, the model accurately represents this test case.

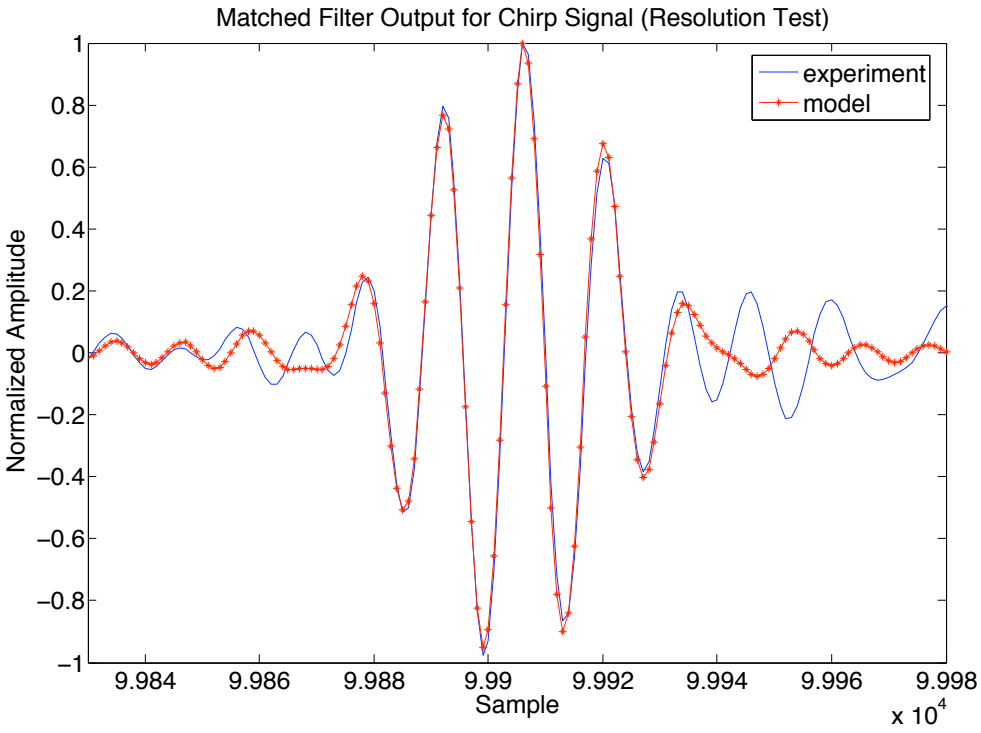

Figure 5.13: Matched filter output comparing the experimental and modeled signals for the resolution test. The compared matched filter results are for the chirp signal.

5.3.3 Test 3 - Long-Range Accuracy

The long-range accuracy test (Section 5.2.3) is used to validate the range measurement of the UGPS using GPS. In this test the UGPS satellite was moored in 14m of water and the UGPS receiver was moored at 6 locations.

This test was modeled for receiver location number 4, which was approximately 580m from the UGPS satellite. The model was set up with an horizontal range between the UGPS satellite and receiver of 582.88m and a receiver depth of 5.61m. The outputs of the matched filters for the modeled and experimentally measured signals are shown in Figure 5.13.

As with the other tests, the modeled results closely match the experimentally measured results.

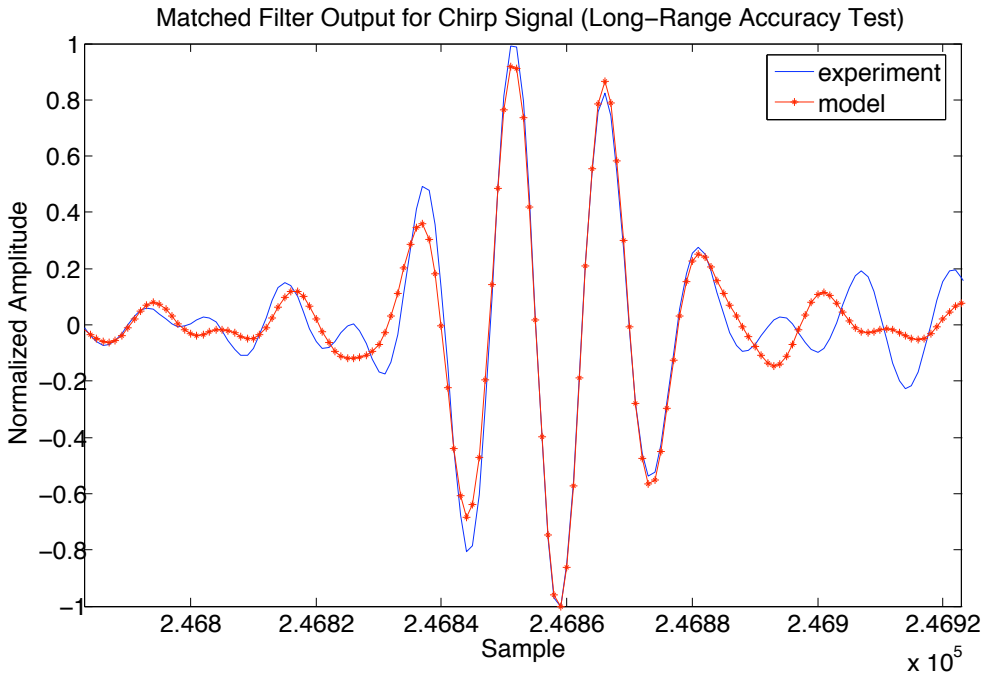

Figure 5.14: Matched filter output comparing the experimental and modeled signals for the long-range accuracy test. The compared matched filter results are for the chirp signal.

5.3.4 Discussion of Model Results

The model performance has been verified against the experimental field tests. The model performed well except for the discrepancies that can be attributed to the projector and hydrophone models. The transient responses of the projector and hydrophone were not modeled, therefore, the model does not perform well for signals with rapidly changing frequencies, such as BPSK and FSK signals. However, for chirp and continuous wave signals, the model performed well. Overall, it has been shown that the model can be employed in designing a full UGPS.

5.3.5 Summary of the Full UGPS Performance

Based on the experimental tests and the error analysis section, the expected operating parameters of the UGPS are:

- The UGPS requires a minimum of 3 satellites, and with the addition of satellites, data redundancy is achieved. Redundancy could be used to decrease the dilution

of precision (DOP).

- The DOP was calculated for a depth of 100m, therefore, the system will perform well to at least this depth.
- UGPS workspace covers a surface area of 1 km^2.
- Within the workspace, the calculated position accuracy of the UGPS receiver is 6.5m, which is a conservative combination of the errors discussed in Section 3.2.
- The system can reliably resolve a receiver motion of 10cm.
- An unlimited number of receivers can operate within the workspace of the UGPS.

5.4 Chapter Summary

In this chapter, the UGPS test system was used to perform four experiments in a realistic underwater environment. These tests quantified several of the error sources theorized in Section 3.2. The tests measured the short and long range accuracy of the test system; the ability to resolve small motions of the receiver; and the position error in the satellite. These tests confirmed the theoretical performance of the UGPS calculated in Section 3.2.

The UGPS test system model was verified in two ways: using a tank test, and by modeling the field tests. The model performed well and was shown to accurately represent the test system under most circumstances. The model, however, did not accurately represent the hydrophone or the projector for signals with rapidly changing frequencies.

Chapter 6

Conclusions and Future Work

6.1 Conclusions

The thesis presents the design, implementation and testing of a new class of positioning system suitable for supporting the operation of autonomous underwater vehicles. The UGPS can provide three-dimensional spatial data to an unlimited number of underwater assets to an accuracy of 6.5m. In contrast to commercially available acoustic positioning systems, the UGPS produces a finite amount of acoustic energy that is independent of the number of receivers. This key feature produces minimal environmental impact.

The thesis presented a review of the state-of-the art of underwater acoustic positioning systems and highlighted the relative advantages and disadvantages of each approach. Combining the best features of these systems and the user specifications for the proposed system, the design requirements of the UGPS concept were generated. A prototype UGPS, consisting of one surface satellite and one underwater receiver, was developed and built to evaluate the UGPS concept. A series of experimental tests were conducted at Elk Lake and the range, accuracy, and precision of the system were evaluated.

A MATLAB model of the UGPS system was also developed and evaluated against the experimental tests conducted at Elk Lake. The model was shown to be an accurate representation of the system and constitutes an important contribution to the research project because it can be used to accurately perform simulations of experimental tests. These simulations can then be employed to develop a full, multi-buoy system with the capability to provide position data to multiple underwater vehicles. Furthermore, the model functionality allows simulation of the UGPS under varying environmental conditions.

Overall, the research results determine that a full UGPS could be implemented with the following operational specifications:

- A minimum of 3 satellites would be required to act as a positioning system. The addition of more satellites produces data redundancy that could be used to decrease the DOP.
- The UGPS will perform well to a depth of at least 100m over a surface work area of 1 km^2.
- A positional accuracy of 6.5m could be achieved within the above spatial boundary.
- An upper bound for the resolution is 10cm.
- An unlimited number of receivers could operate within the workspace.

6.2 Future Work

The feasibility and preliminary design of an UGPS has been presented in this thesis. Based on the outcomes of this research project, it is now possible to design and implement a full UGPS system. A full system, employing 3 or more satellites, would enable multiple underwater vehicles to determine their location from the acoustic signals and precise depth measurement using an on-board pressure sensor. However, prior to the development of a full UGPS, further research and development work is required. The following goals should be achieved before a full UGPS system is built:

- Utilise the current UGPS model and incorporate the transient response of the projector and hydrophone. This would allow accurate simulation of a wider variety of acoustic signals.
- Extend the model to a multi-satellite UGPS so more thorough testing can be performed using the model before requiring further field-testing.
- Develop the means to acoustically communicate data from the UGPS satellite to receiver. This is an essential component of the UGPS that is required when the UGPS satellites are not moored.
- Add the functionality to use the sound velocity profile of the water in the UGPS position calculation.

- Replace the GPS receivers in the UGPS satellites with higher accuracy models. This would significantly increase the accuracy of the UGPS.

A full UGPS would be an asset to the University of Victoria Ocean Technology Laboratory and would further advance the AUV program.

Appendix A

UGPS System Details

A.1 UGPS Satellite

A.1.1 Additional Pictures

Figures A.1, A.2, A.3, A.4, A.5, A.5, A.7 and A.8 show details of the UGPS satellite. Figures A.9 shows the UGPS satellite in a test tank; this was the first time the UGPS satellite was tested. Figure A.10 is a picture of the UGPS satellite moored in Elk Lake for the precision test (Test 2).

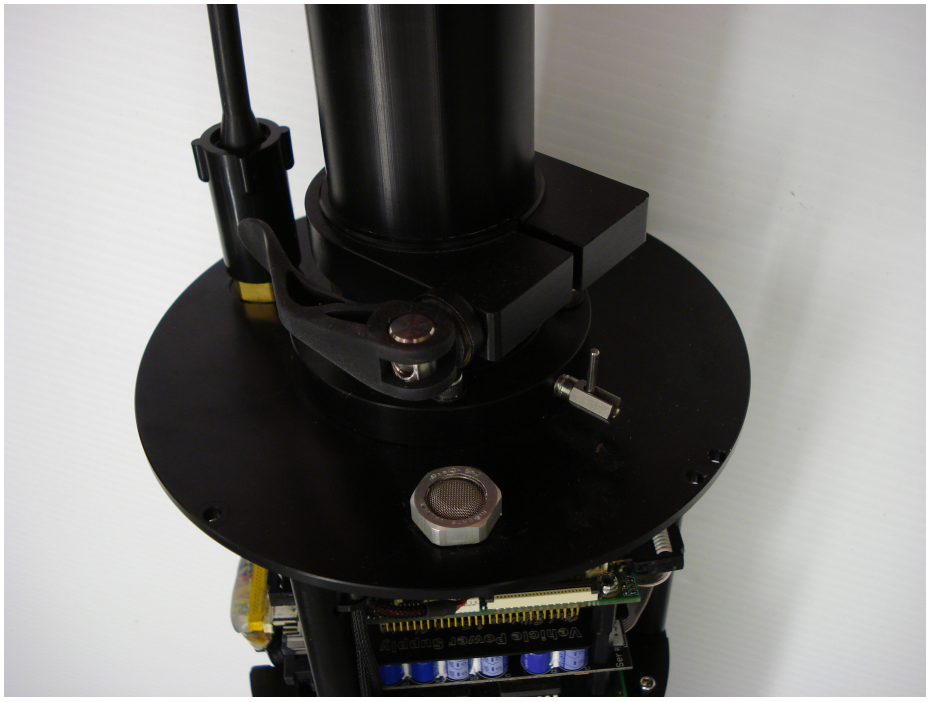

Figure A.1: Photograph of the top surface of the UGPS satellite housing. Key components in this photo are the charging connector, quick release handle enabling the satellite to separate for shipping, and the pressure relief valve.

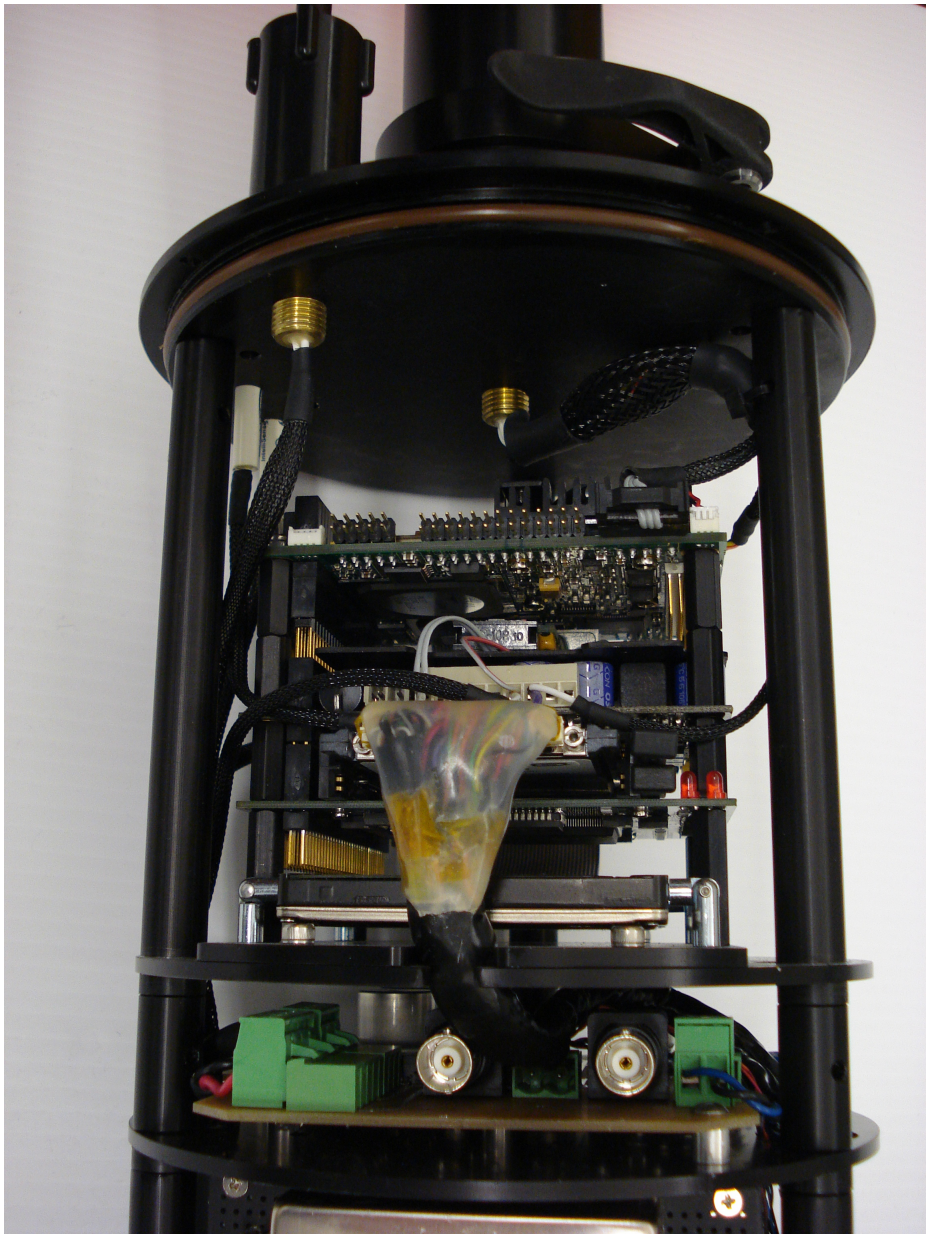

Figure A.2: Photograph of the UGPS satellite computer. The PC-104 computer controls all functionality of the satellite.

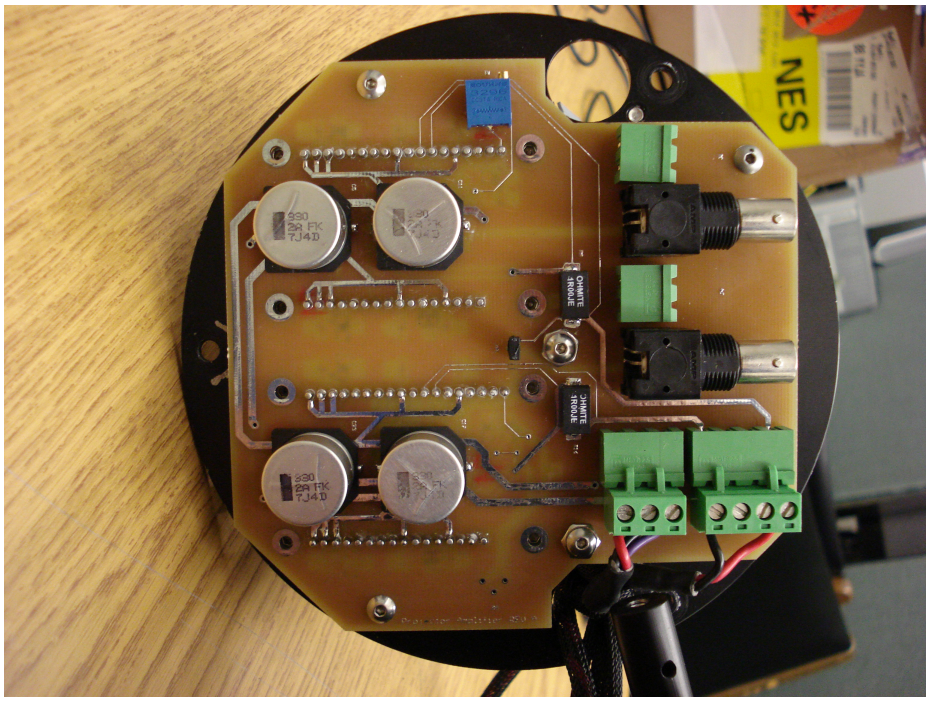

Figure A.3: Photograph of the acoustic projector amplifier in the UGPS satellite.

Figure A.4: Photograph showing the blind stab connectors at the bottom of the UGPS satellite pressure vessel. These connectors allow the majority of the satellite hardware to be removed while the projector stays fixed to the housing.

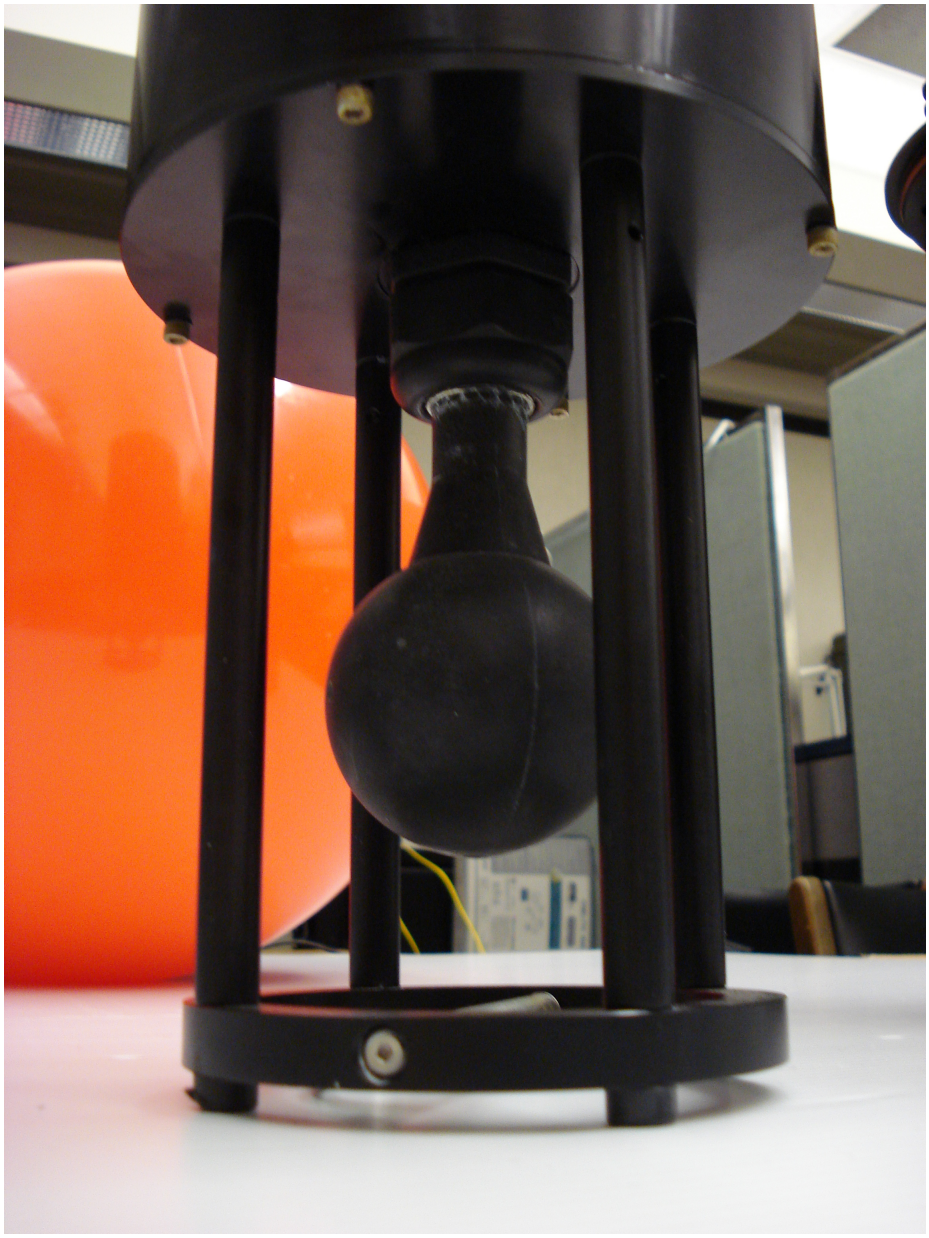

Figure A.5: Photograph of the acoustic projector mounted in the UGPS satellite. Note that the bottom surface of the satellite housing is flat; this surface reflects the acoustic signal from the projector, thereby producing a multi-path signal in the Short Range Accuracy test (Test 1).

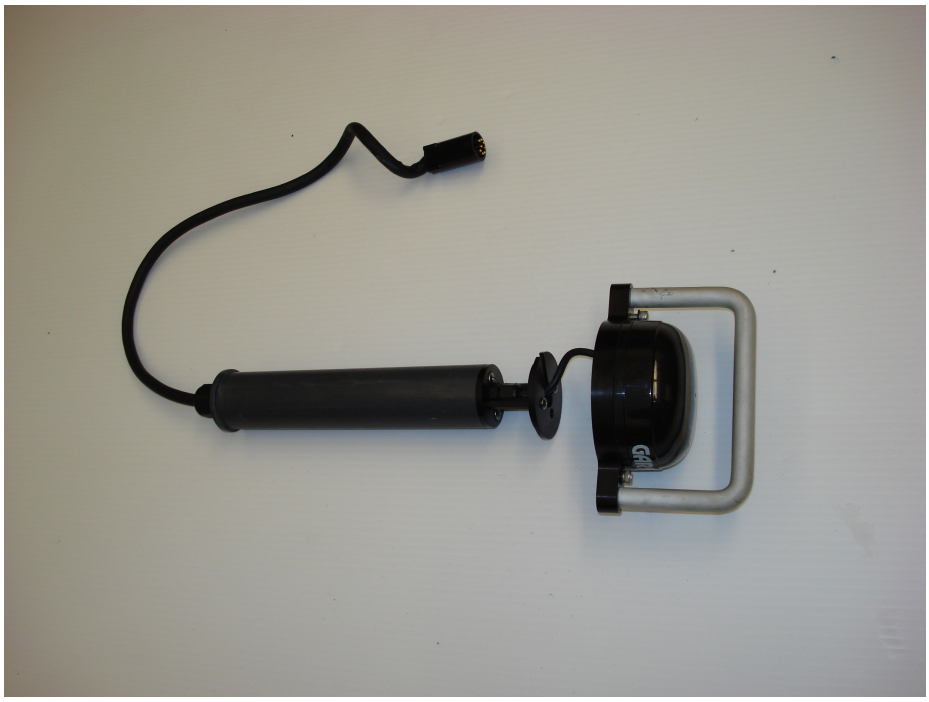

Figure A.6: Photograph of the wireless Ethernet module that is mounted inside the orange float of the UGPS satellite. The Garmin GPS is mounted to the top of the float.

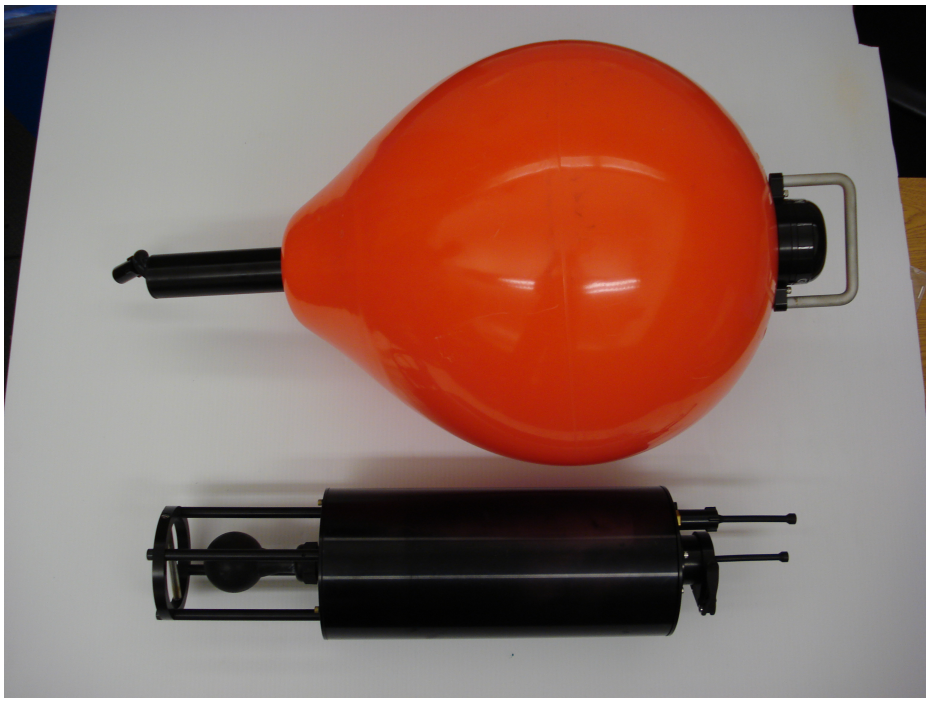

Figure A.7: Photograph of the UGPS satellite in its disassembled state.

Figure A.8: Photograph of the UGPS satellite packed for transport.

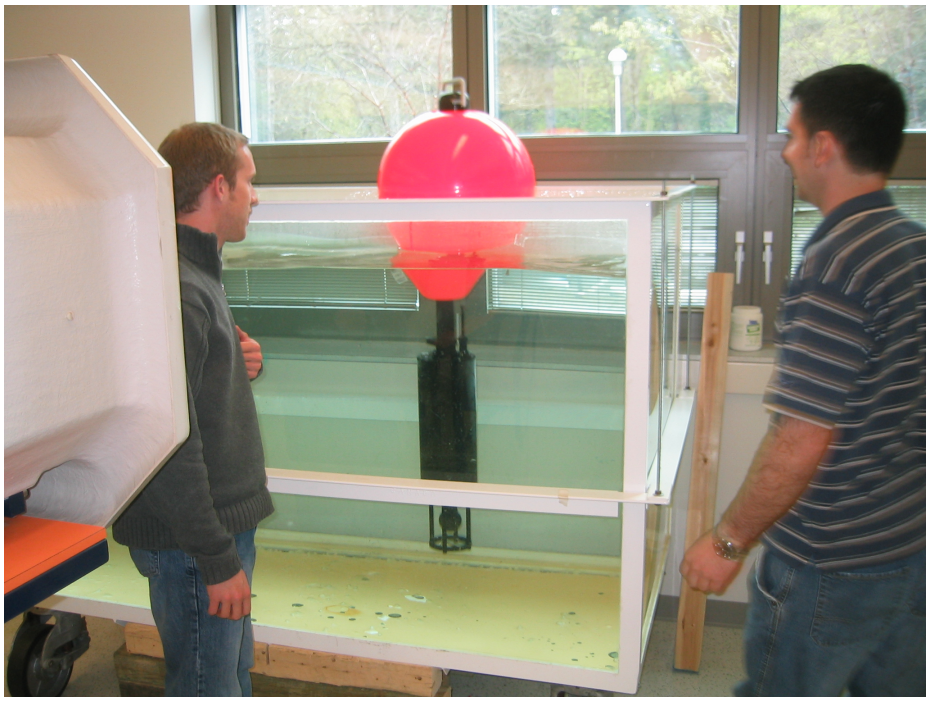

Figure A.9: Photograph of the first tank test of the UGPS satellite.

Figure A.10: Photograph of the UGPS satellite moored for the resolution test (Test 2).

A.1.2 Components of PC104 Computer

Table A.1 contains a list of components that make up the PC-104 computer in the UGPS satellite.

Table A.1: Summary of Components in PC-104 Stack

Component	**Specifications**
Processor board	KONTRON Embedded Computers AG. Kontron MOPSlcd7-PIII/700 MHz, Module with VGA/ LCD, Ethernet & SSD
Analog I/O board	National Instruments NI DAQCard-6062E (for PCMCIA), 500kS/s, 12-Bit Analog Input Multifunction DAQ
PCMCIA board	Aaeon PCM-3116 PC-104 PCMCIA/CompactFlash Module
Hard drive	Samsung 40GB/5400rmp/8M/PATA hard drive
Power supply	Tri-M HESC104 UPS High Efficiency PC/104 Power Supply with Smart Charging

A.1.3 Software

Figures A.11, A.12, A.13, A.14 andA.15 are screen shots of the 5 interface tabs of the UGPS satellite GUI.

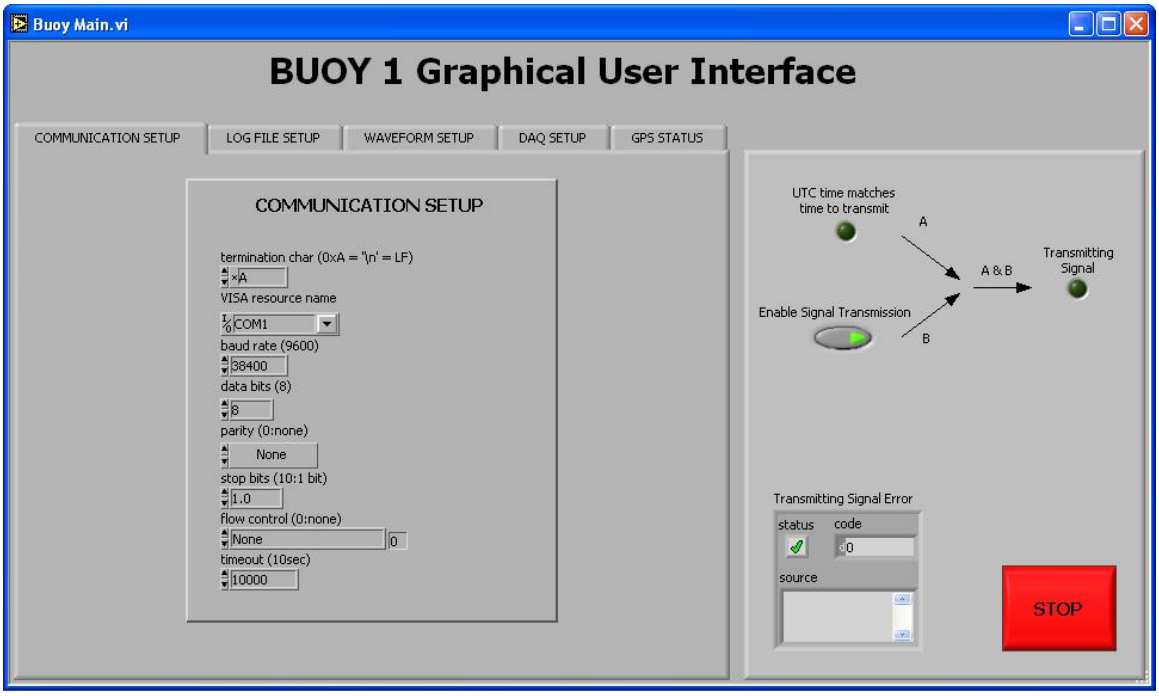

Figure A.11: Graphical user interface of the UGPS satellite, Communications Setup tab. This tab is used to setup the EIA-232 communications interface for the Garmin GPS unit.

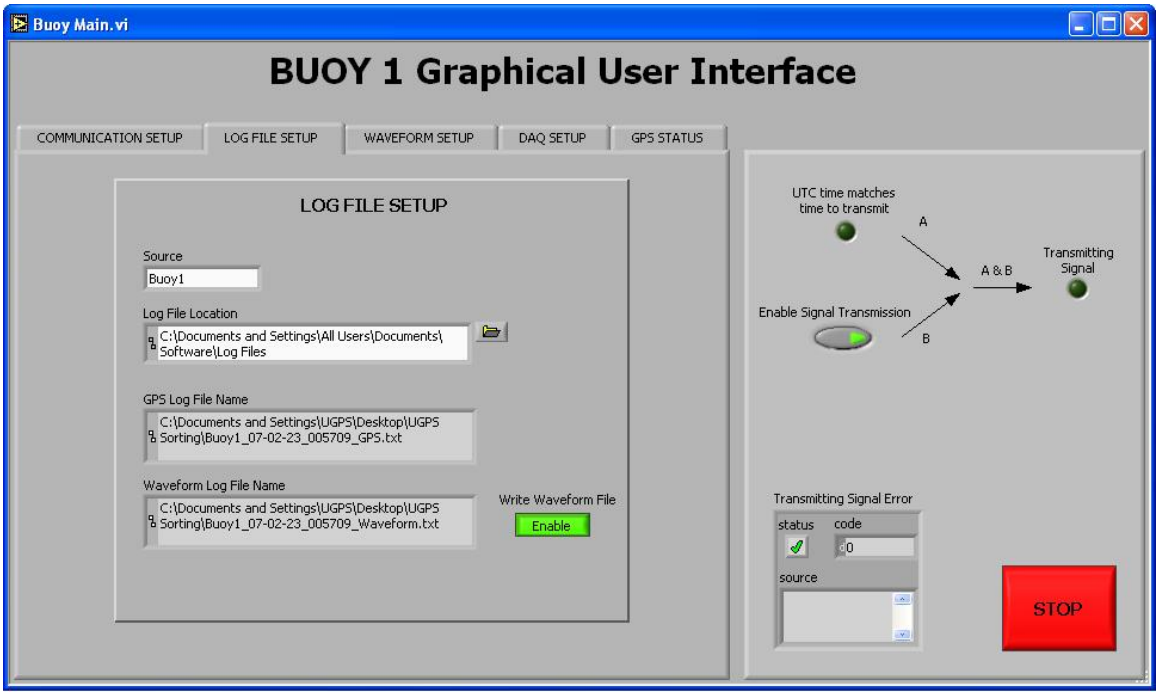

Figure A.12: Graphical user interface of the UGPS satellite, Log File Setup tab. Used to set the location and name of the log files that are created. These log files archive the GPS position of the UGPS satellite and the waveform that is transmitted. The 'Write Waveform File' button allows the user to select whether or not the transmitted waveform is to be logged.

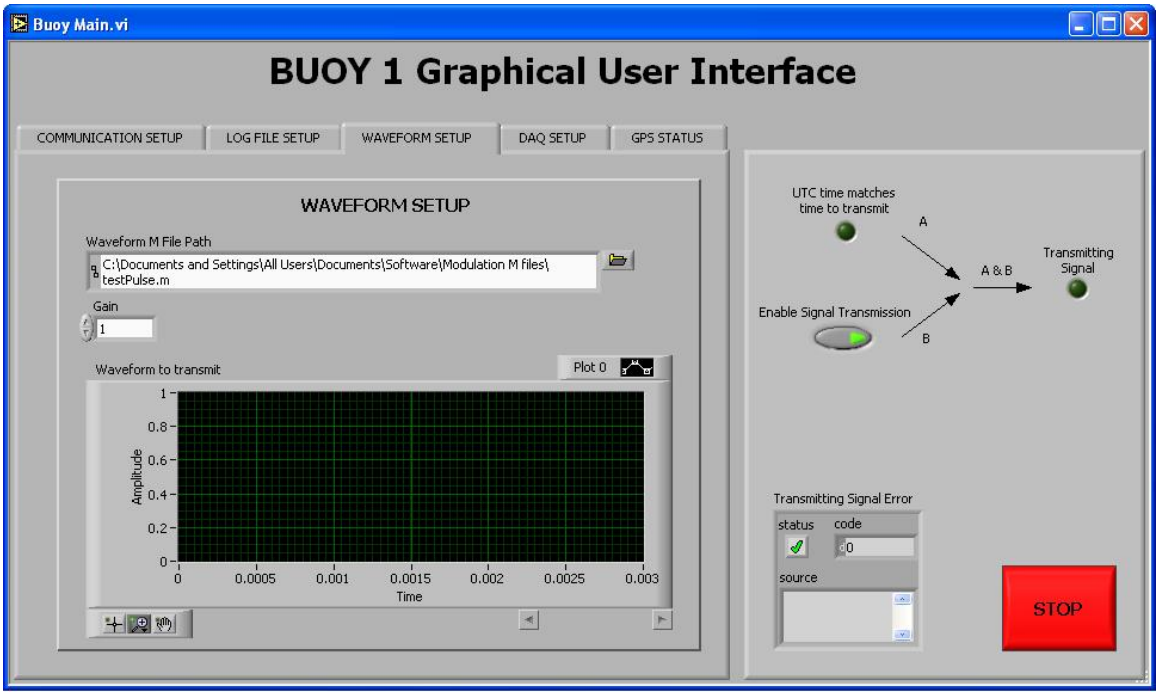

Figure A.13: Graphical user interface of the UGPS satellite, Waveform Setup tab. Used to select the location of the MATLAB file used to generate the transmitted waveform. The user can set the gain of the transmitted signal and inspect the waveform generated from the MATLAB file.

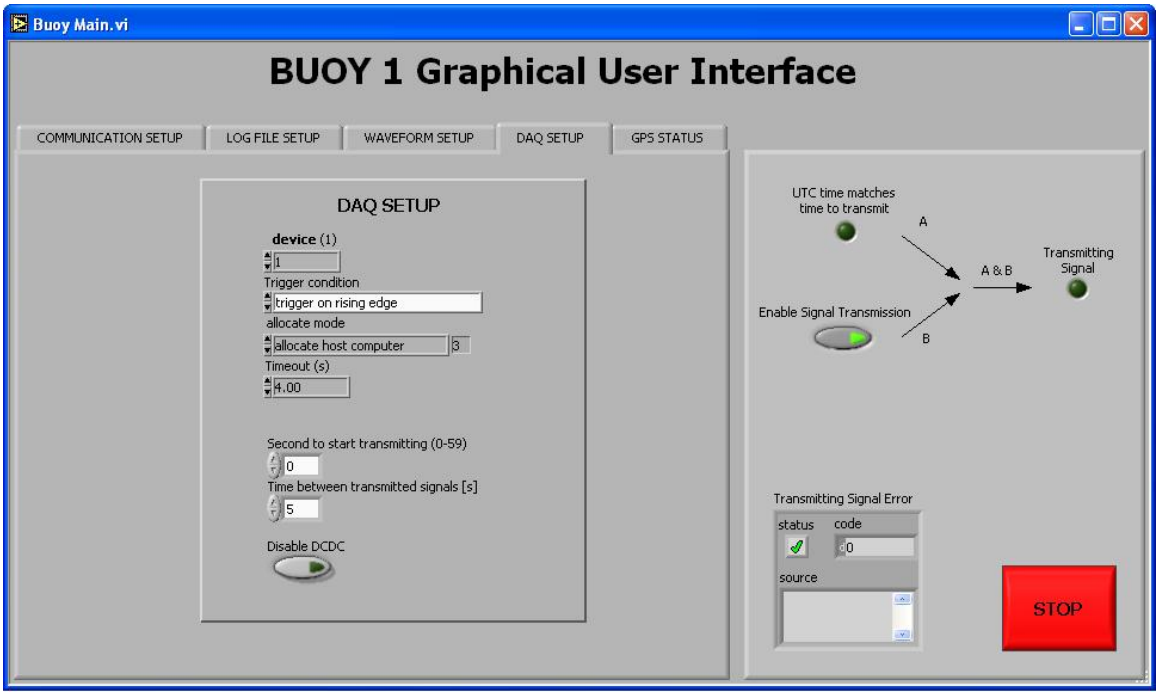

Figure A.14: Graphical user interface of the UGPS satellite, DAQ Setup tab. Setup the various features of the National Instruments DAQ card. The user can select the interval to transmit acoustic signals as well as the time, relative to the start of each UTC synchronized minute, that the signal will be transmitted. Finally the user can disable the DCDC which turns off the acoustic projector.

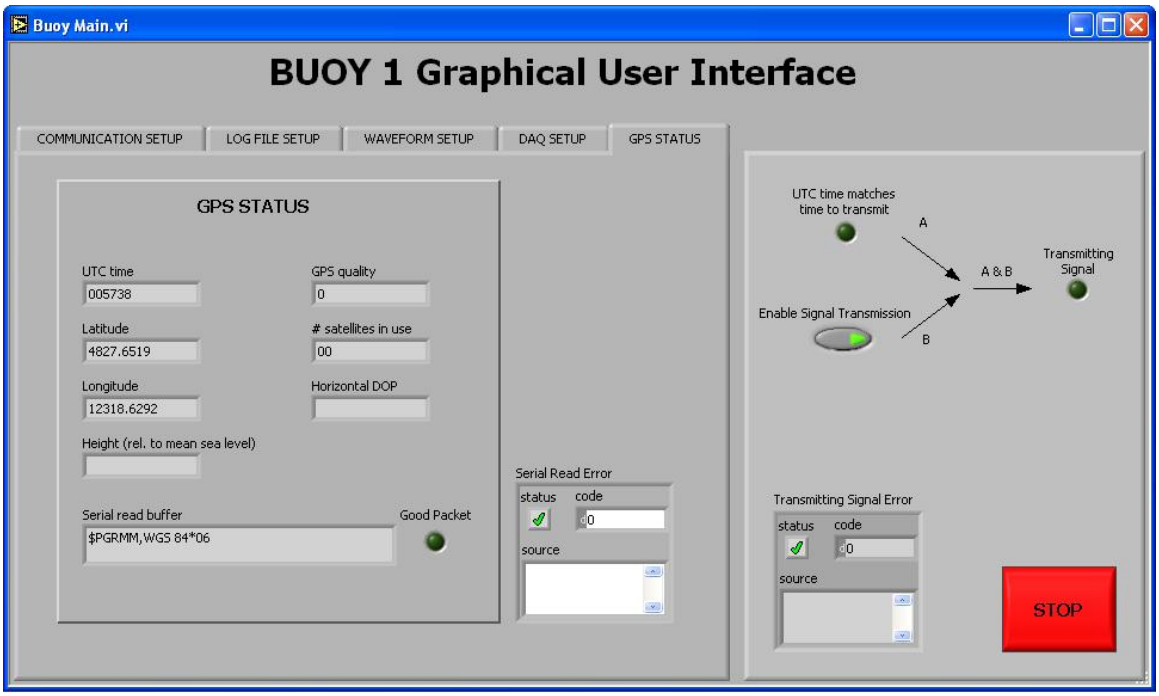

Figure A.15: Graphical user interface of the UGPS satellite, GPS Setup tab. This tab displays information related to the Garmin GPS unit. The user cannot modify GPS settings in this tab, however, the status of the GPS can be observed.

A.2 UGPS Surface Station

A.2.1 Software

Figures A.16, A.17, A.18, A.19, A.20, A.21, A.22 and A.23 are screen shots of the 8 interface tabs of the UGPS receiver GUI.

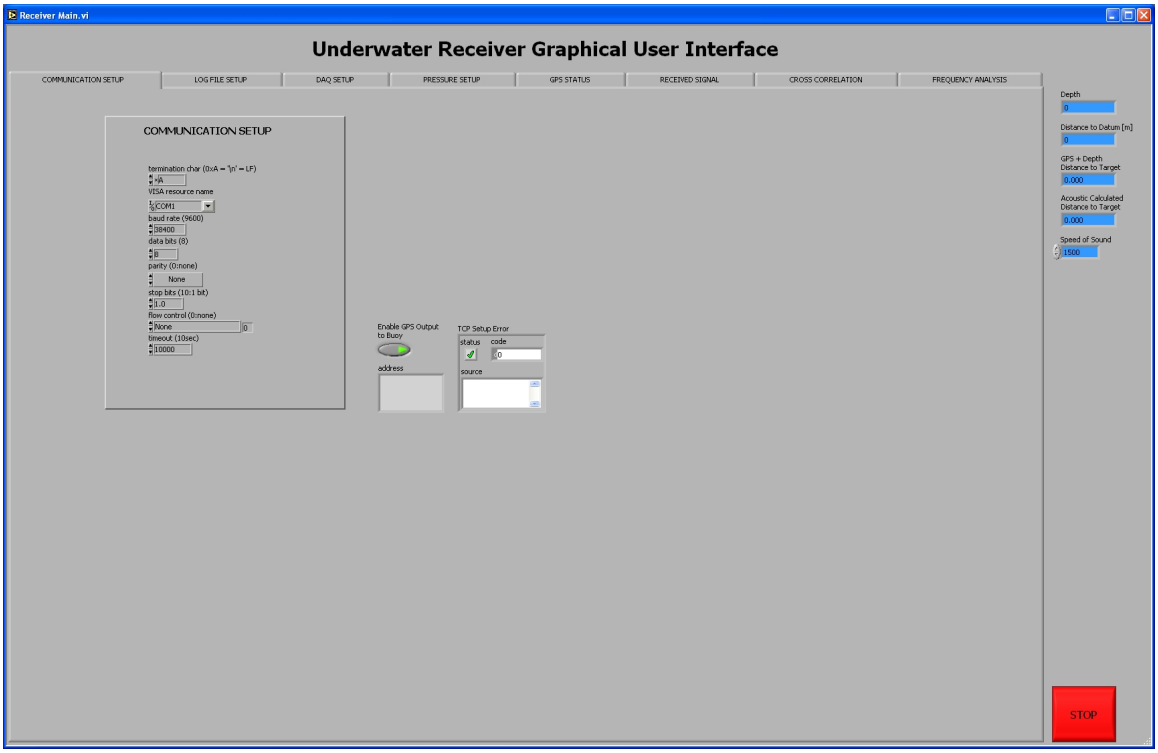

Figure A.16: Graphical user interface of the UGPS receiver, Communications Setup tab. Used to setup the EIA-232 communications interface settings for the Garmin GPS unit.

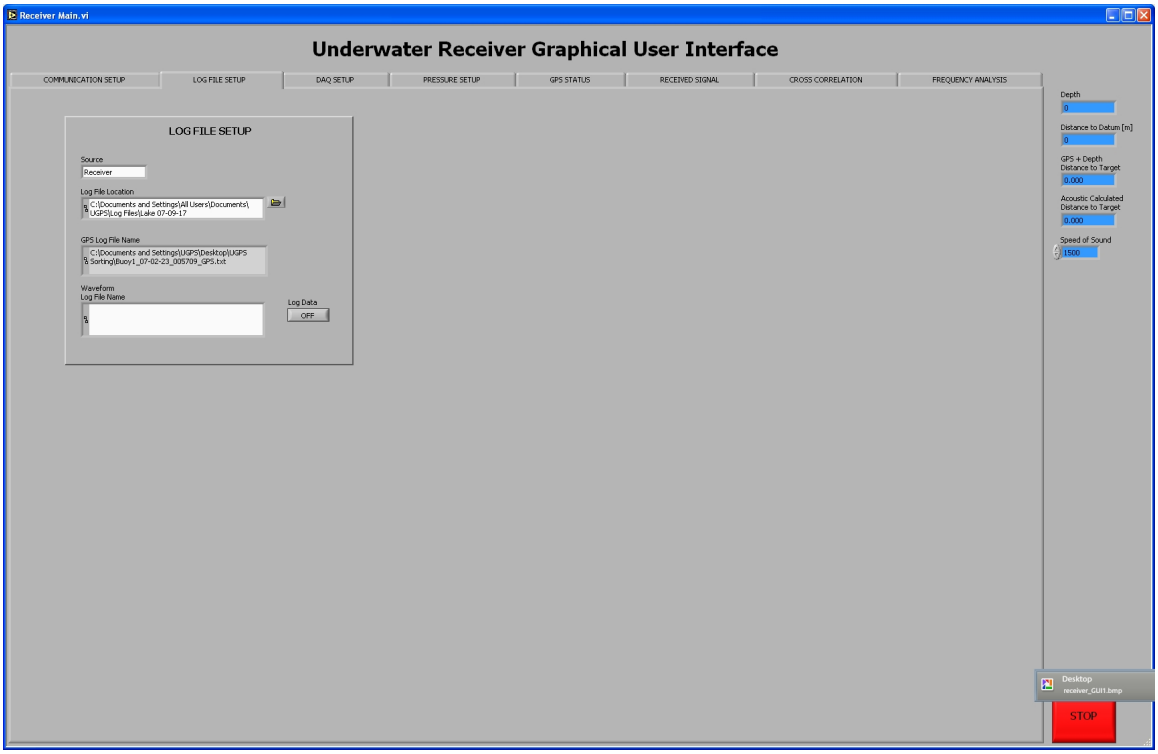

Figure A.17: Graphical user interface of the UGPS receiver, Log File Setup tab. Used to set the location and name of the log files that are created. These log files archive the GPS position of the UGPS receiver and the waveforms that are received. The 'Log Data' button allows the user to select whether or not the waveform is to be logged.

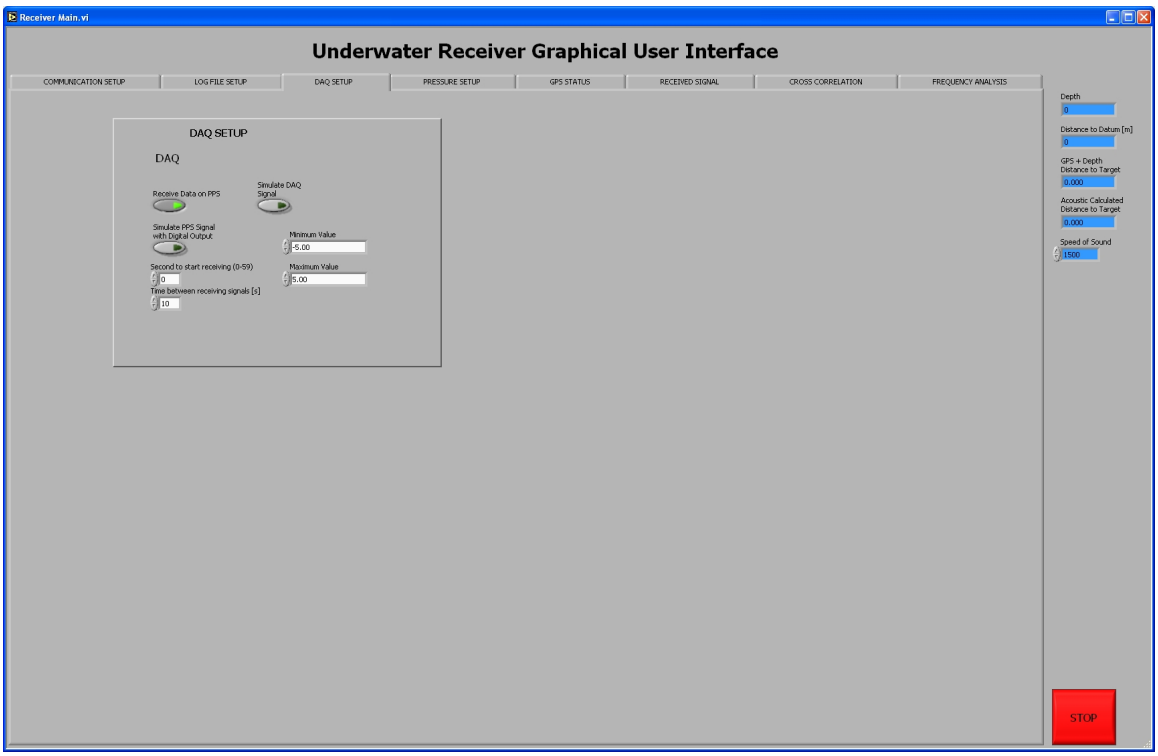

Figure A.18: Graphical user interface of the UGPS receiver, DAQ Setup tab. Setup the various features of the National Instruments DAQ card. The user can select the interval to receive acoustic signals as well as the time, relative to the start of each UTC synchronized minute, that the signal will be received. When testing in an area where GPS signals cannot be received, the user can select the 'Simulate PPS Signal with Digital Output' button to test the functionality of the receiver. Also, if the transducer is not in the water acoustic data can be simulated to test the other functionality of the receiver.

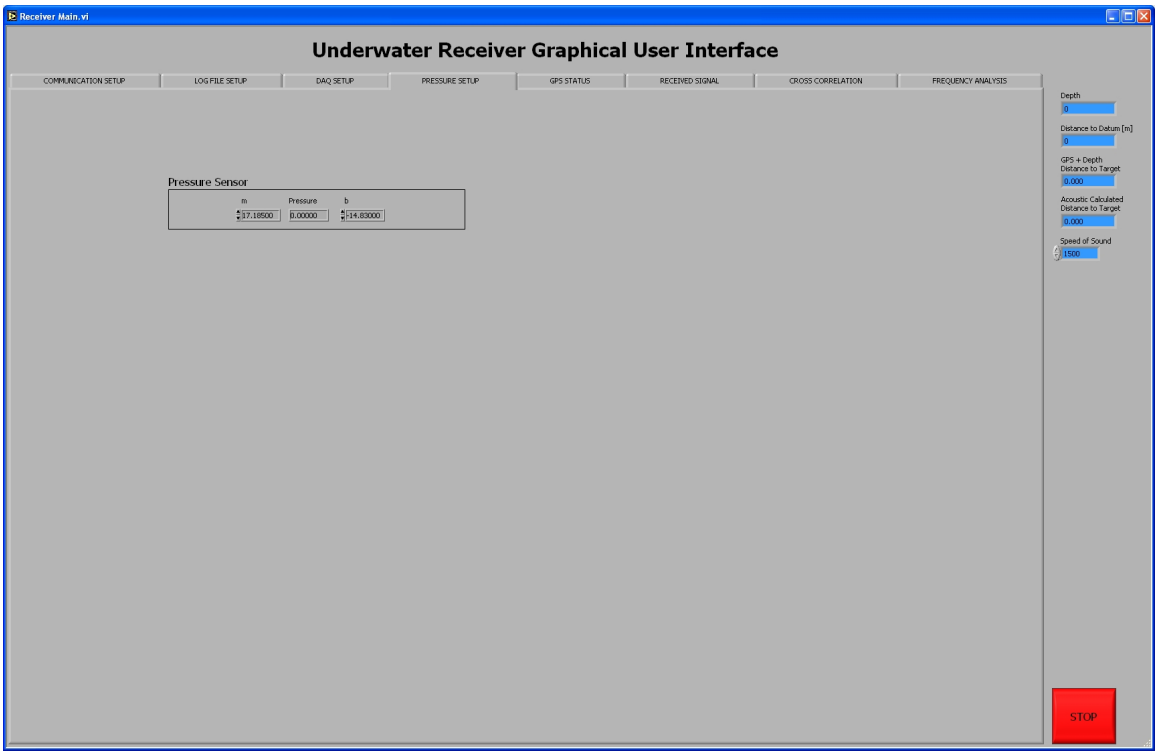

Figure A.19: Graphical user interface of the UGPS receiver, Pressure Setup tab. This tab is used to calibration parameters of the pressure sensor in the UGPS receiver. The pressure sensor has a linear output that must be scaled and offset to convert the raw output voltage into a pressure. The pressure is used to calculate the depth of the receiver.

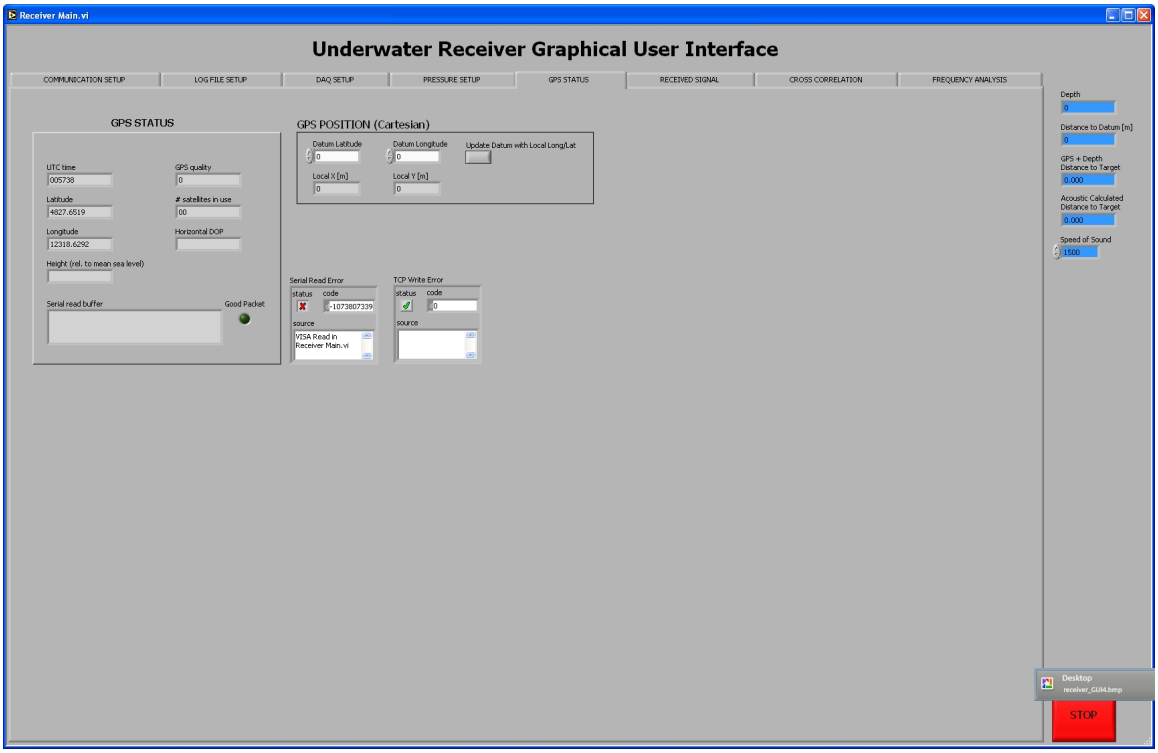

Figure A.20: Graphical user interface of the UGPS receiver, GPS Status tab. This tab displays information related to the Garmin GPS unit. The user cannot modify GPS settings in this tab, however, the status of the GPS can be observed. In addition, a datum can be set so that the position of the receiver is displayed in cartesian coordinates relative to the datum. This is useful feature during field testing because the datum can be set to the position of the UGPS satellite, thereby displaying the position of the receiver relative to the satellite.

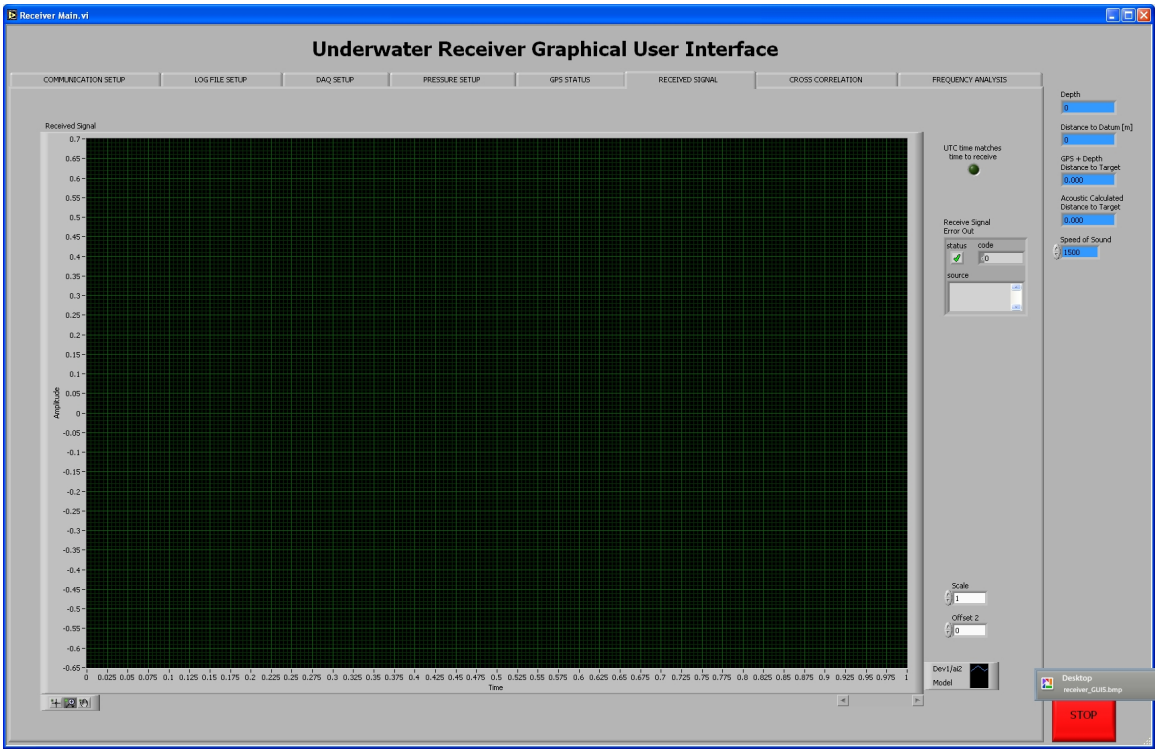

Figure A.21: Graphical user interface of the UGPS receiver, Received Signal tab. In this tab the received signal is graphed. This tab is used to visually inspect the received signal.

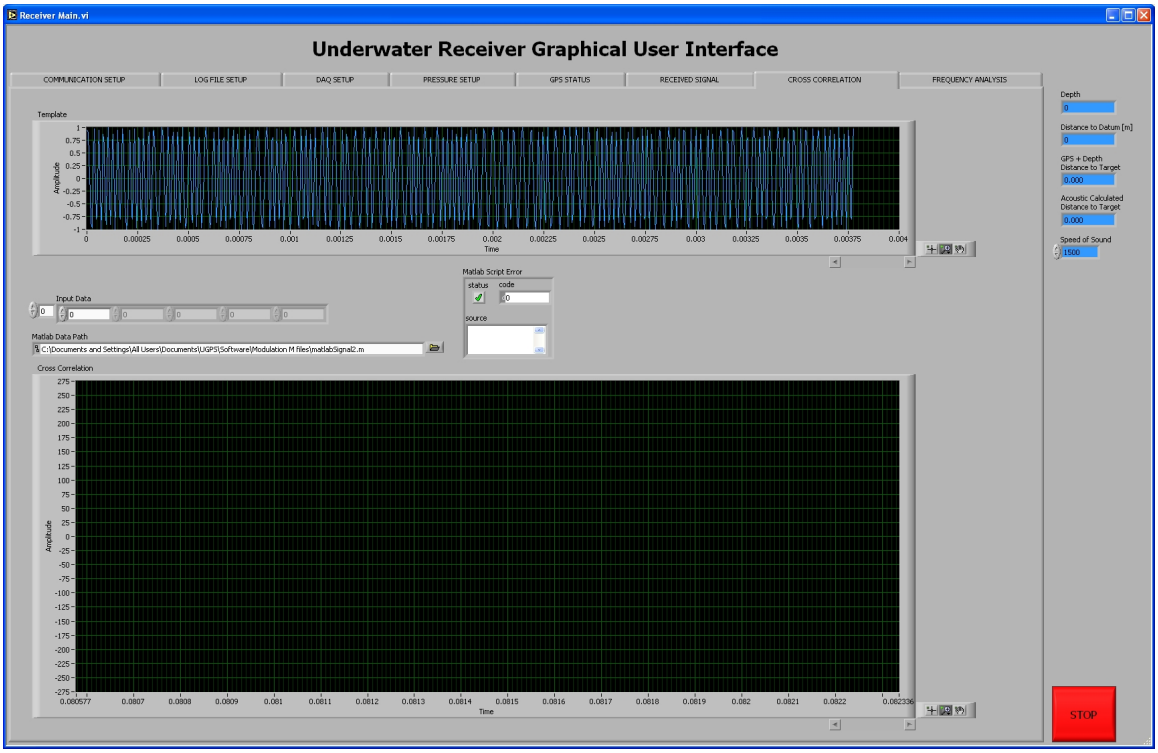

Figure A.22: Graphical user interface of the UGPS receiver, Cross Correlation tab. The received signal is correlated with a local copy of the transmitted waveform emitted by the UGPS satellite. The cross correlation is useful during a test to observe the quality of a received signal.

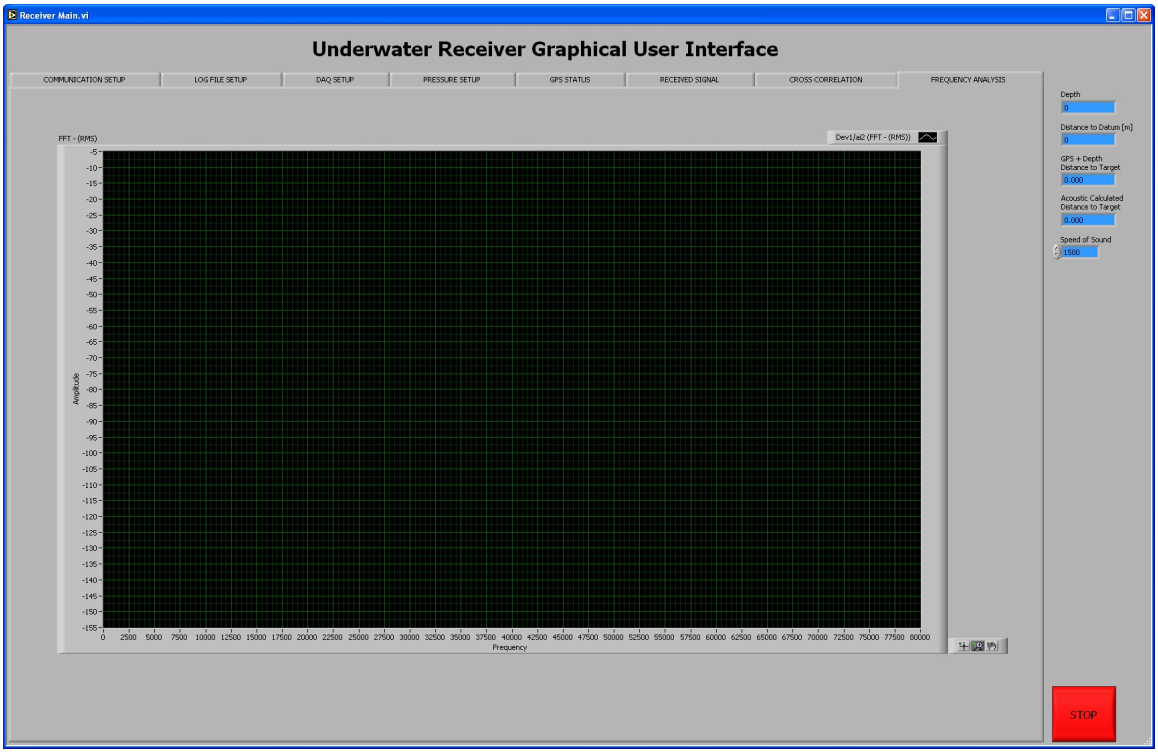

Figure A.23: Graphical user interface of the UGPS receiver, Frequency Analysis tab. Produces a Fast Fourier transform of the received signal. This is useful for identifying the amplitude and frequency of acoustic noise that may affect the quality of the received signal.

Appendix B

ITC 1032 Projector Specifications

ITC-1032

S/N 1146

INTERNATIONAL TRANSDUCER CORP.
Subsidiary of Channel Technologies
869 Ward Drive Santa Barbara, CA 93111

REVISIONS				
ZONE	LTR	DESCRIPTION	DATE	APPROVED
	D	RDRWN & REV'D PER ECO No. 6310 P.G.S	11-23-93	

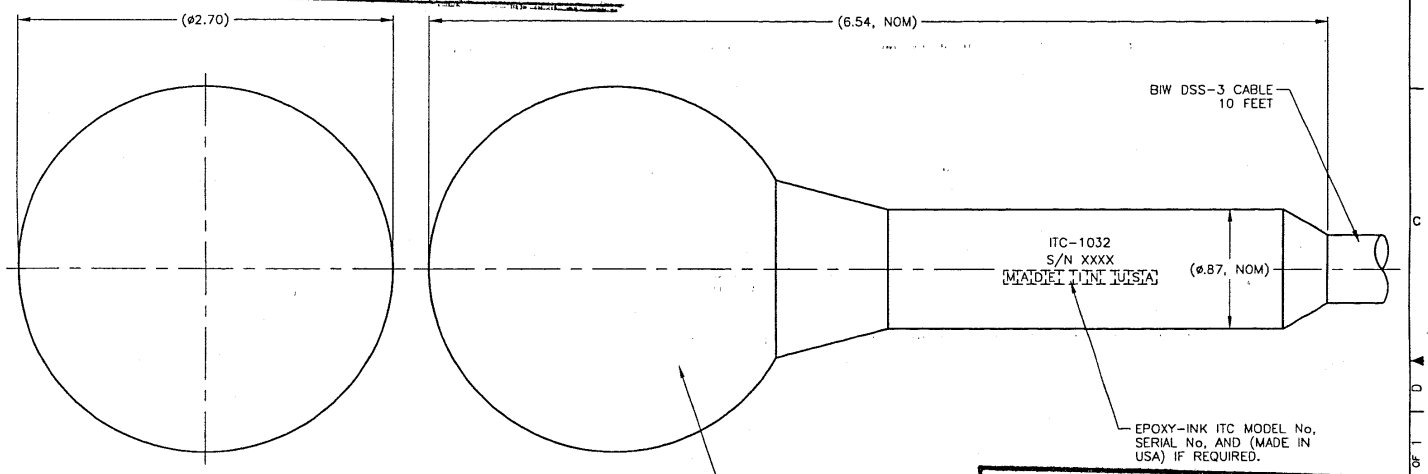

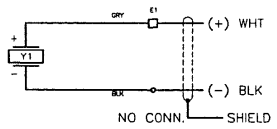

WIRING DIAGRAM (REF)

		UNLESS OTHERWISE SPECIFIED: DIMENSIONS ARE IN INCHES TOLERANCES DECIMALS .XX ± .02 ANGULAR ± — .XXX ± — DO NOT SCALE DRAWING	CONTRACT NO.	INTERNATIONAL TRANSDUCER CORP. SANTA BARBARA, CA 93111-2920
			DRAWN P.G.S DATE 11-23-93	OUTLINE & INSTALLATION ITC 1032
		MATERIAL LISTED	CHECK	
		FINISH NONE	DESIGN	
009761	ITC 1032		DESIGN ACTIVITY	SIZE C | FSCM NO. 17892 | DWG NO. 009760 | REV. D
NEXT ASSY	USED ON	TREATMENT NONE	CUSTOMER	SCALE 2 : 1 | SYS A | PATH C:\COMPLETE | SHEET 1 OF 1
APPLICATION				

009760 SHT 1 OF 1

Polar Plot Hard Copy

FQM_polar_plot_Hard_Copy.vi
c:\LABVIEW\Pamsv17\GQM-2b\Gqm2b_pl.llb\FQM_polar_plot_Hard_Copy.vi
Last modified on 5/3/02 at 7:11 AM
Printed on 11/2/04 at 1:34 PM

UNCLASSIFIED

ITC- 1032 Serial Number 1146

'O' Mark @ 0 degrees

International Transducer Corp.

Test Tank 2
869 Ward Dr. Santa Barbara, CA
Tue, Nov 02, 2004 1:13:31 PM

Directivity Pattern XY Plane
25 kHz

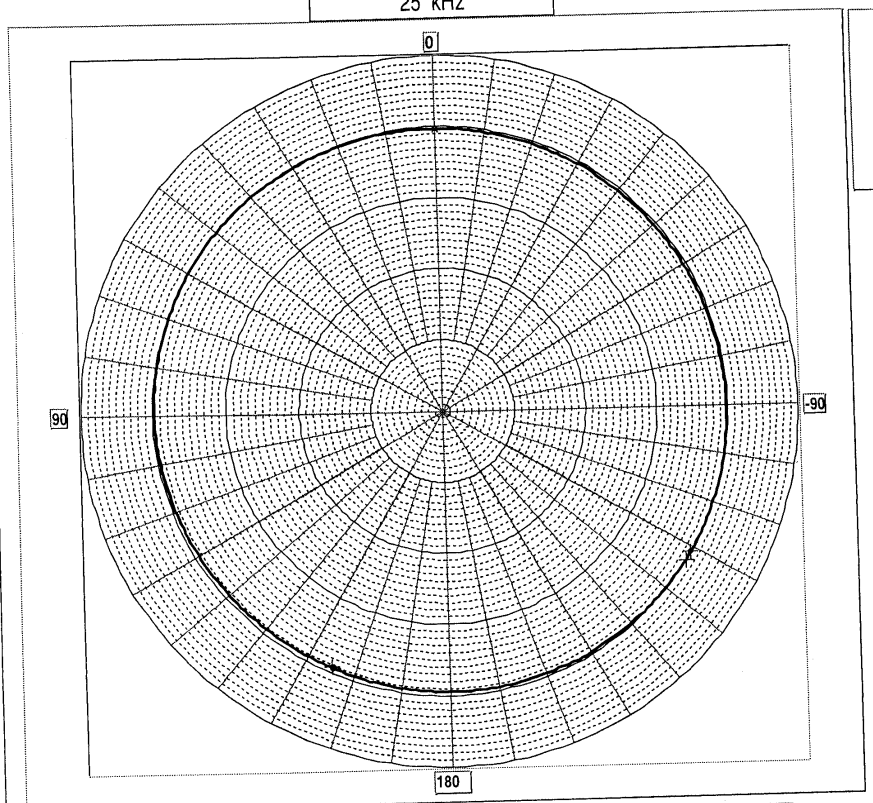

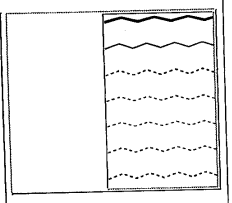

UNCLASSIFIED

Graph Info.

Outer Circle	10 dB
Center	-40 dB
dB/Div	1 dB

	Angle	Ord
Cursor 1	0.00	-0.25
Cursor 2	-204.90	-0.67
Cursor 3	-123.00	-0.09
Cursor 4	-120.90	-0.10

Page 1 Polar Plot Hard Copy

FQM_polar_plot_Hard_Copy.vi
c:\LABVIEW\Pamsv17\GQM-2b\Gqm2b_pl.llb\FQM_polar_plot_Hard_Copy.vi
Last modified on 5/3/02 at 7:11 AM
Printed on 11/2/04 at 2:21 PM

UNCLASSIFIED

ITC-1032 Serial Number 1146 'O' Mark @ 90 degrees cable @ 180 degrees	**International Transducer Corp.** Test Tank 2 869 Ward Dr. Santa Barbara, CA Tue, Nov 02, 2004 1:13:31 PM

Directivity Pattern XZ Plane
25 kHz

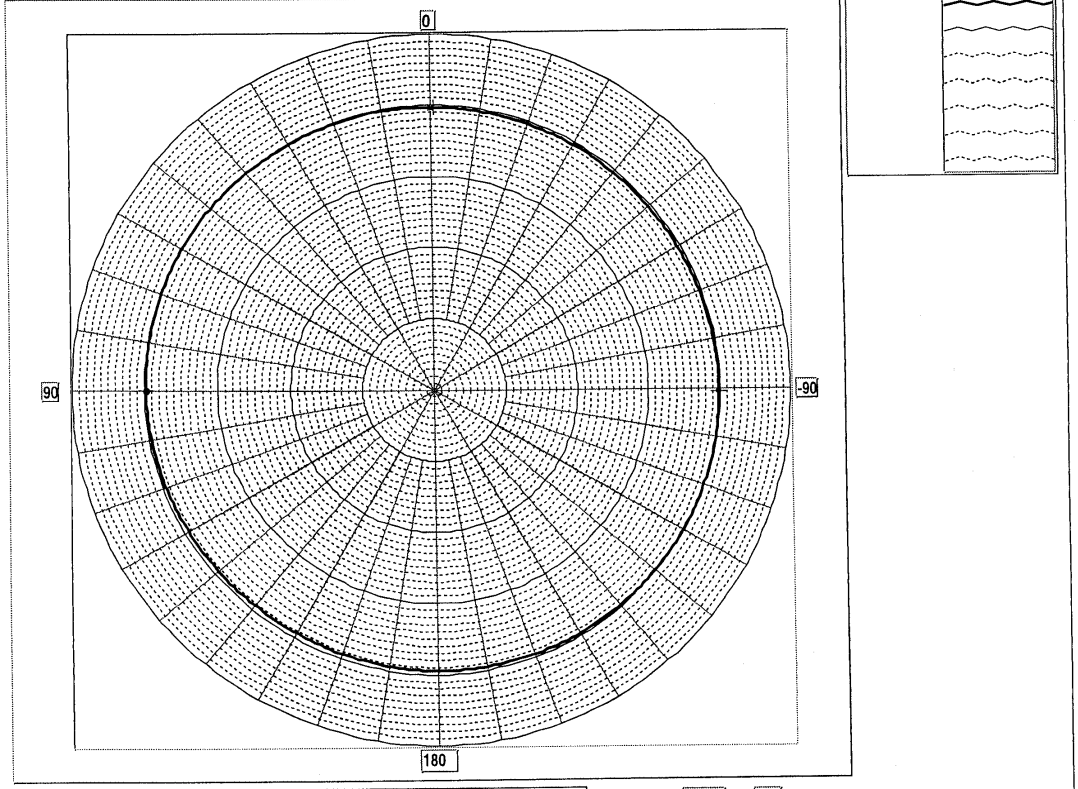

UNCLASSIFIED

Graph Info.

Outer Circle	10 dB
Center	-40 dB
dB/Div	1 dB

	Angle	Ord
Cursor 1	0.00	-0.25
Cursor 2	89.75	-0.25
Cursor 3	-0.50	-0.27
Cursor 4	-90.80	-0.19

UNCLASSIFIED

ITC-1032 Ser. No. 1146 w.o. S1032-04

Capacitance @ 1 kHz.: 32,160 pF Loss Tan : 0.3 % (shl'd to low)
Insulation Resistance @ 1000 Vdc : >1 Gohm +/-,shl'd +,- shl'd/ Water
Water Temp: 18 deg.C
(With DSS-3 Cable)

International Transducer Corp.

Test Tank 2

869 Ward Dr. Santa Barbara, CA

Tue, Nov 02, 2004 1:19:23 PM

WATER ADMITTANCE

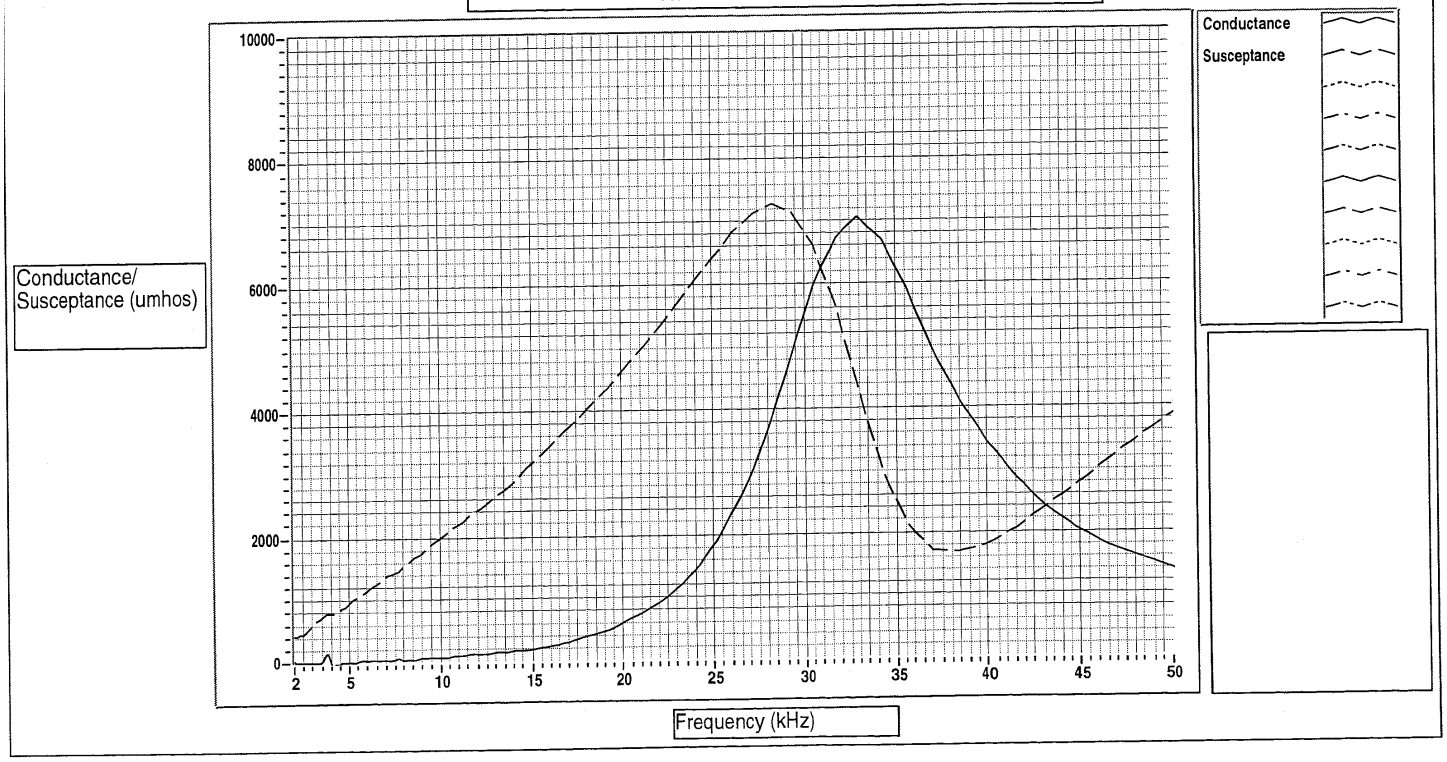

UNCLASSIFIED

ITC-1032 Ser.No. 1146 Response @ 'O' Mark

Test Dist : 2m
Test Depth: 1.5m
Water Temp: 18 deg C
Stand: 6069#9

International Transducer Corp.

Test Tank 2
869 Ward Dr. Santa Barbara, CA
Tue, Nov 02, 2004 1:19:23 PM

Transmit Voltage Response

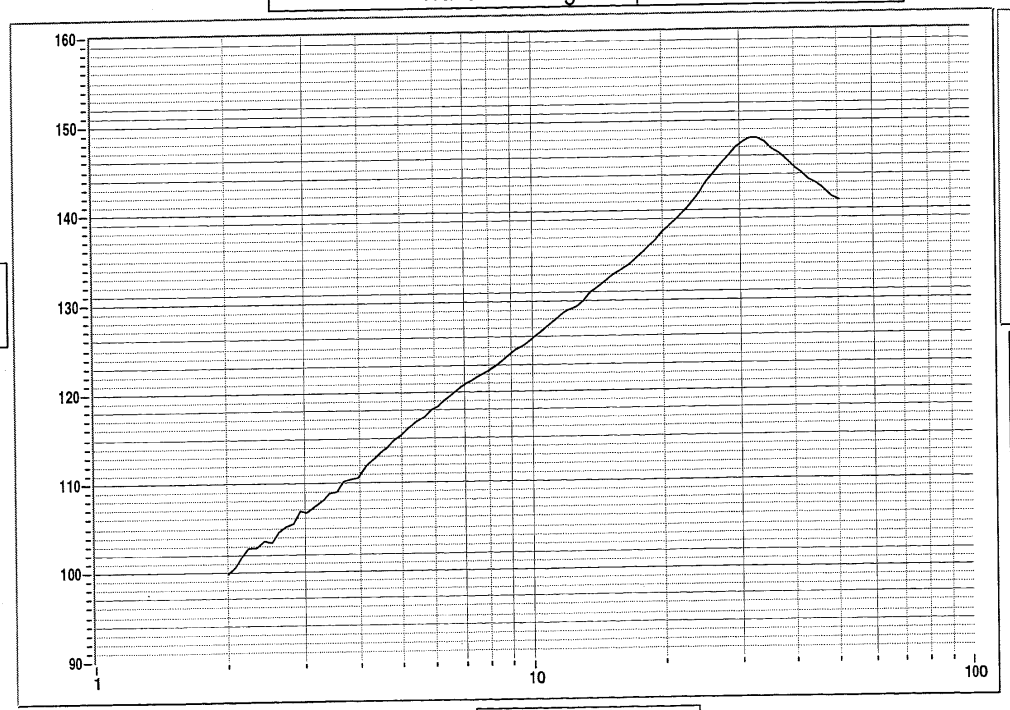

Appendix C

Reson TC4013 Hydrophone Specifications

HYDROPHONE SENSITIVITY

RESON

Under Test:	TC4013-1	Amplitude:	9.5 Vrms	Temperature:	20.67°C 2005 -04- 13
S/N:	1005055	Pulse Width:	1400.0 µs	Depth:	1.0 m
Reference:	TC4033	Rep Rate:	66.7 ms	Distance:	0.50 m
Date:	2005-04-06	Averages:	8	Tested by:	HHP 050406
Session, Run:	956, 37				
Comment:	PHO @ 250Hz: -212.1dB.				

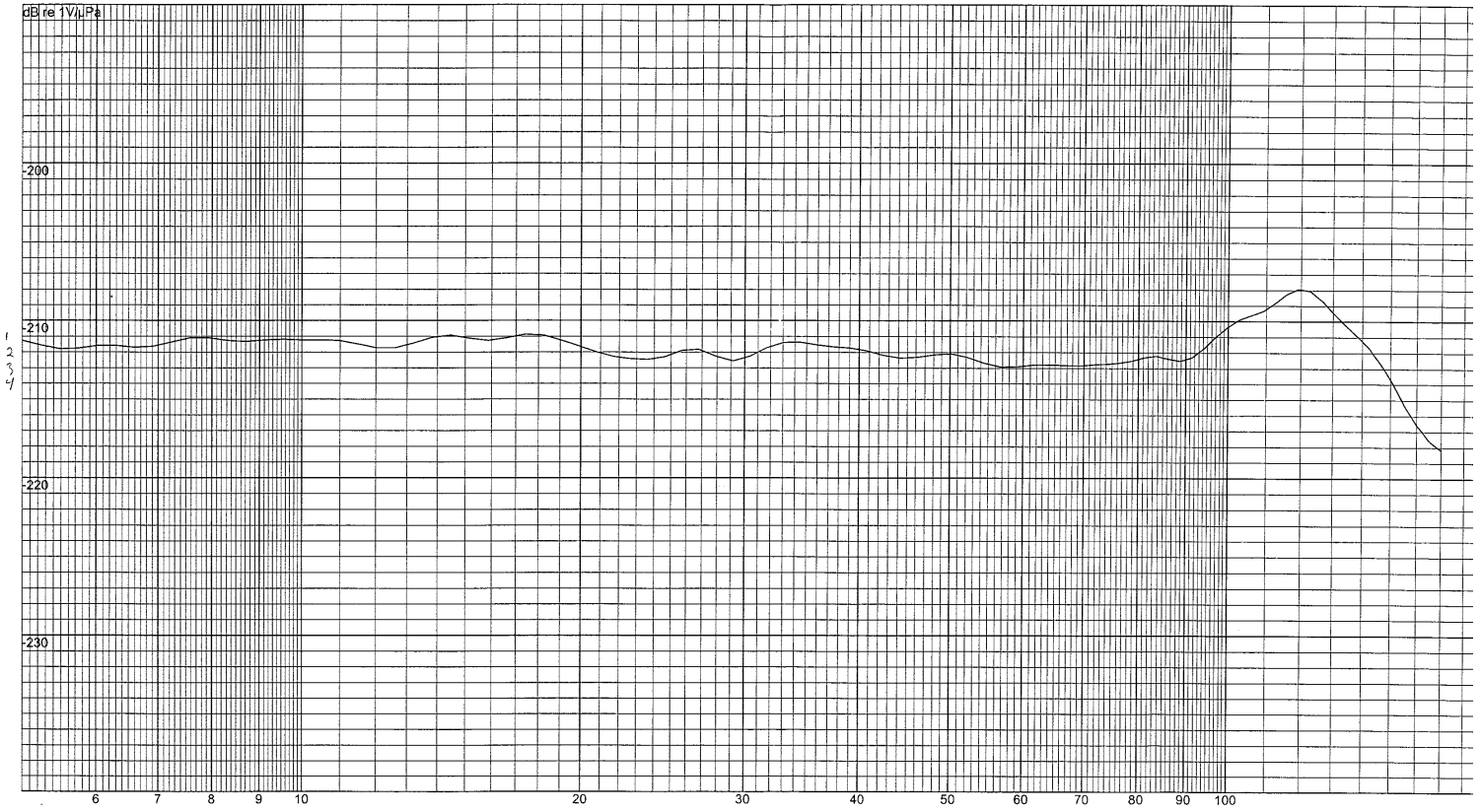

IMPEDANCE SUMARY

RESON

Under Test:	TC4013-1
S/N:	1005055
Date:	2005-04-06
Session, Run:	956, 41
Comment:	

Amplitude:	10.0 Vrms
Pulse Width:	3000.0 µs
Rep Rate:	33.3 ms
Averages:	4

Temperature:	20.67°C
Depth:	1.0 m
Cal Resistor:	0.0 ohms
Tested by:	HHP

2005 -04- 13

050406

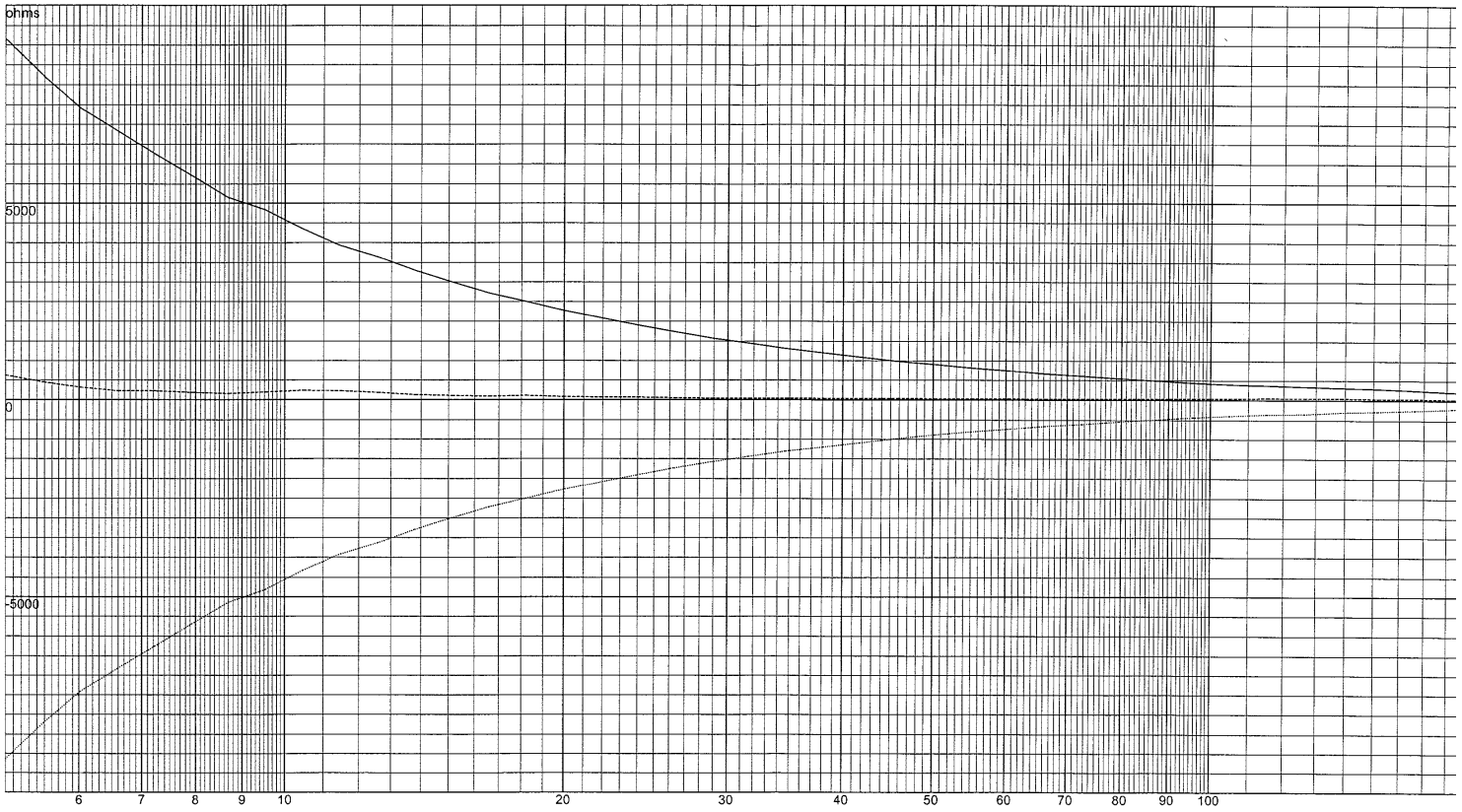

HYDROPHONE DIRECTIVITY

Under Test:	TC4013-1	Amplitude:	20.0 Vrms	Temperature:	20.67°C
S/N:	1005055	Pulse Width:	150.0 µs	Depth:	1.0 m
Reference:	TC4033	Angle:	-180.0° to 180.0°	Distance:	0.50 m
Date:	2005-04-06	Frequency:	100.00 kHz	Tested by:	HHP 050406
Session, Run:	956, 36				
Max RR:	-209.5 dB re 1µPa/V at 1m				
Comment:	Horizontal.				

2005 -04- 13

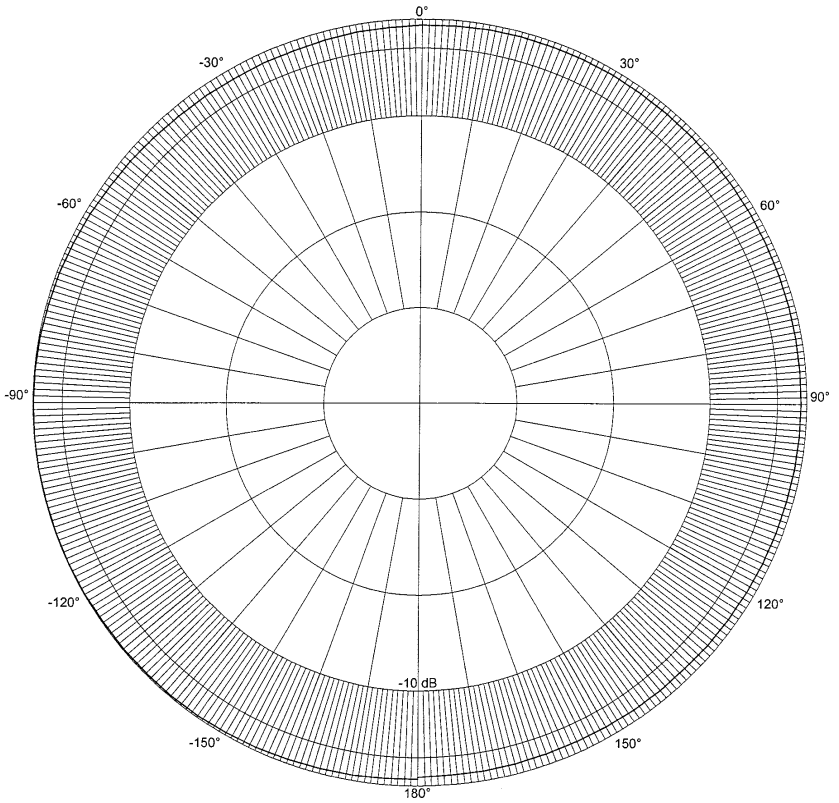

HYDROPHONE DIRECTIVITY

Under Test:	TC4013-1
S/N:	1005055
Reference:	TC4033
Date:	2005-04-06
Session, Run:	955, 10
Max RR:	-209.0 dB re 1µPa/V at 1m
W:	341.4°
Comment:	Vertical.

Amplitude:	10.0 Vrms
Pulse Width:	150.0 µs
Angle:	-180.0° to 180.0°
Frequency:	100.00 kHz

Temperature:	20.74°C
Depth:	1.0 m
Distance:	0.50 m
Tested by:	HHP 050406

2005 -04- 13

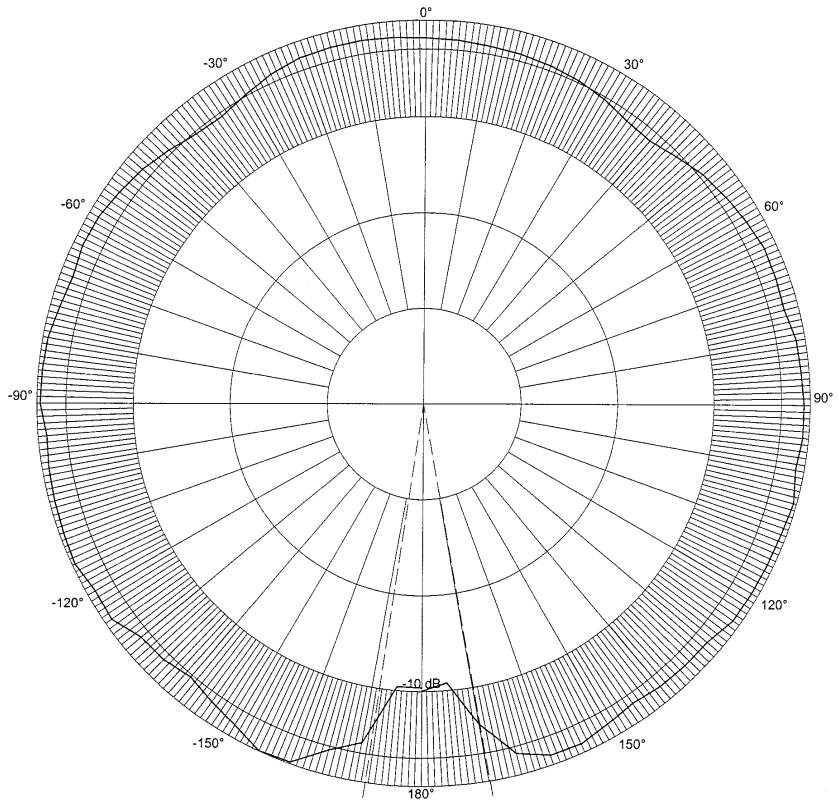

Appendix D

Source Code of the UGPS Model

```
% model of the UGPS satellite data aquisition system

function outputSignal = buoyDAQ(inputSignal)

maxVoltage = 10; % [volts]
minVoltage = -10; % [volts]
resolution = 12; % [bit]
outputFs = 200000; % output sampling frequency [Hz]

halfRange = (maxVoltage - minVoltage)/2; % [volts]
quantization = (maxVoltage - minVoltage) / ((2^resolution) - 1); % [volts/quanta]
inputFs = round(1/inputSignal.Ts); % rounded input sampling frequency [Hz]

% resample the input signal to the output sampling rate (outputFs)
inputResampled = resample(inputSignal.InputData, outputFs, inputFs);

outputResampled = inputResampled;
for m = 1:length(outputResampled)
    % limit the output signal to maxVoltage and minVoltage
    if(outputResampled(m) > maxVoltage)
        outputResampled(m) = maxVoltage;
    elseif(outputResampled(m) < minVoltage)
        outputResampled(m) = minVoltage;
    end
    % quantize the signal
    outputResampled(m) = outputResampled(m) + (halfRange + quantization);
    outputResampled(m) = (outputResampled(m) / quantization) - 1;
    outputResampled(m) = round(outputResampled(m));
    outputResampled(m) = outputResampled(m) * quantization;
    outputResampled(m) = outputResampled(m) - halfRange;
end

outputSignal = iddata(outputResampled, inputResampled, 1/outputFs);
outputSignal.intersample = 'foh';
outputSignal.InputName = 'Buoy DAQ Input Signal';
outputSignal.InputUnit = 'Volt';
outputSignal.OutputName = 'Buoy DAQ Output Voltage';
outputSignal.OutputUnit = 'Volt';
outputSignal.TimeUnit = 'Second';
outputSignal.Name = 'buoyDAQSignal';
```

```
% model of the UGPS satellite projector amplifier

function outputSignal = projectorAmp(inputSignal)

load('projectorAmpModel_20070626');

modelFs = round(1/model.Ts);
inputDataFs = round(1/inputSignal.Ts);
modelData = iddata(resample(inputSignal.InputData, modelFs, inputDataFs),resample↙
(inputSignal.InputData, modelFs, inputDataFs),1/modelFs);
modelData2 = sim(model, modelData);
modelData3 = resample(modelData2.OutputData, inputDataFs, modelFs);

outputSignal = iddata(modelData3,inputSignal.InputData, inputSignal.Ts);
outputSignal.InputName = 'Projector Amplifier Input Voltage';
outputSignal.InputUnit = 'Volt';
outputSignal.OutputName = 'Projector Amplifier Output Voltage';
outputSignal.OutputUnit = 'Volt';
outputSignal.TimeUnit = 'Second';
outputSignal.Name = 'projectorAmpSignal';
```

```
% model of the UGPS satellite projector

function outputSignal = projector(inputSignal)

outputSignal = inputSignal;

TVR_table =           [80 90  100   106 111 115 117 119 121.5   124 126 127.2   128.4↙
129.6   130.8   132 133.2   134.4   135.6   136.8   138 139 140 141 142 143 144 145 146↙
147 147.5   148 148 148 147.59  147.18  146.76  146.35  145.94  145.53  145.12  144.71↙
144.29  143.88  143.47  143.06  142.65  142.24  141.82  141.41  141 141];
freq_table = 1000.*   [0    1   2   3   4   5   6   7   8       9   10  11      12      13↙
14      15  16      17      18      19      20  21  22  23  24  25  26  27  28  29  30↙
31  32  33  34  35  36  37  38  39  40  41  42  43  44  45  46  47  48  49  50 100];

inputFs = round(1/inputSignal.Ts);
outputFs = 2000000;
inputResampled = resample(inputSignal.InputData, outputFs, inputFs);

%%%%%%%%%%%%%%%%%% instantaneous frequency %%%%%%%%%%%%%%%%%%
b = hilbert(inputResampled);
magnitude = abs(b);
magnitude_RMS = magnitude * sqrt(0.5);
phase = angle(b);
instPhase = unwrap(phase);
c = diff(instPhase);
d = [c ; c(length(c))];
instFreq = d /(2*pi*(1/outputFs));
% plot(instFreq); figure;
% plot(decimate(instFreq,5))

for i = 1:length(instFreq)
    if(instFreq(i) > 80000)
        instFreq(i) = 80000;
    elseif (instFreq(i) < 0)
        instFreq(i) = 0;
    end
end
%%%%%%%%%%%%%%%%%%%%%%%%%%%%%%%%%%%%%%%%%%%%%%%%%%%%%%%%%%%%%%%%

TVR = interp1(freq_table, TVR_table, instFreq);
outputResampled = inputResampled .* (10.^( (TVR + 20 .* log10(magnitude_RMS) ) ./ 20) .*↙
10^-6);

outputSignal.OutputData = resample(outputResampled, inputFs, outputFs);
outputSignal.InputName = 'Projector Input Voltage';
outputSignal.InputUnit = 'Volt';
outputSignal.OutputName = 'Projector Output Pressure';
outputSignal.OutputUnit = 'Pascal';
outputSignal.TimeUnit = 'Second';
outputSignal.Name = 'projectorSignal';
```

```
% model of the UGPS acoustic channel (water)

function outputSignal = channel(inputSignal, range, RXdepth, TXdepth)

bottom = 200; % depth of ocean bottom
C = 1480.5;  % sound speed [m/s]
T = 10;    % temperature [degrees C]
SNR = 300;  % signal to noise ratio [dB]

R = sqrt((RXdepth-TXdepth)^2 + range^2) % propagation distance [meters]
R2 = sqrt((RXdepth+TXdepth)^2 + range^2) % surface bounce multi-path
R3 = sqrt(((bottom-TXdepth)+(bottom-RXdepth))^2+range^2) % bottom bounce multi-path
outputSignal = inputSignal;
sampleFreq = round(1/inputSignal.Ts); % Hz

delay = R/C; % delay [seconds]
signal = resample(inputSignal.InputData, 1000000, sampleFreq);

%%%%%%%%%%%%%%%%%% instantaneous frequency %%%%%%%%%%%%%%%%%%
b = hilbert(signal);
% magnitude = abs(b);
phase = angle(b);
instPhase = unwrap(phase);
c = diff(instPhase);
d = [c ; c(length(c))];
instFreq = d / (2*pi*1/1000000);
% figure; plot(instFreq);
for i = 1:length(instFreq)
    if(instFreq(i) > 300000)
        instFreq(i) = 300000;
    elseif (instFreq(i) < 0)
        instFreq(i) = 0;
    end
end

%%%%%%%%%%%%% Transmission Loss %%%%%%%%%%%%%%%%%%%%%%%%%
T = 10;
D = 0.005;
pH = 8;
S = 0.5;
f1 = 0.78*sqrt((S/35))*exp(T/26);
f2 = 42*exp(T/17);
f = instFreq/1000;
alpha = 0.106*(f1*f.^2)./(f1^2+f.^2).*exp((pH-8)/0.56)+0.52*(1+(T/43))*(S/35)*((f2*f.^2)./↙
(f2^2+f.^2))*exp(-D/6)+0.00049*f.^2*exp((-T/27)+(D/17));

SL_DB = 20*log10(R); % spherical spreading loss
AL_DB = alpha*R;
TL_DB = SL_DB + AL_DB; % transmission loss [dB]

TL = 10.^(TL_DB/20); % transmission loss
TLsignal = signal./TL;
```

```
%%%%%%%%%%% Delay %%%%%%%%%%%%%%%%%%%%%%%%%%
% direct path signal with propagation delay
padding = zeros(round(delay*1000000), 1);
delaySignal = [padding ; TLsignal];

% surface multi-path signal with propagation delay
padding2 = zeros(round(R2/C*1000000), 1);
delaySignal2 = [padding2 ; TLsignal];

% ocean bottom multi-path signal with propagation delay
padding3 = zeros(round(R3/C*1000000), 1);
delaySignal3 = [padding3 ; TLsignal];

% add zeros at the end of the direct path signal to make it the same length
% as the multi-path signal
longestLength = length(delaySignal2)-length(delaySignal);
delaySignal = [delaySignal ; zeros(longestLength, 1)];

% combine direct path and multi-path signals
combinedSignal = delaySignal - delaySignal2;

%%%%%%%%%%%%%%% DOPPLER SHIFT %%%%%%%%%%%%%%%%%%%%%%%%%%%%%%%%%%%%%%%%%%%%
dopplerSignal = resample(combinedSignal,14805,14805);
dopplerSignal2 = [dopplerSignal zeros(1, length(combinedSignal) - length(dopplerSignal))];

%%%%%%%%%%%%%%% Noise %%%%%%%%%%%%%%%%%%%%%%
noiseSignal = awgn(dopplerSignal2, SNR);

%%%%%%%%%%%%%%% OUTPUT SIGNAL %%%%%%%%%%%%%%%%%%%%%%%%%%%%%%%%%%%%%%%%%%%%

noiseSignal = resample(noiseSignal, sampleFreq, 1000000);
padding4 = zeros(length(noiseSignal)-length(inputSignal.InputData), 1);

outputSignal = iddata(noiseSignal, [inputSignal.InputData ; padding4], inputSignal.Ts);
outputSignal.intersample = 'foh';
outputSignal.InputName = 'Channel Input Pressure';
outputSignal.InputUnit = 'Pascal';
outputSignal.OutputName = 'Channel Output Pressure';
outputSignal.OutputUnit = 'Pascal';
outputSignal.TimeUnit = 'Second';
outputSignal.Name = 'channelSignal';
```

```
% model of the UGPS receiver hydrophone

function outputSignal = hydrophone(inputSignal)

outputSignal = inputSignal;

freq_table = 1000*[0    1   2   3   4   5   6   7   8   9   10  11  12  13  14  15  16  17↙
18  19  20  21  22  23  24  25  26  27  28  29  30  31  32  33  34  35  36  37  38  39  40↙
41  42  43  44  45  46  47  48  49  50  51  52  53  54  55  56  57  58  59  60  61  62  63↙
64  65  66  67  68  69  70  71  72  73  74  75  76  77  78  79  80  81  82  83  84  85  86↙
87  88  89  90  91  92  93  94  95  96  97  98  99  100];
OCV_table = [-211.3 -211.3  -211.3  -211.3  -211.3  -211.3  -211.6  -211.5  -211.1  -211.2↙
-211.2  -211.2  -211.8  -211.5  -211    -211.1  -211.2  -211    -210.9  -211.3  -211.6↙
-212.1  -212.3  -212.4  -212.3  -212.1  -211.8  -212    -212.3  -212.5  -212.4  -212↙
-211.6  -211.4  -211.3  -211.4  -211.5  -211.6  -211.7  -211.8  -211.9  -212    -212.1↙
-212.2  -212.3  -212.3  -212.3  -212.2  -212.2  -212.1  -212.1  -212.23 -212.36 -212.49↙
-212.62 -212.75 -212.88 -213    -212.9  -212.9  -212.9  -212.8  -212.8  -212.8  -212.8↙
-212.8  -212.8  -212.8  -212.8  -212.8  -212.8  -212.8  -212.7  -212.7  -212.7  -212.6↙
-212.6  -212.6  -212.5  -212.5  -212.4  -212.4  -212.3  -212.2  -212.2  -212.3  -212.3↙
-212.4  -212.4  -212.5  -212.4  -212.3  -212.1  -212    -211.78 -211.56 -211.34 -211.12↙
-210.9  -210.68 -210.4];

%%%%%%%%%%%%%%%%%% instantaneous frequency %%%%%%%%%%%%%%%%%%

b = hilbert(inputSignal.InputData);
magnitude = abs(b);
magnitude_RMS = magnitude * sqrt(0.5);
phase = angle(b);
instPhase = unwrap(phase);
c = diff(instPhase);
d = [c ; c(length(c))];
instFreq = d * (1/inputSignal.Ts)/(2*pi);

for i = 1:length(instFreq)
    if(instFreq(i) > 80000)
        instFreq(i) = 80000;
    elseif (instFreq(i) < 0)
        instFreq(i) = 0;
    end
end
%%%%%%%%%%%%%%%%%%%%%%%%%%%%%%%%%%%%%%%%%%%%%%%%%%%%%%%%%%%%%%%%%%%

OCV = interp1(freq_table,OCV_table,instFreq);
outputSignal.OutputData = inputSignal.InputData .* 10^6 .* 10.^(OCV/20);
outputSignal.InputName = 'Hydrophone Input Pressure';
outputSignal.InputUnit = 'Pressure';
outputSignal.OutputName = 'Hydrophone Output Voltage';
outputSignal.OutputUnit = 'Volt';
outputSignal.TimeUnit = 'Second';
outputSignal.Name = 'hydrophoneSignal';
```

```
% model of the UGPS receiver hydrophone amplifier

function outputSignal = hydrophoneAmp(inputSignal)

load('hydrophoneAmpModel_20070626');

modelFs = 1000000;
inputDataFs = round(1/inputSignal.Ts);
modelData = iddata([],resample(inputSignal.InputData,modelFs,inputDataFs),1/modelFs);
modelData2 = sim(model, modelData);
clear model;
modelData3 = resample(modelData2.OutputData, inputDataFs, modelFs);
outputSignal = iddata(modelData3,inputSignal.InputData, inputSignal.Ts);

outputSignal.InputName = 'Hydrophone Amplifier Input Voltage';
outputSignal.InputUnit = 'Volt';
outputSignal.OutputName = 'Hydrophone Amplifier Output Voltage';
outputSignal.OutputUnit = 'Volt';
outputSignal.TimeUnit = 'Second';
outputSignal.Name = 'hydrophoneAmpSignal';
```

```
% model of the UGPS receiver data aquisition system

function outputSignal = receiverDAQ(inputSignal)

maxVoltage = 5; % [volts]
minVoltage = -5; % [volts]
resolution = 16; % [bit]
outputFs = 500000; % output sampling frequency [Hz]

halfRange = (maxVoltage - minVoltage)/2; % [volts]
quantization = (maxVoltage - minVoltage) / ((2^resolution) - 1); % [volts/quanta]
inputFs = round(1/inputSignal.Ts); % rounded input sampling frequency [Hz]

% resample the input signal to the output sampling rate (outputFs)
inputResampled = resample(inputSignal.InputData, outputFs, inputFs);

outputResampled = inputResampled;
for m = 1:length(outputResampled)
    % limit the output signal to maxVoltage and minVoltage
    if(outputResampled(m) > maxVoltage)
        outputResampled(m) = maxVoltage;
    elseif(outputResampled(m) < minVoltage)
        outputResampled(m) = minVoltage;
    end

    % quantize the signal
    outputResampled(m) = outputResampled(m) + (halfRange + quantization);
    outputResampled(m) = (outputResampled(m) / quantization) - 1;
    outputResampled(m) = round(outputResampled(m));
    outputResampled(m) = outputResampled(m) * quantization;
    outputResampled(m) = outputResampled(m) - halfRange;
end

outputSignal = iddata(outputResampled, inputResampled, 1/outputFs);
outputSignal.intersample = 'foh';
outputSignal.InputName = 'Receiver DAQ Input Signal';
outputSignal.InputUnit = 'Volt';
outputSignal.OutputName = 'Receiver DAQ Output Voltage';
outputSignal.OutputUnit = 'Volt';
outputSignal.TimeUnit = 'Second';
outputSignal.Name = 'receiverDAQSignal';
```

Bibliography

[1] (2009) VENUS website. [Online]. Available: http://venus.uvic.ca

[2] K. Asakawa, H. Yoshida, H. Ochi, H. Mikada, K. Kawaguchi, K. Mitsuzawa, and Y. Shirasaki, "Cabled ocean observatory network of next-generation and AUV's role," *Intelligent Mechatronics and Automation, 2004. Proceedings. 2004 International Conference on*, pp. 218–223, 26-31, 2004.

[3] M. Whitford, "In the swim." *GPS World*, vol. 16, no. 4, pp. p14 – 22, 20050401. [Online]. Available: http://ezproxy.library.uvic.ca/login?url=http://search.ebscohost.com/login.aspx?direct=true&db=mth&AN=16695238&loginpage=Login.asp&site=ehost-live&scope=site

[4] B. Howe and J. Miller, "Integrated acoustics systems for ocean observatories," *Scientific Use of Submarine Cables and Related Technologies, 2003. The 3rd International Workshop on*, pp. 51–56, June 2003.

[5] K. Shirai, J. Akizono, and T. Hirabayashi, "Development of underwater ultrasonic positioning system for construction machines," *Underwater Technology, 2004. UT '04. 2004 International Symposium on*, pp. 139–144, April 2004.

[6] R. Somaraju and J. Trumpf, "Frequency, temperature and salinity variation of the permittivity of seawater," *Antennas and Propagation, IEEE Transactions on*, vol. 54, no. 11, pp. 3441–3448, Nov. 2006.

[7] R. J. Urick, *Principles of Underwater Sound*, 3rd ed., D. Heiberg and J. Davis, Eds. McGraw-Hill Book Company, 1983.

[8] A. El-Rabbany, *Introduction to GPS, The Global Positioning System*, 2nd ed. Artech House, 2006.

[9] J. b.-Y. Tsui, *Fundamentals of Global Positioning System Receivers A Software Approach*, K. Chang, Ed. John Wiley & Sons, Inc., 2000.

[10] (2009) Graphic of GPS segments. [Online]. Available: http://www.somerwil.nl/gps/images/stories/gps/SEGMENTS.gif

[11] E. Rowan, "LBL Underwater Positioning," *Hydro International*, vol. 12, no. 1, January/February 2008.

[12] R. Stokey and T. Austin, "The navicomputer: a portable long baseline navigation system designed for interface to an autonomous underwater vehicle," *OCEANS 2000 MTS/IEEE Conference and Exhibition*, vol. 3, pp. 2115–2121 vol.3, 2000.

[13] (2009) Acoustic underwater positioning and navigation systems HiPAP and HPR. [Online]. Available: http://www.km.kongsberg.com/ks/web/nokbg0240.nsf/AllWeb/FF57C18363FAD917C1256A7E002B9F2F?OpenDocument

[14] T. Austin, "The application of spread spectrum signaling techniques to underwater acoustic navigation," *Autonomous Underwater Vehicle Technology, 1994. AUV '94., Proceedings of the 1994 Symposium on*, pp. 443–449, Jul 1994.

[15] B. Bingham and W. Seering, "Hypothesis grids: improving long baseline navigation for autonomous underwater vehicles," *Oceanic Engineering, IEEE Journal of*, vol. 31, no. 1, pp. 209–218, Jan. 2006.

[16] G. Ramadass, V. Jayakumar, S. Zacharia, S. Ramesh, S. Ramji, A. Nosov, V. Kuznetsov, S. Dremuchev, K. Kuznetsov, and A. Paramanov, "Integrated navigation system for remotely operable vehicle for 6000m water depth," *Oceans 2007*, pp. 1–5, 29 2007-Oct. 4 2007.

[17] M. Larsen, "Synthetic long baseline navigation of underwater vehicles," *OCEANS 2000 MTS/IEEE Conference and Exhibition*, vol. 3, pp. 2043–2050 vol.3, 2000.

[18] C. E. G. LaPointe, "Virtual long baseline (VLBL) autonomous underwater vehicle navigation using a single transponder," Master's thesis, Massachusetts Institute of Technology. Dept. of Mechanical Engineering., 2006.

[19] S. Smith and D. Kronen, "Experimental results of an inexpensive short baseline acoustic positioning system for AUV navigation," *OCEANS '97. MTS/IEEE Conference Proceedings*, vol. 1, pp. 714–720 vol.1, Oct 1997.

[20] K. Vickery, "Acoustic positioning systems. a practical overview of current systems," *Autonomous Underwater Vehicles, 1998. AUV'98. Proceedings Of The 1998 Workshop on*, pp. 5–17, Aug 1998.

[21] M. Audric, "GAPS, a new concept for USBL [global acoustic positioning system for ultra short base line positioning]," *OCEANS '04. MTTS/IEEE TECHNO-OCEAN '04*, vol. 2, pp. 786–788 Vol.2, Nov. 2004.

[22] F. Napolitano, F. Cretollier, and H. Pelletier, "GAPS, combined USBL + INS + GPS tracking system for fast deployable & high accuracy multiple target positioning," *Oceans 2005 - Europe*, vol. 2, pp. 1415–1420 Vol. 2, June 2005.

[23] P. Batista, C. Silvestre, and P. Oliveira, "A sensor based homing strategy for autonomous underwater vehicles," *Control and Automation, 2006. MED '06. 14th Mediterranean Conference on*, pp. 1–6, June 2006.

[24] B. Allen, T. Austin, N. Forrester, R. Goldsborough, A. Kukulya, G. Packard, M. Purcell, and R. Stokey, "Autonomous docking demonstrations with enhanced REMUS technology," *OCEANS 2006*, pp. 1–6, Sept. 2006.

[25] P. Rigby, O. Pizarro, and S. Williams, "Towards geo-referenced AUV navigation through fusion of USBL and DVL measurements," *OCEANS 2006*, pp. 1–6, Sept. 2006.

[26] M. Morgado, P. Oliveira, C. Silvestre, and J. Vasconcelos, "USBL/INS tightly-coupled integration technique for underwater vehicles," *Information Fusion, 2006 9th International Conference on*, pp. 1–8, July 2006.

[27] J. Ferrel and M. Barth, *The Global Positioning System and Inertial Navigation*, S. Chapman, Ed. McGraw-Hill, 1998.

[28] G. Xu, *GPS Theory, Algorithms, and Applications.* Springer-Verlag Berlin Heidelberg New York, 2003.

[29] B. R. Mahafza, *Radar Systems Analysis and Design Using MATLAB.* Boca Raton, FL, USA: CRC Press, Inc., 2000.

[30] M. Stojanovic. (2006) Underwater wireless communications: Current achievements and research challenges. [Online]. Available: http://www.mit.edu/~millitsa/resources/pdfs/newsletter-oes.pdf

[31] M. Deffenbaugh, J. Bellingham, and H. Schmidt, "The relationship between spherical and hyperbolic positioning," *OCEANS '96. MTS/IEEE. 'Prospects for the 21st Century'. Conference Proceedings*, vol. 2, pp. 590–595 vol.2, Sep 1996.

[32] (1998) ES310 Introduction to Naval Weapons Engineering, course syllabus. [Online]. Available: http://www.fas.org/man/dod-101/navy/docs/es310/SNR_PROP/snr_prop.htm

[33] (2008) HLS Research, Acoustic Toolbox. [Online]. Available: http://oalib.hlsresearch.com/Modes/AcousticsToolbox/

[34] A. Alcover, P. Oliveira, and A. Pascoal, "Underwater acoustic positioning systems based on buoys with GPS," in *Proceedings on the Eight European Conference on Underwater Acoustics, 8th ECUA*, S. Jesus and O. Rodriguez, Eds., 2006.

[35] *NI DAQCard-6062E Family Specifications*, National Instruments, http://www.ni.com/pdf/manuals/370724c.pdf, December 2005.

[36] M. A. Ainslie and J. G. McColm, "A simplified formula for viscous and chemical absorption in sea water," *The Journal of the Acoustical Society of America*, vol. 103, no. 3, pp. 1671–1672, 1998. [Online]. Available: http://link.aip.org/link/?JAS/103/1671/1